Department of Electrical and Computer Engineering

Supervisory Control of Full Converter Wind Generation Systems to Meet International Grid Codes

Hasmina Tari Mokui

This thesis is presented for the Degree of

Doctor of Philosophy

of

Curtin University

March 2017

Declaration

To the best of my knowledge and belief this thesis contains no material previously published by any other person except where due acknowledgment has been made.

This thesis contains no material which has been accepted for the award of any other degree or diploma in any university.

Signature : ……

Date : 31/03/2017 ……...

Abstract

Large penetration of wind power in recent electricity market has forced transmission system operators (TSOs) to set new requirements in connecting the wind farms into the grid. These requirements emerge as the grid codes which require wind farms to ride through the fault and support the stability of the adjacent network following severe network disturbances. Specifically, the wind farms are required to be able to withstand during faults, to have extended voltage control by injecting reactive current component during faults as well as to have active power provision during faults and its restoration after fault clearance. The main objective of this thesis is to propose and implement an improved control scheme for full converter wind generation systems to comply with the aforementioned grid code requirements.

The first part of this thesis will review recent trends in grid connected FCWGs particularly to comply with the international grid codes. Recent wind status will be presented followed by benefits of utilizing FCWGs in fulfilling the grid requirements. Existing research works on FCWGs related to fault ride through (FRT) capability and reactive power support will be also included in the discussion. The research gaps in grid connected FCWGs are identified and used to set the direction and aims of this research.

The second part of the thesis will review technical requirements of connecting wind farms to the power grid. Applying the most stringent requirements in wind integration to the grid, Australia will be compared to some selected countries in terms of required FRT capability, active power and frequency control as well as reactive power and voltage control.

In the third part of this thesis, the transient responses of grid connected FCWGs will be examined. Dynamic modelling and control of FCWGs will be presented including general analysis on voltage control of FCWGs. In addition, theoretical analyses are also discussed to give supplementary justification on the simulation results. The results of this study can assist in improving FRT capability of the FCWGs.

The fourth part of the thesis presents extended PQ capability of FCWGs in compliance with Australian grid codes. The grid side converter control will be assessed in order to temporarily increase maximum converter current during the fault. Prioritization of reactive power over real power and vice versa will give different perspectives in recovering voltage stability during the fault events.

The fifth part of the thesis presents the impacts of the grid compliance FCWGs on the stability of the weak grid. A practical testing network is applied in order to investigate the impacts of the proposed FCWGs during selected symmetrical and asymmetrical faults. Two different fault locations are chosen in order to assess the response of FCWGs with regard to fault distance.

The sixth part of the thesis proposes an enhanced reactive power allocation approach for FCWGs. The approach uses voltage drops at PCC and the wind speeds to define a power index for the PQ control. Coordinated controllers allow distribution of reactive power support among FCWGs. Power indexes are implemented both at the machine side and grid side controllers such that it can be activated when voltage sag is detected at the point of common coupling (PCC). Simulations are presented for a test system consisting of FCWGs connected to power grid subject to balanced and unbalanced faults. The aim of proposed power index is not only to distributed reactive power support among FCWGs but also reduce tear and wear of DC link during fault onset.

The final part of the thesis proposes a new supervisory active and reactive power control (SPQC) that considers the individual FCWG wind speeds within the wind farm to improve the overall reactive power support to the network. The main idea is

for the wind turbines that are delivering less active power to inject more reactive power or temporarily increase their current ratings such that FCWG is able to help the nearby generators and loads to recover during severe fault conditions while working under safe operating area. The control command is centralized and the SPQC is independent of the wind turbine technology. Therefore, the proposed method may also be applied to other types of variable speed wind turbines. This will be beneficial for wind farm operator in providing reactive power support during fault among different level of wind speed.

DEDICATION

Verily, with the hardship, there is relief

(QS 94:6)

To my parents, my country, my “teachers” within my entire life and those who never stop seeking and sharing knowledge.

ACKNOWLEDGMENT

First of all, I would like to express my sincere gratitude and appreciation to my supervisor, Professor Mohammad A.S. Masoum for his invaluable supervision, encouragement, and beneficial suggestions throughout this research work. His moral support and constant guidance on both my research works and career have been priceless. I also would like to thank my associate-supervisor, Dr. Mansour Mohseni, for his assistance, brilliant ideas, and encouragement during the course of this research work. His precious advices and experiences really inspire me in improving my research attitude.

Furthermore, I would like to express my gratitude to the Chair Person (Professor Syed Islam), the University Graduate Studies Committee and the Associate Deputy Vice-Chancellor of Research Training for the constant support and beneficial suggestions during my PhD journey in Curtin University. Also, I would like to thank the examiners for their interests to my work and advices for the improvement of my thesis.

I also would like to express my deepest gratitude to Australian and Indonesian Partnerships for the Australian Development Scholarships that provides financial support throughout my Ph.D. thesis.

A special thanks to all my families and relatives, especially my parents, sisters, nieces and brothers in law. Your constant prayers and supports have sustained me so far. Last but not least, I would also like to thank all of my friends and colleagues who supported me to strive towards my goals.

TABLE OF CONTENTS

Table of Figures

List of Tables

List of Abbreviations

FCWG	Full converter wind generator
DFIG	Doubly fed induction generator
FSIG	Fixed speed induction generator
GSC	Grid side converter
MSC	Machine side converter
FRT	Fault ride thorough
PCC	Point of common coupling
PI	Proportional-integral
PLL	Phase locked loop
TSO	Transmission system operator
WPP	Wind power plant
WTG	Wind turbine generator
SCR	Short circuit ratio
SCC	Short circuit capacity

List of symbols

V_g	Grid voltage
V_{PCC}	Voltage at the point of common coupling
I_{dc}	DC link current
V_{dc} and $V_{dc,max}$	Rated and maximum value of the DC link voltage
I_c and $I_{c,max}$	Converter rated and maximum current
V_c and $V_{c,max}$	Converter rated and maximum voltage
I_{dg} and I_{qg}	Direct and quadrature components of the actual grid side converter reference current
I^*_{dg} and I^*_{qg}	Direct and quadrature components of grid side converter reference current
$\hat{I}^*_{dg}$ and $\hat{I}^*_{qg}$	Direct and quadrature components of grid side converter reference current, $I^*_{qg,}$ during the fault
P_g and Q_g	Active and reactive power output of full converter wind generator
$P_{Pre\text{-}fault}$	Pre-fault output power of FCWG (proportional to wind speed)
ΔI_{dg}	The current difference between direct current component, I_{dg} before and after fault
ΔV_{dc}	The voltage difference between DC link voltage, V_{dc} before and after fault
v_{wind}	Wind speed
S_{WT}	The rated power of wind turbine
Z_{weak}	The impedance of the weak grid

V_{sag}	The voltage at the equipment terminals during the fault
Z_S	The source impedance at the PCC
Z_F	The impedance between the PCC and the fault.
z	The impedance of the feeder per unit length
d	The distance between the fault and the PCC

Chapter 1. Introduction

1.1 STATEMENT OF THE PROBLEM

In the last decade, there is an exceptional interest towards utilization of renewable energy due to global energy crisis and the need for clean energy. Among numerous sources of renewable energy, wind power has a major role in electricity supply due to its mature technology as well as clean and economical characteristics. Market, manufacturing and investment of wind energy have expanded worldwide reaching most regions including Asia Pacific. China, India, Japan and Australia are Asia-Pacific countries with more than 1000 MW installed wind capacity by the end of 2013 [1].

As the penetration of wind power in the networks has increased largely, the TSOs have set the grid codes that require the wind farms to be capable of riding through the fault and support the stability of adjacent network upon network faults. Previously, grid code requirements were merely focused on wind farm protection without considering its effect on grid stability. However, the latest international grid codes no longer accept any wind farm disconnection during network disturbance; instead, it should remain intact to support neighbouring grid stability during fault and inject the reactive power upon fault clearance [2-7].

This thesis proposes supervisory control scheme for full converter wind generation systems (FCWGs) to comply with the most rigorous grid technical regulations imposed by international electricity markets. The main contribution of this study is an integration of supervisory control and protection scheme of FCWGs considering their intermittent characteristics and transient responses in meeting the grid codes whereas previous researches have merely focused on the improvement of the

individual FRT capability of the wind turbines as well as active and/or reactive power control.

1.2 RESEARCH MOTIVATION

Recent concern in wind power integration is not only about the quality of delivered power but also their controller ability to help with improving the stability of the network. Different countries apply different technical regulations on wind farm connection to the existing grid [7-11]. These conditions impose more constraints on wind farms requiring them to operate close to/at their critical limits.

Active power production and reactive power exchange is highly dependent on the technology of the wind farm. Being intermittent energy sources, application of power electronic has enhanced efficiency and performance of the wind farms [6, 12-14]. For example, integration of power converter technology in variable speed wind turbines allows for better PQ control. This has become the market trend and the most common applied topologies are DFIGs and FCWGs.

Compared to DFIG, FCWG is becoming a more viable and attractive option in the recent wind power market [6, 13-15] due to its ability to fully control P and Q through the GSC and the MSC [16], as well as better performance and smoother grid connection under various speed range operations [17, 18]. In addition to that, PMSG based FCWGs also allow the gearless constructions such that this technology is more cost effective compared to DFIG which is also popular in the market. Due to these outstanding characteristics, FCWG is chosen to be investigated in this thesis.

Recent literatures about enhanced FRT of FCWGs are mostly focused on the improvement of individual converter controllers at the wind turbine level. Meanwhile, intermittent characteristics of wind power cause different wind level across the wind park and the individual choice of reactive power set-points for the wind turbines in the park can take into account their respective wind conditions. In addition to that, cutting edge technology in power electronic make it possible to temporary extend the limit of power converter in order to maximize reactive power support during faulty events. Research gaps regarding the aforementioned issues are

the main motivation for the proposed supervisory control of the FCWGs in order to comply with the most stringent grid codes. Details on these research gaps will be discussed in Chapter 2.

1.3 RESEARCH OBJECTIVES

The main objective of this research is to generate a supervisory control scheme for FCWGs so that they can comply with the most demanding international grid codes. Detail plans to achieve the main objective are as follows:

1) The recent technical requirements for wind integration will be overviewed in order to discover the most up-to-date issues regarding grid code compliance.
2) An analytical and simulation based study will be performed in order to investigate transient behavior of FCWGs under various fault scenarios. The characteristic of existing controllers for FCWGs and its drawbacks leading to poor fault ride-through capability of FCWGs will also be identified.
3) Based on identified limitations of conventional controllers for FCWG, various scenarios in providing reactive power support will be investigated, particularly in regard to maximum converter capacity.
4) Reactive power allocation method considering different wind level within a wind park will be developed to comply with FRT requirements outlined in the international grid codes.
5) Investigating the positive impacts of grid code compliant control scheme on the stability of the adjacent network. The FCWGs equipped with proper FRT capability will be interconnected to the practical weak power grids in order to provide stability support to the corresponding networks.
6) Finally, supervisory P-Q control loops of FCWG will be suggested to support the transient stability of neighboring grid, as requested by international grid codes. The proposed supervisory controller will be designed to provide reactive power injection under network disturbance and have fast active power restoration during fault clearance. The comparison of the conventional control scheme and the proposed one will be carried out under realistic fault conditions.

1.4 THESIS STRUCTURE

Overall, this thesis comprises eight chapters with organization as follows.

1) Chapter 1 provides thesis objectives and motivation, thesis organization as well as a brief explanation about thesis contribution.
2) Chapter 2 presents literature review on recent trends in grid connected FCWGs, particularly in compliance with the grid codes.
3) Chapter 3 assesses the most stringent grid codes in comparison with international standards. In this Chapter, the most updated Australian grid codes will be compared with the most recent requirements from selected countries.
4) Chapter 4, the transient responses of grid connected FCWGs will be examined. Dynamic modelling and control of FCWGs will be presented including general analysis on voltage control of FCWGs. In addition, theoretical analyses are also discussed to give supplementary justification on the simulation results. The results of this study can assist in improving FRT capability of the FCWGs.
5) Next is Chapter 5 presenting extended PQ capability of FCWGs. The GSC control will be assessed in order to temporarily increase maximum converter current during the fault. Simulation compares the two different grid codes and prioritization of reactive power over real power and vice versa will give different perspectives in recovering voltage stability during fault event.
6) Chapter 6 presents the impacts of the grid compliance FCWGs on the stability of the weak grid. A practical test network is applied in order to investigate the impacts of the proposed FCWGs during selected symmetrical and asymmetrical faults. Two different fault locations are chosen in order to assess the response of FCWGs with regard to fault distance.
7) Chapter 7 of the thesis proposes enhanced reactive power allocation of FCWGs. The approach uses voltage drops at PCC and the wind speeds to define a power index for PQ control of FCWGs. Coordinated controllers allow distribution of reactive power support among FCWGs. Power indexes are implemented both at the machine side and grid side controllers such that it can be activated when voltage sag is detected in the common point. Simulations are presented for a test

system consisting of FCWGs connected to power grid subject to balanced and unbalanced faults. The proposed power index is not only to distributed reactive power support among FCWGs but also reduce tear and wear of DC link during fault onset.

8) Chapter 8 proposes a new supervisory active and reactive power control (SPQC) that considers the individual FCWG wind speeds within the wind farm to improve the overall reactive power support to the network. The main idea is for the wind turbines that are delivering less active power to inject more reactive power or temporarily increase their current ratings such that FCWG is able to help the nearby generators and loads to recover during severe fault conditions while working under safe operating area. The control command is centralized at the common point and the SPQC is independent of the wind turbine technology. Therefore, the proposed method may also be applied to other types of variable speed wind turbines. This will be beneficial for wind farm operator in providing reactive power support during fault among different level of wind speed.
9) Finally, contributions and future research works are presented in Chapter 9.

1.5 LIST OF AUTHOR'S PUBLICATIONS

The main content of the thesis is based on the following published articles:

C1. **H. T. Mokui**, M. Mohseni, and M. A. S. Masoum, "Investigating the Transient Responses of Fully Rated Converter-based Wind Turbines," in the proceedings of the *21st Australasian Universities Power Engineering Conference (AUPEC 2011),* Brisbane, Australia, 25-28 September 2011.

C2. **H. T. Mokui**, M. Mohseni, and M. A. S. Masoum, " Implementation of Space Vector Based Hysteresis Current Control for Full Converter Wind Generation System, " in the proceedings of the IEEE PES ISGT Asia, Perth, Australia, 13 – 16 November 2011.

C3. **H. T. Mokui**, M. A. S. Masoum, M. Mohseni, and M. Moghbel, "Power System Transient Stability Enhancement using Direct Drive Wind

Generators," in the proceedings of the *2012 IEEE Power and Energy Society General Meeting,* San Diego, USA, 22 – 26 July 2012.

C4. **H. T. Mokui**, M. A. Masoum, and M. Mohseni, "Fault ride through Capability of Fixed Speed Induction Generators connecting to Full Converter Wind Generation System within Weak Network," in the proceedings of the *2014 IEEE 5th International Symposium on Power Electronics for Distributed Generation Systems (PEDG),* Galway, Ireland, 24 -27 June 2014.

C5. **H. T. Mokui**, M. A. Masoum, and M. Mohseni, "Enhanced Reactive Power Allocation of Full Converter Wind Generation System," in the proceedings of the *2014 IEEE 5th International Symposium on Power Electronics for Distributed Generation Systems (PEDG),* Galway, Ireland, 24 -27 June 2014.

C6. **H. T. Mokui**, M. A. Masoum, and M. Mohseni, "Review on Australian Grid Codes for Wind Power Integration in Comparison with International Standards", Accepted for presentation and publication, *Australasian Universities Power Engineering Conference (AUPEC 2014)*, Perth, Australia, 28 September – 1 October 2014.

Chapter 2. Trends in Grid Connected Full Converter Wind Generation Systems

2.1 INTRODUCTION

Wind power can be considered as a mature technology and its integration into the existing grid gets special attention in the field of renewable energy. With regard to this, FCWG technology equipped with full power electronics becomes more preferred in order to gain the whole benefits of wind integration. This chapter will review recent trends associated with penetration of FCWGs into power network. Section 2.2 presents an overview on the recent wind energy status worldwide including in Australia and Section 2.3 highlights main benefit of FCWGs over other wind turbine technologies. Section 2.4 investigates PQ control strategies applied to FCWGs including FRT capability and reactive power support to the network followed by conclusions.

2.2 RECENT WIND ENERGY STATUS

Recently, renewable energy sources have more functionalities than just as energy sources. Their roles become mainstream including for energy security improvement, cleaner and healthier environment establishment, mitigation of greenhouse gas emission, as well as more job and educational opportunities.

Figure 2-1 depicts the total new investments on renewable energy sources worldwide by the end of 2013 and wind power is accounting for more than one-third of the total investment [19]. From early 1980s to the end of the 1990s, worldwide wind capacity increased about twice folds for every three years while electricity cost from wind power decreased to about one sixth [17]. Besides, with averaged cumulative annual growth rate of about 21.4% since the end of 2008, the global installed capacity

worldwide has boosted up from about 39 GW at the end of 2003 to about 318 GW at the end of 2013 [19].

Figure 2-2 shows the total installed capacity of wind power in the past decade. According to renewable energy indicator [19], the top five countries for total generation of wind power by 2013 are China, United States, Germany, Spain and India. China and Germany are also on the list of countries with the most annual investment in wind power capacity.

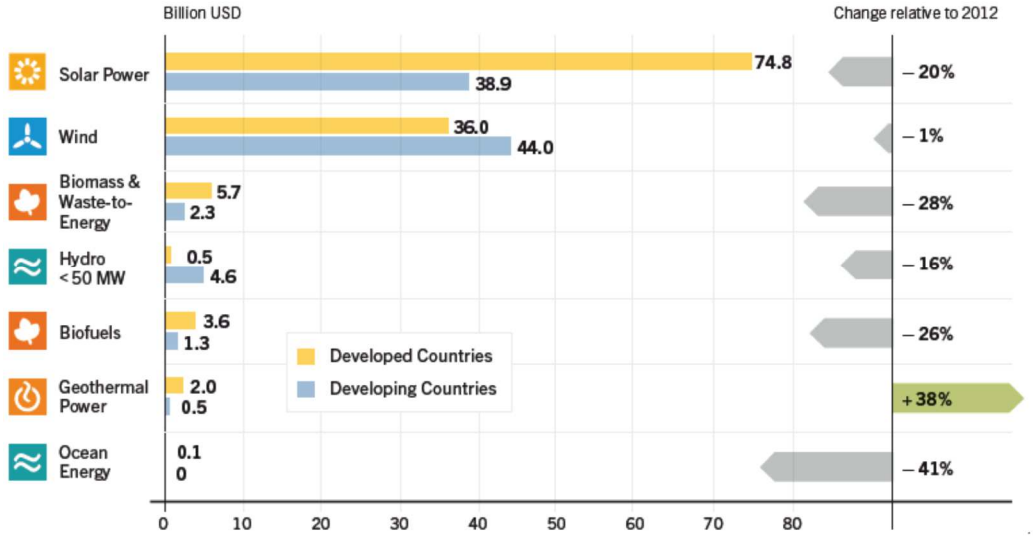

Figure 2-1 Global new investment in renewable energy by technology, developed and developing countries, 2013 [19].

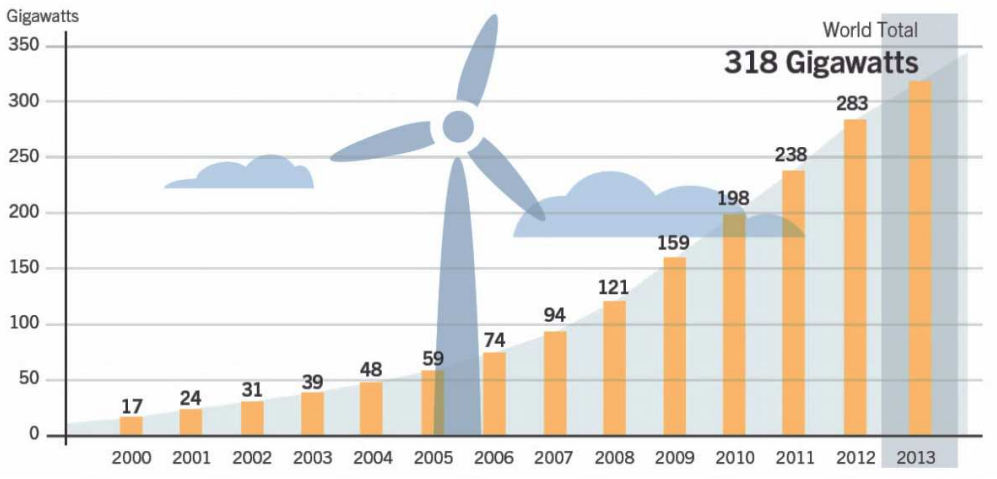

Figure 2-2 Wind power total world capacity, 2000–2013 [19].

On 23 June 2015, Australian Government [20] has announced the amendment of large scale Renewable Energy Target (RET) from 41,000 GWh to 33,000 GWh. The amended RET basically set that by 2020; at least 23.5% of the Australia's electricity will be generated from renewable energy sources such as wind. According to [21], Australia is one of the countries with excellent wind resources, particularly along its south-western, southern and south-eastern coastlines as well as some isolated areas in the eastern regions. The Australian utilization of wind energy for electricity has increased with the average rate of 35.9%/year in the periods 1999-2000 and 2011-2012 [21].

Figure 2-3 illustrates trends in total wind electricity generation in Australia within the last two decades [21]. In period 2011 to 2012, wind power generation contributed about 6.1 TWh which is 2.4% of the total electricity generation in Australia. These figures confirm that wind power generation is the fastest growing renewable energy source in Australia. Moreover, in 2012 [21], large wind farms having more than 100 MW capacities contribute to about 40.6% of the total wind installed capacity in Australia and by the end of 2012, 66 large wind farms were under operation with total installed capacity of 2.584 GW. There is a positive confident that this trend will keep increasing, particularly with commitment of the new government to keep involve in the RET by 2020.

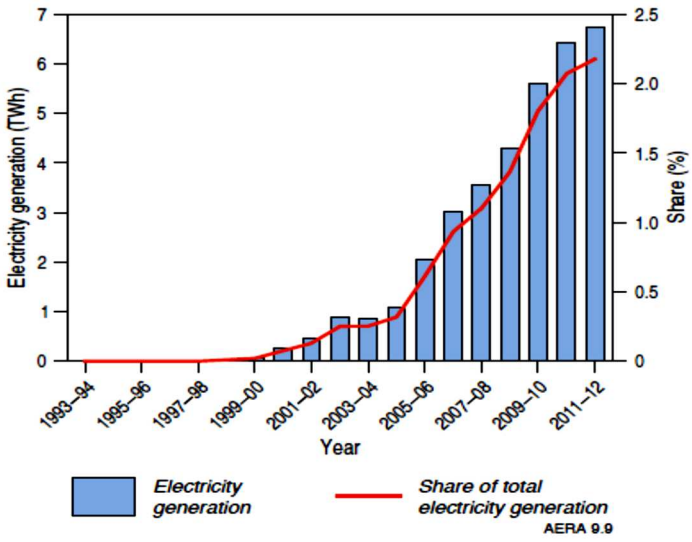

Figure 2-3 Wind electricity generation in Australia [21].

In Australia, large wind farms are mostly located in South Australia, Victoria and Western Australia [21]. Technical regulations for grid connected wind farms within South Australia and Victoria are set by the Australian Energy Market Operator (AEMO) while Western Power (WP) acts as the TSO for Western Australian network. Even though the aforementioned TSOs are in the same country, they apply different technical regulation.

2.3 EXAMINING WIND TURBINE TECHNOLOGIES

The main objective of wind energy generation is to convert mechanical energy produced by the blades into electrical energy by minimizing the total cost of energy production. In addition to cost optimization, there are other requirements need to be considered in order to maximize power delivery into the power grid [15]:

(1) Fulfilling grid requirements, explained in Chapter 3. of this thesis.
(2) Availability and reliability of WTGs in any condition and temperature range.
(3) Applying variable speed in order to enable optimal match between generator and the aerodynamic of the rotor.

The aforementioned requirements highly determine WTG technology to be installed within a wind farm. Accounting for 13.1% of the total market shares, Vestas manufactures most WTGs worldwide, followed by Goldwind, Enercon, Siemens and GE Wind respectively (Figure 2-4).

Even though there are rooms for future improvements, recent WTG technologies based on their ability to control speed and their type of power control can be classified into 4 main categories [6, 15, 17]. The following sections will briefly examine these WTG technologies including their advantages and disadvantages.

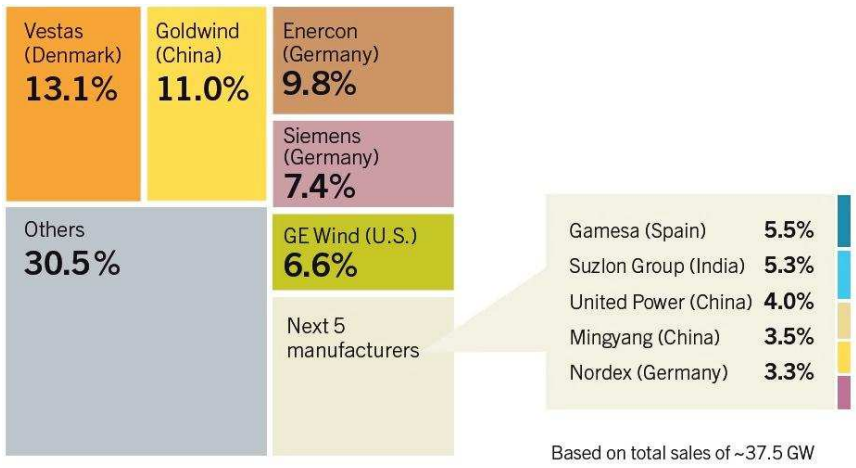

Figure 2-4 Market shares of top 10 wind turbine manufacturers, 2013 [19].

2.3.1 Fixed speed induction generator

This type of machine consists of induction generator (squirrel cage or wound rotor) directly connected to the grid through a transformer with configuration as shown in Figure 2-5.

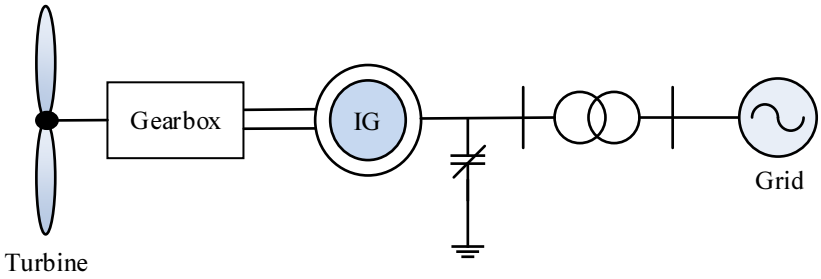

Figure 2-5 Configuration of FSIGs.

FSIGs are well known for their simple installation, economical cost, as well as brushless and rugged constructions. However, during network fault they are very susceptible to rotor over speed that may lead to the activation of its protection and under voltage tripping scheme [22]. These actions are aimed to protect the wind turbines as well as maintain the network security and stability following contingencies due to voltage collapse within the network. Ideally, the FSIGs are installed within stiff network in order to avoid such issues. On the contrary, FSIGs

are mostly located far away from the grid [23]. Meanwhile, the TSO set the grid codes that require the wind farms to remain intact during the fault and if possible contribute to the stability of the nearby network.

There are several methods published to improve FRT capability of FSIGs, either aimed to reduce their rotor over speed or providing reactive power compensation during the fault. These methods include application of fast pitching techniques at the pitch angle controller, dynamic braking resistor, FACTS devices, and superconducting magnetic energy storage (SMES) [22, 24-30]. Nevertheless, additional reactive power compensation equipments also cause an increase to the total cost of wind turbine generation.

There are FSIGs that are still operating nowadays and contributes about 20% to 30% of global wind capacity, mostly installed in the 1980s to 1990s [31]. Within that era, technology in power electronic converter has not advanced as nowadays, therefore the aforementioned machine has low FRT capability.

2.3.2 Wounded rotor induction generator with rotor resistance control (Dynamic slip control).

The rotor windings of the WTG are connected with variable resistors in order to control the slip. Electronic control system is responsible to adjust variable resistor so that the slip is in proportional with the resistance (Figure 2-6). In such way, the WTGs can vary their speeds.

Apart from its limited variable speed, this type of WTG still requires soft starter and reactive power compensation [6] contributing to low FRT capability as well. The fact that it has limited variable speed, causing this type of WTG is not popular as other variable speed configurations (i.e. DFIGs and FCWGs).

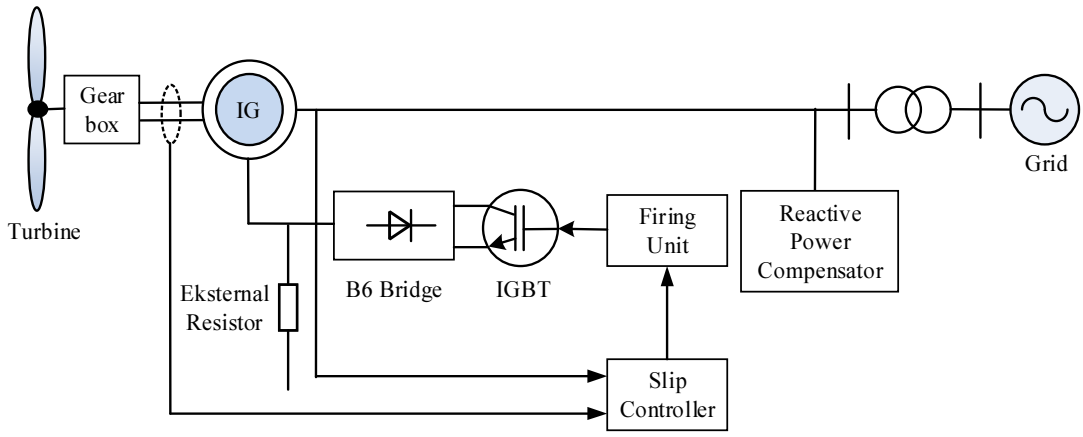

Figure 2-6 Configuration of wounded rotor induction generator with rotor resistance control.

2.3.3 Doubly fed induction generator

In this configuration, the stator part of WTGs is directly connected to the grid while a back to back converter connects the rotor side of machine to the grid via slip rings as illustrated in Figure 2-7. The back to back converter consists of two bidirectional converters connected via DC link, where one side of converters attached to the machine rotor and the other one to the grid.

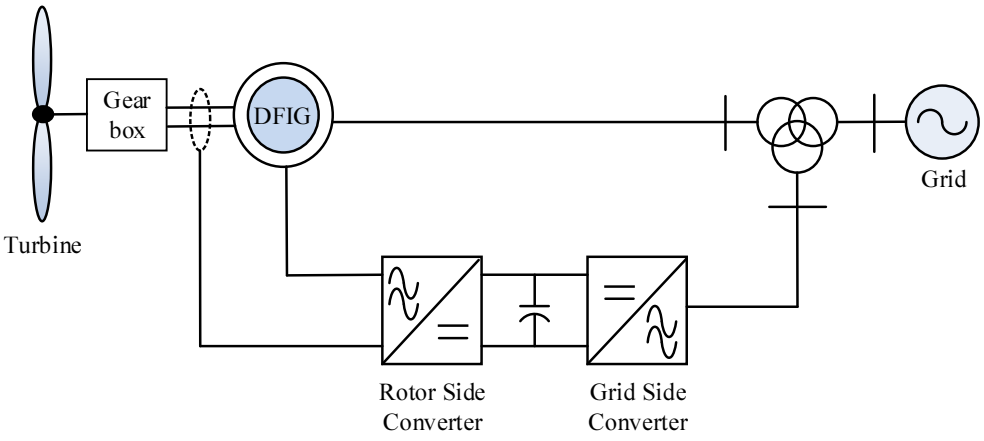

Figure 2-7 Configuration of DFIG.

As harnessing wind power is increasing, the TSOs set the grid codes that oblige the wind farms to ride through the fault and support the stability of nearby grid during severe network faults. Implementation of grid codes worldwide has been reported in

various works and mostly suggested the utilization of variable speed generators such as DFIGs [32-35] and FCWGs [3, 16, 36-38]. Recently, DFIG configuration has proven as the most popular solution for modern wind farms [13, 39] since its power converter capacity is only about 30% to 40 % of the total wind generator rating. However, the limited size of power converter also becomes the major drawbacks for the DFIG as it causes inherent problems for DFIGs to ride through under voltage sags. The voltage dip can cause the surge current in the rotor side converter and voltage ripple at the DC link capacitor which might destroy these electronic components unless protection equipment such as crowbar and energy capacitor system (ECS) are installed [17, 32]. In addition, DFIG configuration also needs mechanical slip-ring/brush gear arrangements which become major concerns in system reliability [17, 40].

2.3.4 Full converter wind generator

In this configuration the generator is connected to the grid via a full scale frequency converter (Figure 2-8) and it has been adopted by some manufacturers such as Siemens, Enercon and Goldwind [15].

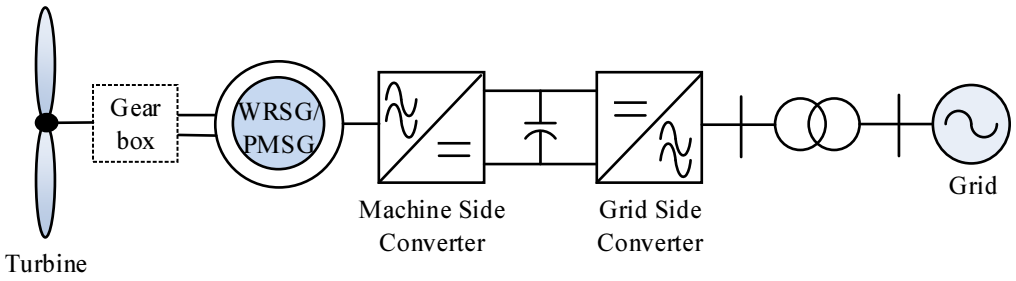

Figure 2-8 Configuration of FCWG.

It is reported in [13, 14] that there are three types of generators normally used for FCWGs, i.e. asynchronous generator, wound rotor synchronous generator (WRSG) and permanent magnet synchronous generator (PMSG). FCWG with asynchronous generator and back-to-back converter can avoid the increase of short circuit power by controlling the fault current at the GSC. Nevertheless, manufacturers producing the

aforementioned configuration is quite low because it is not technically feasible for a multipole direct drive operation as with PMSG [41]. In contrast, its counterparts (i.e. PMSG and WRSG) dominate the wind turbine markets in the best seller power range [6, 12, 14, 41, 42]. PMSG based FCWG can omit the use of gearbox that reduces the total weight, maintenance cost, and noise generation [43, 44]. Due to these characteristics, it is predicted that PMSG will be the most adopted wind generator in the future [13-15]. However, the total cost for PMSG is higher as compared to the WRSG due to the increased price of rare-earth magnet [14].

Superconducting generators for FCWGs are superior to PMSG in terms of low weight, small sizes and high efficiency [45]. AMSC has announced a 10MW offshore Sea Titan [46] based on superconducting generators. However, this technology still have some technical challenges such as a necessity to maintain cryogenic systems [47]. In addition to that, the aforementioned technology still require further research in order to improve the generator system reliability and its maintenance [47, 48].

Being low cost solution, FCWG system with externally excited SG is also such a mature wind generator technology. Enercon [14, 41, 49] has successfully manufactured up to 7.5-MW of such wind generator with gearless construction and the company is still aiming for manufacturing increased wind generator capacity.

The use of frequency converters allow FCWG has better capability to ride through the fault by providing reactive power compensation as well as smooth grid connection over different range of wind speed [6, 13, 14]. Generally, this concept has more excellences as compared to DFIG, due to its simple configuration, slip ring elimination, possible for gearless configuration as well as better speed control and grid support capability [13, 16, 17, 50]. The possibility of gearless construction causes this configuration to have low cost as well as less wear and tear at the gearbox thus significantly reducing the total maintenance cost.

2.4 PQ CONTROL SCHEMES FOR FCWGS

2.4.1 Modelling techniques for FCWGs

In modelling the dynamic of wind energy conversion system as in FCWGs, it is important to comply with the physic of the power system and the level of complexity depends on the target of investigation. The electricity producing wind turbines are usually presented as complex electromechanical system which represent the electrical (i.e. generators, frequency converters and their control systems) and mechanical components (i.e. shaft system, turbine rotors and their control system) [51].

While modelling of various types of generators, converter, mechanical shafts and control system are well established in the literature, modelling of wind turbine is more complex as it includes the aerodynamic system [17]. Specifically in modelling interaction of wind farm into large system, there are two common approaches used, i.e. detailed modelling and aggregate modelling. Previously, transient study on large scale wind farm is modelled in detail which increase system complexity and contribute to lower simulation speed. It is argued in [52] that aggregate modelling can simplify modelling and reduce time simulation, but do not significantly reduce the accuracy compared to the detailed modelling. However, in investigation of control features of the wind turbine during transient event requires both detailed and aggregate model [51]. Furthermore, the FCWGs are modelled using fundamental frequency approach and its control schemes determine the behaviour of wind turbine within normal and network faults. Vector control techniques usually used to control the frequency converter since these techniques allows decoupled control of reactive and active power [36]. In the vector control, the rotating reference frame is utilized based on AC flux or voltage and then this rotating frame is used to project the currents.

2.4.2 Power converters for FCWGs

In FCWGs, power converters connect the stator of machine to the grid. The MSC normally controls the current flowing into the generator to adjust the torque resulting to control of rotational speed [14, 42]. During normal and fault condition, this converter balances active power production while maximizing power extraction from wind turbine. Moreover, the GSC must ensure that the wind turbine has the ability to meet the grid requirements, i.e. providing reactive power support while performing fast active power response [14, 42].

According to [14], the single cell power converters for wind turbines are divided into 3 main categories, i.e unidirectional power converters, 2 level power converter (2L-BTB), and multilevel power converter. These three configurations are also commonly applied to FCWGs. In unidirectional concept, the MSC can apply diode rectifier or semi controlled rectifier as in [53]. In addition to that, a DC-DC boost converter is also installed in between rectifier and the inverter of power conversion system to reach the power level in MWs. Simple configuration as well as cost effective solution are two major benefits of the aforementioned configuration. However, the main drawback of diode rectifier is causing the low frequency pulsations that can trigger shaft resonance, either for multiphase or 12-pulses [54].

The 2L-BTB, well known as back to back power converters, is the most common power configuration applied to the wind power conversion. Besides PMSGs, DFIGs-based WTs frequently use this type of power converter. Simple structures, well proven robust and reliable performance are the main advantages of the aforementioned power converter. Nevertheless, 2L-BTB may have larger switching losses and reduced efficiency when the power and voltage range of WTG are increased [14]. Another drawback of 2L-BTB is the need of bulky output filter to lessen the voltage gradient and decrease the THD [14, 55].

Multilevel power converters are the solution for achieving required performance with the available switching devices. However, they can only be used for FCWGs sized between 3 to 7 MW in order to achieve cost efficient design. In addition, as the

power converters and their auxiliary controllers are increased, the converter reliability and the total cost will increase as well [14].

2.4.3 Maximum wind power control

It is worth noting that the amount of energy generated from a WTG depends on wind characteristics in the site as well as applied control strategies. By applying maximum power point tracking (MPPT) algorithm, the MSC controls turbine rotational speed in order to achieve maximum generated power and limit them to not exceed nominal power when the wind speed increases. During excessive wind, applied MPPT algorithm also keep the DC link voltage as constant as possible, meaning that the decoupling of GSC and MSC is achieved [6].

MPPT control algorithm for wind turbine can be divided into 4 categories. Details on these control techniques as well as their implementation on FCWG system are presented as follows.

1) Tip speed ratio (TSR) control. The work in [56] applies TSR control for a megawatt PMSG-based FCWGS with diode bridge rectifier and a dc–dc four-level boost converter in the MSC. It is necessary for TSR control to measure both wind and turbine speed. This method really depends on the anemometer to measure the wind speed in order to maintain optimal control. Apart from its simplicity, it is difficult for TSR control to achieve optimal wind speed while adding an external anemometer will lead to a more cost and complex system [6, 57].
2) Power signal feedback (PSF) control. This method can be divided into optimum power feedback control and the optimum torque feedback control [57]. Implementation of these two PSF based control methods for FCWG system are shown in [58] and [59] consecutively. PSF control requires maximum power curves data of the turbine, obtained from simulations or practical tests. A predictor or an observer may substitute the power curve as a function of the power and the wind speed. Nevertheless, since the blade

aerodynamics and wind speed change all the time, it is difficult to force the wind turbine to work off peak of the C_p curve simultaneously [6, 57, 60].

3) Hill climbing search (HCS) control. This MPPT technique is also called as perturb and observe (P&O) method, due to its characteristic to perturb the control variable and observe whether to increase or decrease power [57, 60]. Photovoltaic system also implements this control technique [6]. Independency from system characteristics and wind speed data are the two main advantages of HCS control. However, due to its perturbation characteristic, the HCS is somehow incapable of tracking the exact MPP under rapidly varying wind speed leading to failure of the whole MPPT control [6, 57, 60]. An intelligent HCS for PMSG was proposed in [61].
4) Fuzzy logic and neural network based control. The main advantages of this MPPT control are fast convergence, parameter insensitivity as well as acceptance of noisy and inaccurate signals. However, the aforementioned control applies complex algorithm and time consuming such that ineffective for practical implementation [57, 60]. The work in [62] shows implementation of such MPPT algorithm.

2.4.4 Ride through capability and grid support of FCWGs

In order to maintain good power quality service to the consumers as well as for the sake of the network, TSOs impose stringent requirements that basically demand the wind farms to have good FRT capability and if possible to inject particular amount of reactive power in response to the voltage drop sensed at the machine terminals.

Good FRT capability means that the wind generator remains connected with the grid in response to any fault event. Theoretically, FCWG can ride through any grid faults (symmetrical or unsymmetrical) as the generator is fully decoupled from the grid through the grid side inverter. Thus, reactive power exchange merely depends on the characteristic of grid side inverter and not by the generator properties [17, 36]. When the fault occurs in the network, the inverter is automatically affected by the grid so that its control over DC link voltage will be limited quickly. The MSC continuously

delivers power normally, however the grid side inverter cannot transfer this power to the grid. As a result, the power surplus in the inverter starts charging the DC link capacitor that leads to the DC link over voltages which potentially damage the DC link itself. As the power imbalance occurs, the rotor of turbine also starts to accelerate and increase the possibility of damaging the converter [36]. Therefore, it is really essential to design an integrated controller to protect the converter from overvoltage/over current while complying with the grid codes.

Despite considering voltage variation issues, the TSOs also address the issue of power quality to maintain a proper functionality of power system [63, 64], such as maximum limit for the total harmonic distortion (THD) and flicker induced by voltage fluctuations. During unbalanced fault, the power of the DC side of the inverter will be interfered by a significant second order harmonic due to modulation between the positive and negative phase sequence components of the voltage and current on the AC side. The inverter will push its limit to remove such harmonic emission which leads to significant reduction of the output power. Coordinated control between generator rectifier and grid side inverter utilizing the PI controller is proposed in [40] to constrain such harmonic power or current in PMSG based FCWG. Harmonic current emission can also be influenced by a converter control malfunction and Reference [65] proposed fractional order controllers to effectively decrease the THD. In the case of output power drop because of flicker, a flicker mitigation controller (FMC) has been proved in [66] to successfully damp the 3p active power oscillations caused by the wind shear and tower shadow effect in full scale wind turbine generation system.

Dynamic control strategies for FCWG has raised many attentions in the literatures and mostly focused on fault ride through (FRT) techniques for voltage source converters (VSC) in wind energy conversion system (WECS) [5, 37, 44, 67] while very few research on current source converter (CSC) based WECS is proposed [39, 68, 69]. This is because PWM CSC only suit for high power medium voltage application such as in large scale offshore wind turbines. While it is crucial to

understand the dynamic of FCWGs in the context of standalone, weak networks and grid connected.

Several ride through schemes for FCWGs proposed in the literatures often involve hardware modification instead of controller performance enhancement [5]. For example, the braking chopper is usually modelled in the DC link for protection and activated when the network experiencing faults. When the DC link exceeds its predefined limit, the chopper dissipates the active power into its resistance part [5]. However, installation of braking chopper require additional cost and might not optimize performance of FCWG since in [37] it shown that its installation on offshore FCWGs with HVDC link did not make best use the network during onshore network fault. Similarly, reference [70] shows that an energy capacitor system (ECS) installed at the terminal side of the wind farms can effectively smoothen the output power fluctuations of the FCWGs. Even though the proposed ECS is claimed to have small size and economical cost, it still requires additional cost for the installation and maintenance.

It has been reported that cascaded control schemes utilizing the classical PI controller are commonly applied for the current controllers at the MSC and/or at the GSC [5, 51, 71] due to its robustness as well as wide stability margin [71]. However, it is reported in [64] that under unbalanced faults, the PI controller has larger overshoot in its response compared to the deadbeat (DB) controller which belongs to the family of predictive controller. The PI controller requires the synchronization algorithm such as provided by a PLL system to extract the positive sequence of the grid voltages. The algorithm under fault provides the phase angle which is synchronized to the positive sequence component of the grid voltages such that the current references remain sinusoidal and balanced. Other drawbacks of PI based controllers are highly sensitive to parameter variations and nonlinearity of dynamic systems [71].

There have been several attempts to improve FRT capability of FCWGs by modifying control strategies of the power converters. In [71], the FRT capability of PMSG-based FCWG can be significantly enhanced by using the parameters of its frequency converter obtained from combination of genetic algorithms (GAs) and

response surface methodology (RSM). However, limitations associated with GAs method still exists, such as no guarantee that the global optimum will be obtained [72] . In addition, GAs is not practically used for real time simulation due to issues on random solution and convergence.

Moreover, in [73] back to back neutral point clamped converter is proposed concurrently controlling both MSC and GSC of PMSG based FCWG. By applying such concurrent control action, an excessive active power during fault can be stored into the generator rotor inertia such that the dc-link can remain constant. It is claimed that by applying this control scheme, activation of brake chopper could be avoided in some cases. But, there is issue with energy loss at PMSG due to drag force induced by the magnetic field parts. This energy loss somehow may reduce the rotational speed of the machine [74], which is avoided in maintaining the stability of power supply.

Another important requirements imposed by the TSOs is the ability of the wind turbine to provide reactive power support to the nearby grid during fault, such as FSIGs (Please see Section 2.3.1). Application of fast pitching techniques at the pitch angle controller, dynamic braking resistor, FACTS devices, and superconducting magnetic energy storage (SMES) [22, 24-30] are normally applied in order to help the FSIGs recovering from contingency. Among aforementioned solutions, SMES is the most effective and efficient energy storage system to help WTs in improving their FRT capability due to its instantaneous large energy discharge [75]. This technology has shown good results when it is implemented into several distributed renewable projects including wind power [75, 76]. However, the material cost of SMES is considerably high even though it is expected to decrease by nearly 30%. In addition to that, a very little temperature change may lead the coil to become unstable and lose energy [77].

It has been discussed before that the GSC is responsible for reactive power exchange between wind turbine and the grid. It has been demonstrated in [2, 3] that FCWGs can improve transient and voltage stability of its adjacent grid by modifying P/Q control scheme of the power converter. It is also shown that the capability of FSIGs

to ride through the fault can be improved by installing FCWGs nearby such as in [5] that implements 3 level neutral point clamped (3L-NPC) for both side power converters in order to meet the grid requirements. The aforementioned study is designed by considering the grid codes set by the Federal Energy Regulatory Commission (FERC) but the effect of extending its converter capacity on PQ control is not shown. Moreover, reference [78] shows that the droop control can be successfully implemented for power sharing between multiple FCWGs such that they can help the weak network recovery in the occurrence of fault.

Based on the aforementioned literatures, it is obvious that to meet the grid code requirements, some modification on power converters is required. However, any change in the control strategy must keep the maximum converter current within the permissible limits [2, 51] and in some way also maintain the DC link voltage stable [39, 51, 79] so that the wind turbine can safely ride through the fault. Again, great advancement in the power electronic technology allows more sophisticated control of the converter that inherently enhances the control and capability of wind farms. For instance, PM3100W power converter from AMSC [80] and Semikron Skiip Intelligent Power Module [81]. Taking full benefit of these properties will enhance the ability of the wind farms to deliver power to the network and contribute to the stability of the network by injecting more reactive power during contingency.

2.5 CONCLUSION

In this chapter, trend in grid integration of FCWGs has been discussed starting with its beneficial over other wind turbine technologies to its positions for network stability as requested by TSOs. The use of advanced power electronics is important such that FCWGs can regulate their voltage reactive power based on requirements imposed in the grid codes. However, proper control strategies are necessary such that the FCWGs can work properly within its safe operational limits while maximizing its potential in helping maintaining network stability during and after fault clearance.

It has been shown that FCWGs have better characteristics in complying with the grid codes compared to the DFIGs which are also popular in the market. Since most

literatures are focused on implementation of DFIGs, there are still rooms for research on FCWGs particularly in designing proper control strategies in meeting the recent grid requirements. The remaining part of this thesis will discuss the improved control strategies of FCWGs in order to diminish current research gap such that they can safely complying with the grid codes.

Chapter 3. Review on Technical Requirements of Grid Connected Full Converter Wind Generation System

3.1 INTRODUCTION

The main objective of power system is to ensure that the power can be supplied continuously to the customers in economic and secure way but still in an accepted level of power quality. Substantial integration of wind power into existing power grid has exposed new issues regarding grid stability. In dealing with these issues, most TSOs stipulate the grid codes requiring the wind farms to have proper FRT capability and supplying reactive power support to the nearby network in need [2-7]. These codes noticeably vary from country to country and mainly depend on characteristics of the existing networks and available resources [7]. Although, grid codes have been reviewed in several literatures including [7-11], they are subject to updates.

Since Australian electricity market applies the most rigorous regulations [8], this chapter provides an international grid code update with a focus on grid code comparisons between western and eastern electricity market of Australia. For a broader outlook, a comparison with international grid codes will also be discussed.

The latest update of the grid codes provided in this chapter will help the Australian TSOs in examining recent regulations in comparison to international practices while also giving some insights to the wind turbine manufacturers, developers and operators in improving their services and/or products in complying with the existing standards.

The structure of this chapter will be as follows. In Section 3.2, a comprehensive review on the technical requirements stated in selected grid codes will be provided. This section will cover requirements in validating stability performances of wind turbines during fault and after fault clearance, i.e. FRT capability, active power and

frequency control, frequency control as well as reactive power and voltage control. Section 3.3 discusses grid code issues related to wind integration including harmonization of grid codes, grid code compliance certificate, as well as future trends of the grid codes. Finally, in Section 3.3 the main remark of this chapter is concluded.

3.2 REVIEW OF GRID CONNECTION REQUIREMENTS

According to [7], the grid codes basically refer to the large wind farms connected to the transmission system instead of smaller stations connected to the distribution systems. As a dynamic system, the behaviour of wind turbines becomes more complex with its integration to the grid. To comply with these dynamic issues, the TSOs basically impose strict grid codes to maintain the standard of electricity services as well as safeguarding the stability and security of supply in electricity market. Nevertheless, due to intermittent nature of wind conditions and market demands, it is also important for wind turbine manufacturers to improve their technologies.

In setting the network requirements, TSOs consider the present situations as well as the future system developments. ENTSO-E as the TSO for European network acknowledges different local network conditions such that the recently approved grid codes [82] do not apply full harmonisation for its network requirements. Since network topology, dynamic system response and stability differs from country to country, the local TSOs apply further requirement within its network. TSOs such as in Spain and Germany set the grid codes for wind integration in two scenarios, i.e. through stringent requirement and/or financial incentives [11].

The main technical requirements presented in the majority of the grid codes include fault ride through (FRT), active power and frequency control, voltage and frequency operating range, reactive power control and voltage regulation, as well as other requirements such as a virtual type test (Eltra and Elkraft grid codes) to verify wind turbine behaviour during fault [7]. Nevertheless, it is predicted in [8, 83] that the

future grid codes will also include inertia emulation and power oscillation damping such as recommended in Spanish [84] and Irish grid codes [85].

Details about these technical requirements particularly for Australian grid codes will be investigated in the following sections.

3.2.1 Fault ride through

There are four main characteristic defined by most grid codes in determining contingency performances of the wind turbines [11] including (1) conditions for which the turbines must remain connected and allowed to be disconnected, normally represented in time domain through the FRT curve at point of connection, (2) voltage support requirement during the disturbance, (3) active power provision during fault, and (4) restoration of active power after fault clearance.

The FRT capability of WTG refers to the ability of the wind generator to remain intact during contingency. This can be investigated by considering its dynamic stability during fault onset as well as fault clearance. Due to specific characteristics of the network, each TSO applies certain FRT capability that might be different to another TSO. For example, ENTSO-E [82] sets the lower limit of the FRT diagram to be applied by each TSOs within the European Network. In addition, ENTSO-E specifies different FRT capability profiles for synchronous power generating modules and power park modules due to specific technical requirements and its financial consequences. Network stability of the grid is very much affected by both machine's fault clearance time and pre-fault operating points (i.e. voltage and apparent power). For the aforementioned reasons, ENTSO-E sets a maximum of 0.25s for the generating unit to withstand during the minimum admissible voltage and a maximum of 3s to regain its pre-fault voltage.

Table 3-1 shows high and low voltage ride through (HVRT, LVRT) requirements applied in the major countries leading in wind power utilization. As can be seen, Spain and Australia have the most stringent HVRT and LVRT compared to the other standards. Moreover, Figure 3-1 and Figure 3-2 show LVRT and HVRT capability required by WP; respectively, while the HVRT curve required by AEMO is

presented in Figure 3-3. Based on aforementioned figures and Table 3-1, WP and AEMO require the generators to allow similar over voltage condition (e.g. 1.3 p.u.); however, WP sets much longer periods than AEMO. Therefore, the Western Australian grid has more stringent requirement as compared to the eastern network regulated by AEMO.

Table 3-1 Technical requirements in international grid codes.

Country (TSO)	LVRT				HVRT		Ref
	During Fault		Fault Clearance		During swell		
	V_{min} [p.u.]	T_{max} [s]	V_{min} [p.u.]	T_{max} [s]	V_{max} [p.u.]	T_{max} [s]	
Australia (AEMO)	0	0.43	0.7	2	1.3	0.06	[86]
Australia (WP)	0	0.45	0.8	0.45	1.3	0.98	[87]
Canada (Hydro Quebec)	0	0.15	0.75	1	1.25	2	[88]
Denmark (Energinet)	0.2	0.5	0.9	1.5	1.2	0.1	[89]
Germany (Tennet)	0	0.15	0.9	1.5	1.2	0.1	[90]
Ireland (EirGrid)	0.15	0.625	0.9	3	N/A	N/A	[85]
Spain (REE)	0	0.15	0.85	1	1.3	0.25	[84]
UK (NGET)	0.15	0.14	0.8	1.2	N/A	N/A	[91]
USA (WECC)	0	0.15	0.9	1.75	1.2	1	[92]

Different to AEMO, WP also specifies that WTGs should be able to withstand safe operation during voltage transients caused by high speed auto-reclosing of transmission lines irrespective of whether or not a fault is cleared during a reclosing sequence. The corresponding LVRT curve is presented in Figure 3-4.

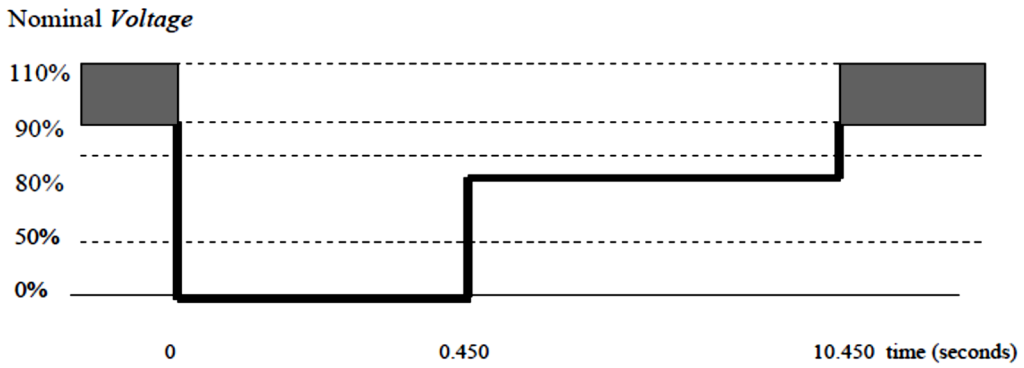

Figure 3-1 Off nominal voltage operation capability requirement for generating units in Western Power Network [87].

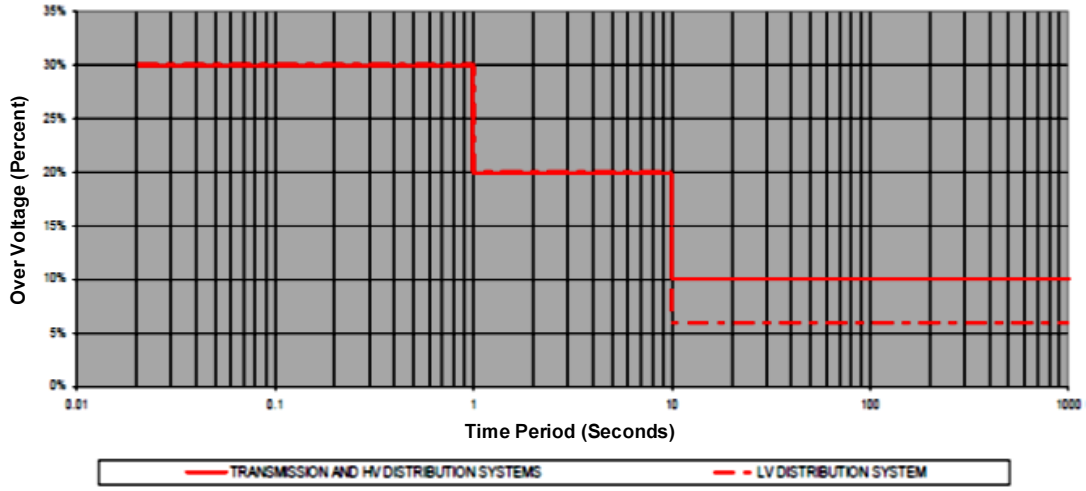

Figure 3-2 Temporary over voltages as stated at WP Grid codes [87].

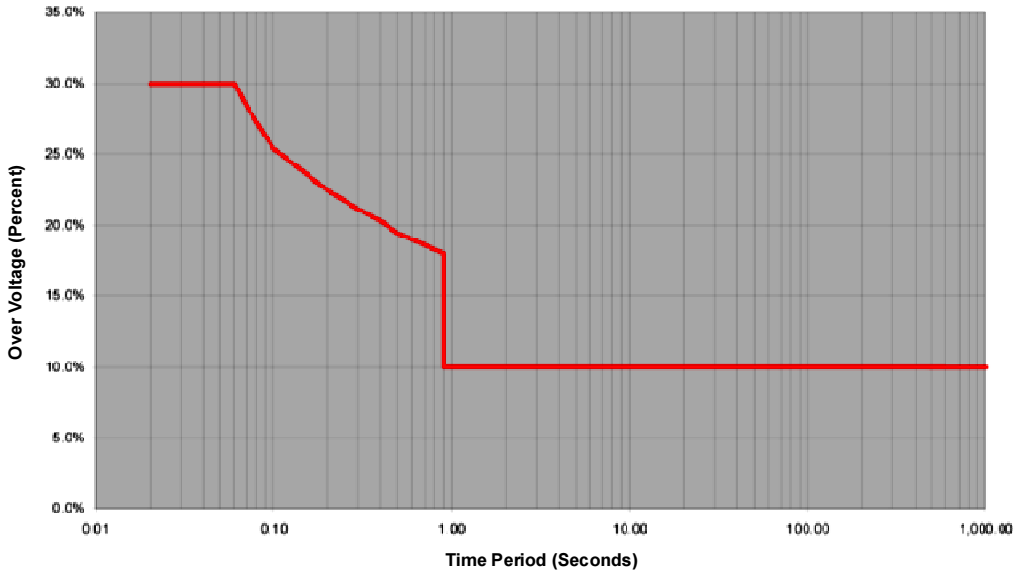

Figure 3-3 Temporary over voltages set by AEMO [86].

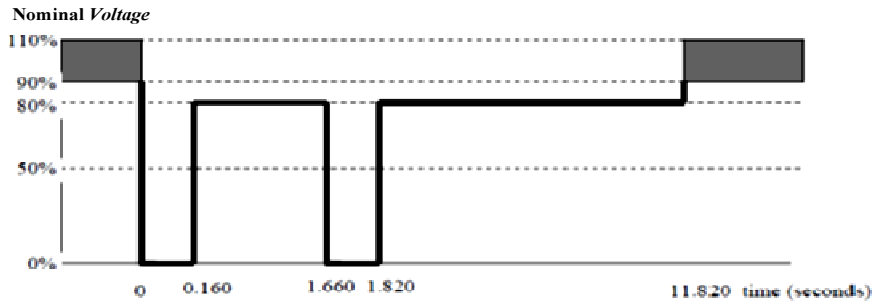

Figure 3-4 Off nominal voltage operation capability requirement for generating units set by WP [87].

Recent WTGs normally consists of synchronous and asynchronous machine. Some countries specify FRT capability requirements for the aforementioned machines due to their natural behavior such as reactive power consumption due to network fault. For instance, German (Tennet) [90] applies two profiles, called limits 1 and 2 (Figure 3-5). In the case that the generating plant cannot fulfil the requirements of limit line 2, by negotiation it is allowed to operate under limit line 1 as long as the minimum reactive current support is guaranteed and the resynchronization time is reduced. Both AEMO and WP demand a continuous uninterrupted operation during and after fault clearance unless specified in the documents [86, 87]. A summary of active power provision is presented in Table 3-2 indicating that AEMO demands a faster active power restoration than WP following a disturbance.

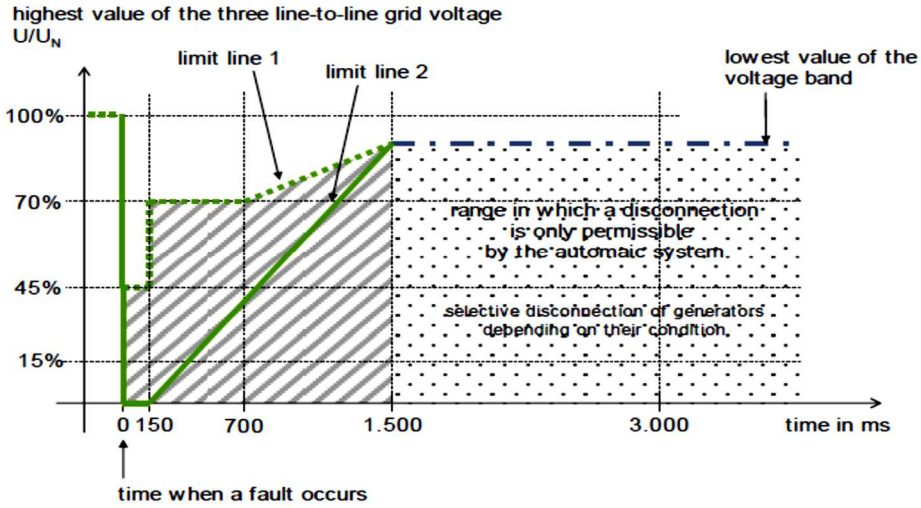

Figure 3-5 FRT curve for grid connected asynchronous generators in Germany [90].

Table 3-2 Comparison of active power provision for AEMO and WP.

	AEMO	WP
Voltage support during disturbance	Required	Required
Active power provision during fault	Generator and its units must remain in continuous uninterrupted operation during a disturbance unless specified in [86]	Generator remains in continuous uninterrupted operation during and following a sudden reduction in required active power considering that the reduction is less than 30% of generator's nameplate rating and the

		required active power remains above the generating unit's registered minimum active power capability.
Restoration of active power after fault clearance	Providing active power of at least 95% of the level existing just prior to the fault, starting from 100 milliseconds after disconnection of the faulted element.	Active power output returns to the generator's pre-fault electric power output within 200 milliseconds after the voltage has returned to about 80-110% of nominal voltage.

3.2.2 Active power and frequency control

Active power and frequency control can be defined as the ability of wind farms to regulate their output power to certain limit through disconnection of wind turbines or simply by activating the pitch control. The aim of active power curtailment is to balance the supply and demand in the electricity network by keeping the system frequency within its safety limit. Both AEMO and WP set the active power control for wind turbines. Table 3-2 shows the comparison of their active power provision assuming wind farms are dispatchable [86, 87] while Table 3-3 presents their active power requirements in comparison to other countries [10, 84-87, 89, 93]. Table 3-3 also provides information regarding the active power control requirements for European Network [82].

Table 3-3 Summary of active power control requirements for selected countries.

Grid Code	Delta Control	Ramp Rate	T_{Start} [s]	$T_{implement}$ [s]
Australia (AEMO)	Yes	Set by TSO, at least 3MW/min or 3%	ASAP	300
Australia (WP)	Yes	Set by TSO, not less than 5%/min	-	-
Ireland (EirGrid)	Yes	Set by TSO, 1-100%/min	ASAP	180
Denmark (Energinet)	Yes	Set by TSO, 10-100%/min	2	30
Spain (REE)	Yes	-	-	-
Germany (Tennet)	-	10%/min	-	-
Canada (Hyrdo Quebec)	-	-	-	-
Europe (ENTSO-E)	-	Set by relevant TSO	ASAP	-

3.2.3 Frequency control

It is compulsory for wind farms to stay in operation when voltage and/or frequency excursion occur either within or beyond the normal operating limits. However, beyond the normal operating condition, time limit is commonly applied and in some cases result in reduced output power production. Frequency control stability and control of the system is very much affected by the rotating masses of synchronous machines [11]. Speed regulation through governor actions controls frequency while the inertia of the synchronous machines is responsible to limit frequency change during fault conditions. In the modern WTGs such as DFIGs and FCWGs, power electronics decouple rotational masses from grid frequency. Failures in power converter of the machines can significantly deteriorate the whole regulation capability of the system.

Due to its significance, most TSOs including WP and AEMO set frequency control as part of the grid requirements. In some grid codes, frequency control does not only state the range of frequencies at which WTGs must stay connected but also the duration that they remain connected, namely the rate of change of frequency (ROCOF) limits. In addition, TSOs within the same control area as in the European Network [82] are required to coordinate the ROCOF setting in order to ensure the whole network stability. Table 3-4 shows the variation of frequency range and ROCOF for selected grid codes [10, 84-87, 89].

Table 3-4 Frequency and ROCOF of selected grid codes.

Country (TSO)	**Frequency [Hz]**		**ROCOF [Hz/s]**
	Min	**max**	
Australia (AEMO)	47.5	52.5	± 4, for more than 0.25s
Australia (WP)	47.5	52.5	up to 4
Canada (Hydro Quebec)	55.5	61.7	-
Denmark (Energinet)	47	52	± 2.5
Germany (Tennet)	47.5	51.5	-
Ireland (EirGrid)	47	52	± 0.5
Spain (REE)	47.5	51.5	± 2
UK (NGET)	47	52	-

Focusing on Australian grid, the base frequency is 50 Hz and Figure 3-6 shows frequency operation capability set by WP. WP [87] allows the maximum of 52.5 Hz for 6 seconds and minimum frequency of 47.5 Hz for 10 seconds and beyond those ranges. In addition, WTGs are allowed to be tripped off from the network in order to avoid further cascading failures.

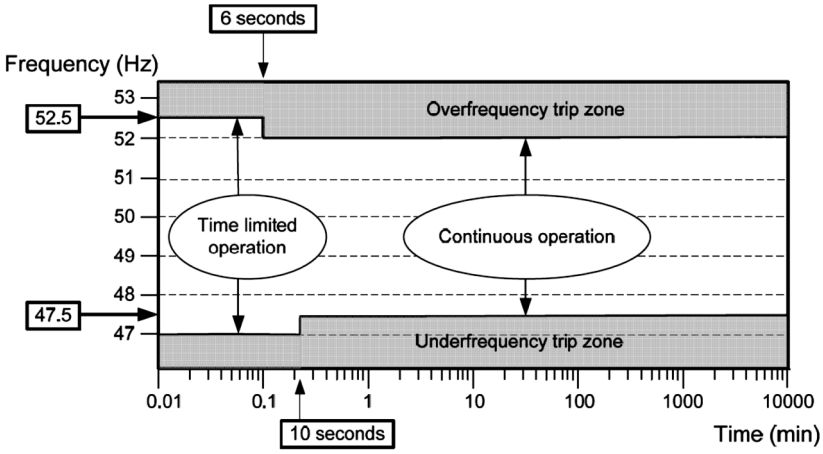

Figure 3-6 Off nominal frequency operation capability requirement for generating in Western Power network [87].

3.2.4 Reactive power and voltage control

Reactive power control is related to the voltage control and the recent grid codes require the wind farms to inject certain amount of reactive power in response to the voltage drop. Most grid codes also specify reactive power ranges for wind turbines as different type of wind turbines will have different reactive power capability. Specification of reactive power capability among grid codes are varied with respect to the considered point at the network, voltage range of the aforementioned point, and the mandatory reactive power capability.

In Australian grid codes, AEMO [86] states that in the case of fault, wind farm is required to provide 4% of the reactive current component (I_q) support for every 1% reduction in the point of common coupling (PCC) voltage, V_{PCC}; while WP demands the wind farms to either have reactive current compensation settable for droop or install remote point voltage control [87]. Similarly, ENTSO-E demands the relevant TSO in the European network to automatically provide reactive power support at the

connection point. ENTSO-E sets the general reactive power provision requirements in terms of V-Q/P_{max} profile. It is the responsibility of the relevant TSO to work with the relevant network operator in order to define this set of requirements [82].

For example, in [89], Danish grid codes set the requirement of wind farm connecting to the grid. As can be seen from Figure 3-7, the working condition of WPP is divided into three areas. Area A (V_{PCC} > 0.9 p.u.) is the condition that wind farm must remain connected to the grid while maintaining its normal power production. Area B (0.2 p.u. ≤ V_{PCC} ≤ 0.9 p.u.) is condition that the requires the wind farm to provide reactive power support while also maintaining its connection to the network. Within this area, a 2% reactive power support is required to respond a 1% voltage drop at the PCC. Area C (V_{PCC} < 0.2 p.u.) is the condition where wind farm is pertmitted to be disengaged from the grid.

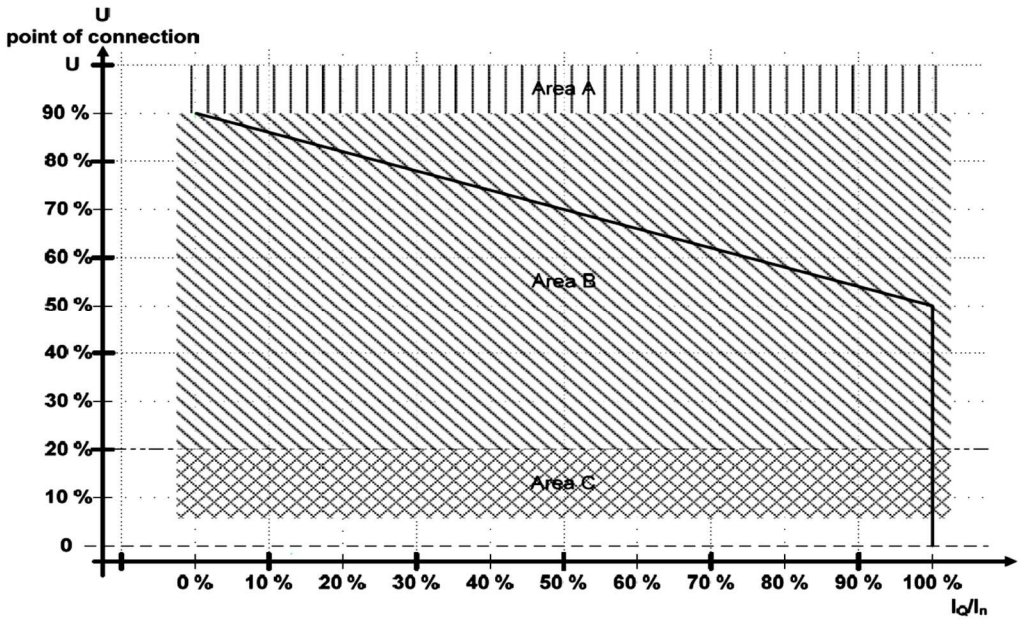

Figure 3-7 Requirement for injecting reactive current component, I_q, during voltage collapse for Danish grid codes [89].

Similar to Danish, German grid code states that the voltage control must provide 2% of reactive current component on the low side of the transformer to compensate for each 1% of voltage drop at PCC [90]. Figure 3-8 illustrates this voltage control in

detail. Summary of reactive power requirement for selected countries is presented in the Table 3-5 [10, 84-87, 89] .

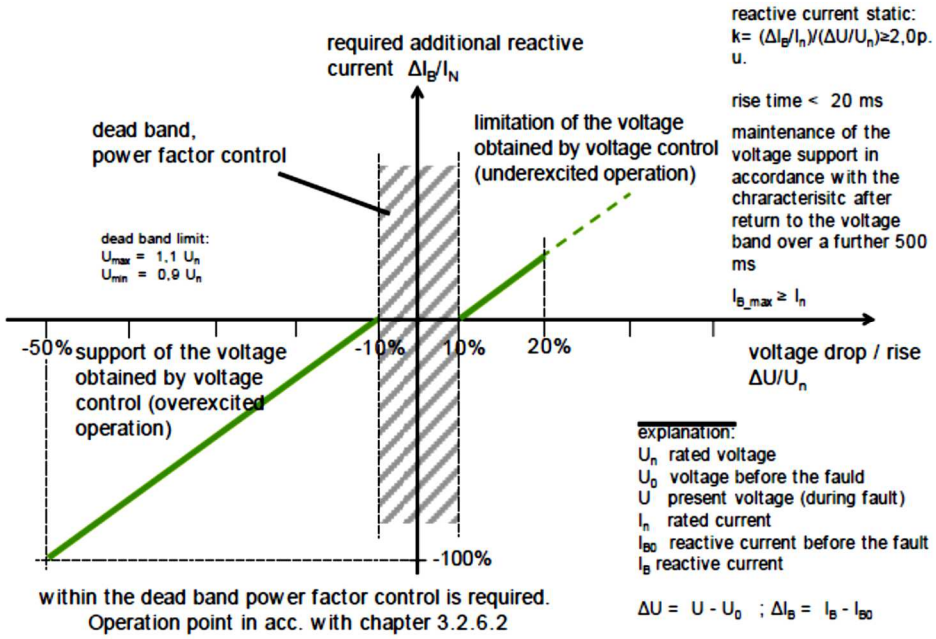

Figure 3-8 Characteristic of voltage control for German grid code [90].

Table 3-5 Reactive power requirements of selected grid codes.

Country (TSO)	Considered point	Q range [p.u.]	Cos φ
Australia (AEMO)	Connection point	0.395 (automatic)	0.9 – 0.95
Australia (WP)	Generator terminal	0.484	0.8 – 0.9[a] 0.95 – 0.95[b]
Canada (HydroQuebec)	HV side of transformer near wind farm	-0.33 – 0.33	0.95 – 0.95
Denmark (Energinet)	Power plant operating point	-0.33 – 0.33	0.95 – 0.95
Germany (Tennet)	Connection point	-	0.95 – 0.925
Ireland (EirGrid)	Connection point	-0.33 – 0.33	0.95 – 0.95
Spain (REE)	-	-0.3 – 0.3	-
UK (NGET)	Grid entry point	-	0.95 – 0.95

[a]Applied to synchronous generators

[b]Applied to induction generators

3.3 GRID CODES ISSUES FOR WIND INTEGRATION

3.3.1 Harmonisation of grid requirements

In recent years, the increasing number of wind turbines within electricity network has created a number of issues including system stability resulting is development of more stringent grid codes and application of power electronics in the existing wind turbines with FSIGs resulting in more sophisticated networks. Moreover, different TSOs have applied different grid requirements giving impact to the gross inefficiency for wind turbine manufacturers and developers. The European network connecting five synchronous areas (i.e. Continental Europe, Nordic, Great Britain, Ireland and Baltic States) is the perfect example of complex interconnected networks. In response to these issues, European Wind Energy Association (EWEA) under grid code working group [94] proposed the following two step approaches:

Step 1- a structural harmonization exercise aiming to the establishment of standard definitions, parameters, units, figures and structure among different grid codes.

Step 2- a technical harmonization exercise aiming to the adaptation of existing grid technical requirements into a new grid code template.

Therefore, in the latest updated European Network Codes, ENTSO-E [82] states that it is vital to establish mutual agreement on requirements for power generating modules in order to maintain system security within interconnected power networks. ENTSO-E acknowledges these requirements under “the cross-border network issues and market integration issues” in order to accurately manage the operation of the internal electricity market and the cross border trade as well to achieve profitable trade through harmonization of all requirements.

Issues on harmonization in Australia are more focused on the need of the dynamic model as well as certification of the wind farms. AEMO [11] stress out the necessity of providing a standard dynamic models in addressing conflicting perspectives between network operators and WTG manufacturers. Network operators requires a standard dynamic model that supports stability study without too much details such

may reduce the ability of running the simulation for extensive networks. On the other hand, the main concerns of WTG manufacturers are on the high accuracy of plant dynamic model to maintain the expected performance and somehow are more focused on transient stability study. By doing this, manufactures are also maintaining their intellectual property rights. As the results, they end up with a very complex model that is unsuitable for large scale system simulations as demanded by network operators.

In order to minimize issues regarding dynamic model of the WTGs, Eirgrid [95] recommended to establish active participation among WTG manufacturers, model developers, and system operators in a transparent and agreed manner since the beginning of the project. Moreover, the WECC Wind Generation Modeling Task Force (now the Renewable Energy Modeling Task Force) of the WECC Modeling and Validation Working Group [96, 97] proposed four generic WTG models, particularly used for positive sequence stability analysis within the power system. The latest versions of two commercial software packages, i.e. GE PSLF^{TM} and Siemens PTI PSS^{TM}E have already implemented the proposed models [97].

3.3.2 Grid code compliance of WTG technologies

Another issue to be addressed is regarding different grid and frequency requirements between the country where the turbine is manufactured and the country where it will be installed [98]. GCC is the certificate that validates the wind turbine compliance with all applicable requirements [98]. GCC consists of two step certifications; (1) a type certificate that verifies the type of WTG in compliance with one or more grid codes according to the relevant procedure and (2) a project certificate that is issued for each wind farm and constructed based on site specific data as well as the type certificate [99, 100].

GCC is conducted by an independent and qualified expert and the certification report normally consists of documents from manufacturer, the measurement report and simulation results [98]. Alliance Power and Data (APD) is an example of consulting companies offering generation compliance testing services [101]. In addition to that,

there is also DNV GL [100], providing independent accredited certification services for the renewable energy industry as well as regularly updating the status of grid codes internationally.

Most grid codes such as in Australia [86, 87] and European Continents [82] require that the new or replacement of power generating unit in the network must pass the test, confirmed with equipment certificate. Certification requirements will be different from country to country as well as from TSO to TSO. Table 3-6 presents comparison of the required testing during commissioning of the WTGs for eastern and western parts of Australia.

Table 3-6 Comparison of GCC certificate in Australia.

	TSOs	
	AEMO	**Western Power (WP)**
Referenced Document	National Electricity Rules Version 63 [86]	Technical Rules for the South West Interconnected Network [87]
Certification for each generator (GCC)	Required	Required
Technical requirements prior to commercial operation	Any new or replacement equipment complies with relevant Australian Standards, the Rules and any relevant connection agreement prior to or within an agreed time after being connected to a transmission network or distribution network, and the relevant Network Service Provider is entitled to witness such inspections and tests.	A generator must comply with clause 3.3 or 3.6 in [87] and the relevant connection agreement prior to commencing commercial operation. Table A11.1 of Attachment 11 in [87] summaries the detail of required tests for synchronous generating units while requirements for non-synchronous generation must be specified by the Network Service Provider.

In response to certification requirements from TSOs, wind turbine and power converter manufacturers keep improving their products and services in compliance with the preferred standards by building their own testing facilities. For example, Vestas, a wind turbine manufacturer with an accumulated market share of almost 50% in Australia, has the capacity to perform up to 900 hours of testing a day distributed on 50 test rigs in their three test centres [102].

Most of wind farms are located far away from their loads such that dynamic reactive compensation is required due to interconnection in many locations. The stringent requirements set by TSOs to provide reactive power support to the grid are sometimes beyond to the capability of the wind turbines. Therefore, there is a need to install ancillary reactive support equipment and control such as the technology applied to Collgar wind farms connecting into Western Power network. AMSC [103] has installed one of its products called D-VAR STATCOM system at each of the main 33kV buses at the site along with multiple mechanically switched capacitor banks controlled by its master controller that allows communication with the Vestas wind farms to automatically provide reactive power solution in need.

3.4 CONCLUSION

Technical requirements of connecting wind turbine in Australia are discussed in details including a comparison with selected international grid codes. Both AEMO and WP enforce rigorous technical requirements for grid integration of WTGs. Differences in international standards has raises issues on harmonization of grid codes and GCC certificate. To comply with the grid codes, the triple parties (TSOs, manufactures and operators) are obliged to cooperate during the commissioning of the projects. The case of Collgar wind farms provides an example of practiced solutions from perspectives of wind related manufacturers in complying with the Western Power grid requirements.

Finally, maintaining sustainable environment needs participation of stakeholders. Increasing trend towards utilization of wind power is very much affected by government policies. In order to reach the Australian 2020 renewable energy target, more projects on wind power followed by incentive schemes are required to motivate and encourage wind manufacturers and developers to build further WPPs that comply with the stringent grid codes imposed by TSOs.

Chapter 4. Transient Response of FCWGs under Network Faults

4.1 INTRODUCTIONS

Most TSOs set more stringent codes regarding wind turbine participation into the existing grid. A comprehensive review on trends in FCWG control strategies in complying with the grid codes has been presented in Chapter 2. From the aforementioned chapter, it is found that it is necessary to modify controller at the power converters. Prior to control modification, it is important to gain good understanding of the transient behavior of the implemented FCWG system.

The main objective of this chapter is to provide an in depth investigation on the transient responses of FCWGs under reactive power control, wind gust as well as balanced and unbalanced voltage sags. Since the machine is fully controlled over the generator and the grid side converter, the impacts of voltage sags on *d-q* control conditions of the converters will also be taken into account. Section 4.2 gives detail explanation on modelling and control system of FCWG, including its mechanical and electrical parts. Then, in Section 4.3, simulation results will be shown and discussed in order to gain a better understanding of transient response of FCWG system. Finally, Section 4.4 concludes the entire content of the chapter.

4.2 MODELLING AND CONTROL OF FCWGS

This section briefly presents an overview of the modelling and control of FCWGs. For the purpose of this research, the FCWG model with volt/var control at GSC based on [104, 105] is implemented. This FCWG system uses salient pole synchronous generator with the gear box which is decoupled from the grid through GSC. The machine is connected to a diode rectifier and DC-DC boost converter,

while the GSC utilizes a self-commutate PWM converter. The control system for pitch control and power converters is based on [104]. A brief explanation of each part will be presented in the following sections. Figure 4-1 illustrates the schematic configuration of applied FCWG system.

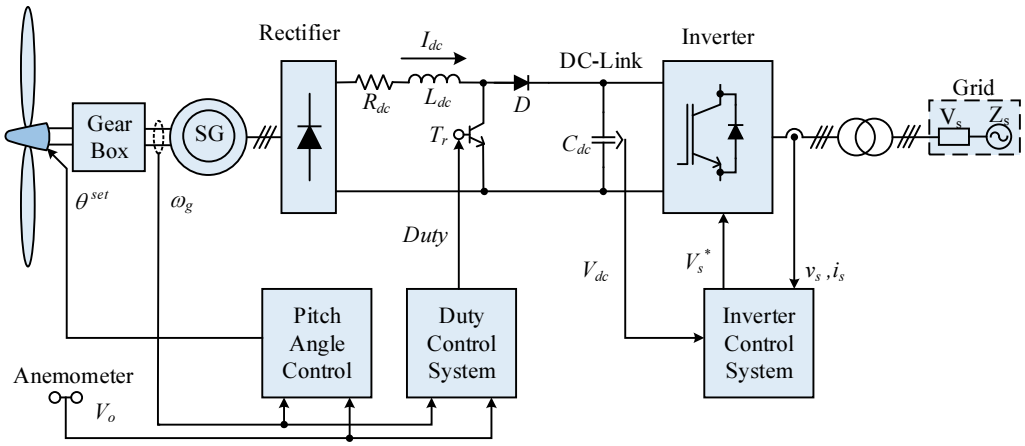

Figure 4-1 Schematic diagram of full scale converter based on wind turbine.

4.2.1 Drive train, aerodynamics and pitch angle control

Similar to other wind turbine concepts, wind power is captured by wind turbine through the blades and then it is converted into mechanical power. The aerodynamic force on turbine needs to be controlled in order to protect the turbine during the wind gust. There are common methods to control turbine aerodynamics, i.e. stall control (passive control), pitch control (active control) and active stall control [6, 17]. During the higher wind speed, either active stall or pitch control could smoothly limit the power produced by rotating blades, while the stall control show a small overshoot and a lower power output. In [36], the simplified aerodynamic model confirms the effect of changes on speed and pitch angle to the aerodynamic power and typically drawn from a two dimensional aerodynamic torque coefficient C_q table. Here, a PI controller with anti-wind-up conceives the pitch angle control, where a servomechanism model is applied to limit the pitch angle and its rate of change.

A low speed high torque mechanical power is commonly converted into electrical power by means of a drive train, consisting of a gearbox and a generator with standard speed. However, for multi-pole generator such as PMSG, it is not necessary

to use a gearbox [6]. A gearbox is particularly placed between low speed rotor shaft and high speed generator shaft. Because this gearbox has a function to adapt the low speed of the rotor shaft (approx. 20 – 50 rpm) to the high speed of generator shaft (mostly about 1000 – 3000 rpm) [106]. For stability analysis considering system response under very intense faults, the drive train is modelled by at least the two-mass-model. The two-mass-model drive train becomes even more crucial in modelling a multi-pole synchronous generator wind turbine [36]. Since there is no gearbox applied in the PMSG, then the gear ratio is 1 (one).

As stated in [36], the drive train system for stability analysis considering severe network disturbances must be approximated by at least a two-mass model (Figure 4-2).

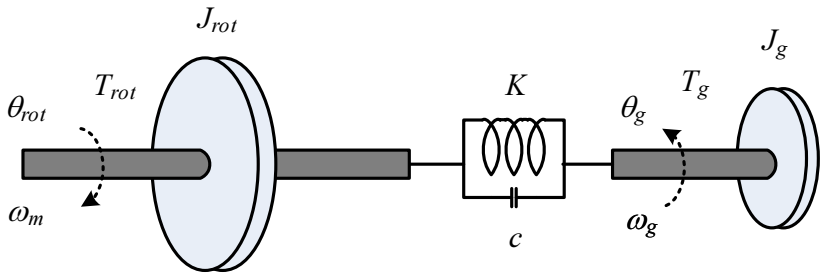

Figure 4-2 Drive train model.

In the wind turbine integration studies, it is common to define the wind turbine mechanical power output as [107]

$$P_w = \frac{1}{2}\pi\rho R^2 v_w^3 C_p(\lambda,\beta) \tag{4-1}$$

where, P_w is the extracted wind power ; ρ is the air density; R is the radius of rotor ; v_w is the wind speed; λ is the tip speed ratio; β is the blade pitch angle; and C_p is the efficiency coefficient of the turbine which is the function of λ and β. Equation (4-1) represents steady state condition such that the dynamic stall effects are not taken into account. The tip speed ratio λ is expressed as [107]:

$$\lambda = \frac{\omega_r R}{v_w} \tag{4-2}$$

where, ω_r is the turbine rotational speed.

In the fully rated converter wind generation, the speed control does not only depend on the generator, but also on the wind turbine drive power characteristics [108], so integrating the two parts is important for dynamic study of the machine. Figure 4-3 presents the pitch control system using a PI controller with anti-wind-up [36, 104]. Its function is to control the generator speed by controlling the pitch angle of the blade and its rate-of-change such that over speeding of the wind turbine can be avoided.

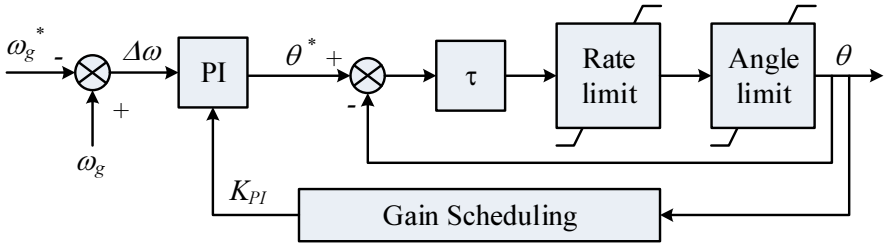

Figure 4-3 Pitch control model.

4.2.2 Synchronous generator

Figure 4-4 presents a SG model expressed in the rotor field reference frame [109]. To simplify, the set of voltage equations for modelling SG is given in Equations (4-3), (4-4), (4-5), and (4-6) [109]:

$$V_{ds} = -R_s I_{ds} - \omega_r \lambda_{qs} + p\lambda_{ds} \tag{4-3}$$

$$V_{qs} = -R_s I_{qs} + \omega_r \lambda_{ds} + \omega_r \lambda_r + p\lambda_{qs} \tag{4-4}$$

where R_s is the stator resistance, λ_r is rotor flux, ω_r is rotor speed in synchronous frame, p is number of pole, I_{ds} and I_{qs} are direct and quandrature currents respectively, while λ_{ds} and λ_{qs} are direct and quadrature stator flux linkages, defined by [109]:

$$\lambda_{ds} = -L_{ls} I_{ds} + L_{dm}(I_f - I_{ds}) \quad (4\text{-}5)$$

$$\lambda_{qs} = -(L_{ls} + L_{qm}) I_{qs} \quad (4\text{-}6).$$

In Equations (4-5) and (4-6), I_f represents the field current in the rotor winding, L_{dm} and L_{qm} are direct and quadrature components of magnetizing inductances of the synchronous generator.

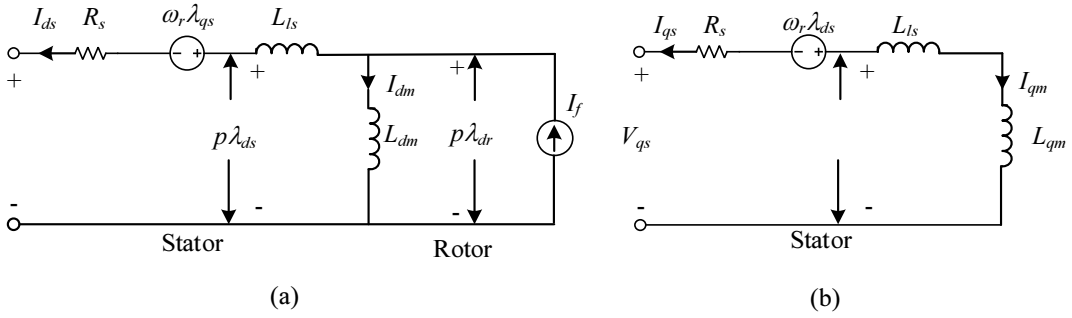

Figure 4-4 Simplified *dq*-axis model of synhcronous generator. (a) *d*-axis circuit. (b) *q*-axis circuit [109].

4.2.3 Full scale converter control

The MSC in this study is composed of diode rectifier, DC-DC boost converter and DC link capacitor [110, 111]. In FCWG, the DC-DC boost converter has two main roles [109]:

(1) Performing maximum power tracking under variable wind speed.

(2) Boosting the dc link voltage to meet suitable voltage ratings of the inverter.

The rectifier converts the AC output of the generator to dc voltage while the DC-DC boost converter controls the rectifier output current, I_{dc}, and the electric power, P_{grid}. Figure 4-5 illustrates the control block of the boost converter.

In the grid side, the PWM inverter adopting the cascaded control scheme is applied (Figure 4-6). This inverter is responsible to maintain the DC-link voltage, $V_{dc,}$ at constant value as well as the flow of reactive power, Q_{grid}, to the grid [36, 110, 111]. The var/voltage control for this study is built based on [104].

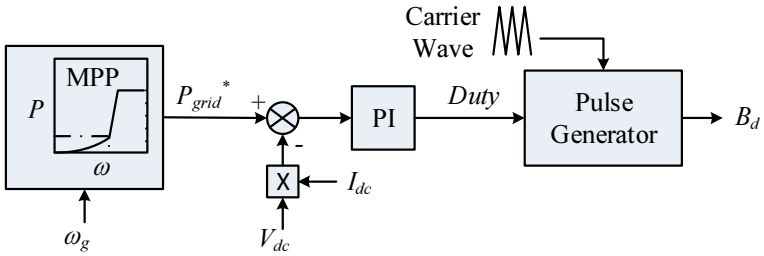

Figure 4-5 Control block diagram of boost converter.

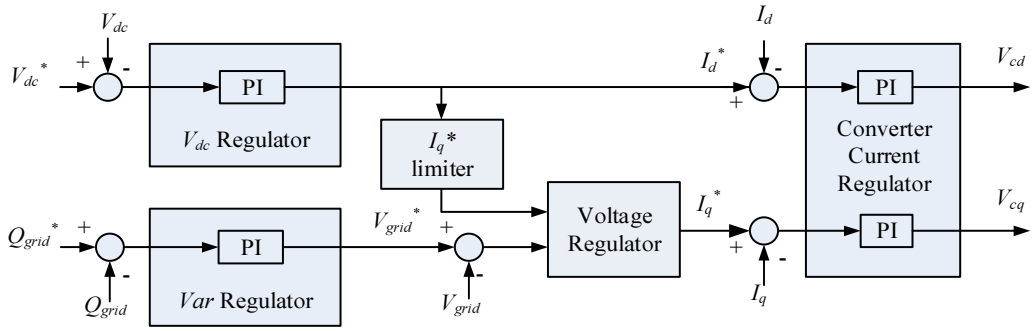

Figure 4-6 Control block diagram of GSC.

Theoretically, full converter based wind turbine can ride through any grid faults (symmetrical or unsymmetrical) as the generator is fully decoupled from the grid through the grid side inverter. Thus, reactive power exchange merely depends on the characteristic of the grid side inverter and not on the generator properties [17, 36].

4.3 SIMULATION RESULTS

The simulation analysis is conducted using MATLAB/SIMULINK. Figure 4-7 shows the voltage divider model of the simulated system, with the schematic diagram and parameters of the machine given in Figure 4-1 and the Appendix A, respectively. The operational status of simulation is presented in Table 4-1. For improving FRT capability, this system is also equipped with voltage regulator in the GSC control (see Figure 4-6).

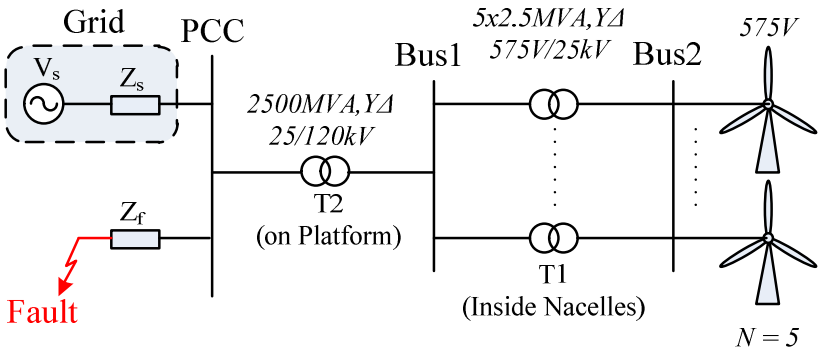

Figure 4-7 Voltage divider model (italic figures are the real parameters for the simulated system and 'N' is the total number of wind turbines).

Table 4-1 Operational status of the simulation.

Definition	Time	
A ramp change in the v_{wind}	$0 < t < 3s$, $4.5s \leq t \leq \infty$,	v_{wind} = 12 m/s; v_{wind} = 15 m/s
A step change in the I_q^*/Q_g control	$0 < t < 3s$, $3s \leq t < \infty$,	$I_q^* = 0$; $I_q^* = 0.25$ PU
3ϕ symmetrical sag at infinite bus	$0 < t < 3s$, $3 \leq t \leq 3.15s$, $3.15 < t \leq \infty$,	$V_{inf\text{-}bus} = 1.0$ PU; $V_{inf\text{-}bus} = 0.5$ PU; $V_{inf\_bus} = 1.0$ PU;
Unbalanced single-phase to ground fault (PF = 1)	$0 < t < 3s$, $3 \leq t \leq 3.2$ s, $3.2 < t \leq \infty$,	$V_a = 1.0$ PU; $V_a = 0.25$ PU; $V_a = 1.0$ PU;

4.3.1 Transient performances under wind gust

In this simulation, the mechanical input torque to the full converter based wind turbine is externally specified in order to emulate the power extracted by the wind turbine. Figure 4-8 shows the simulation results with a ramped-up wind speed from 12 to 15 m/s starting at the t = 3.0 s. As the wind speed ramps up, the rotor accelerates from about 0.98 to about 1.01 p.u. and the electric power, P_g, raises from 0.7 M p.u. This extracted power, P_g, keeps increasing and start decreasing once it reaches its maximum extraction point. In addition, output reactive power, Q_g can be maintained at approximately 0 p.u. under any given output electric power level, P_g. This indicates that the decoupled control of active and reactive powers in the

generator is functioning. In full converter wind generation system, the maximum power output of the maximum power point tracking (MPPT) is the reference power for the MSC (see Figure 4-5). The pitch control will be automatically activated to control the rotational speed when the reference power exceeds the rated power of the generator such that the output of the generator will not surpass the rated power.

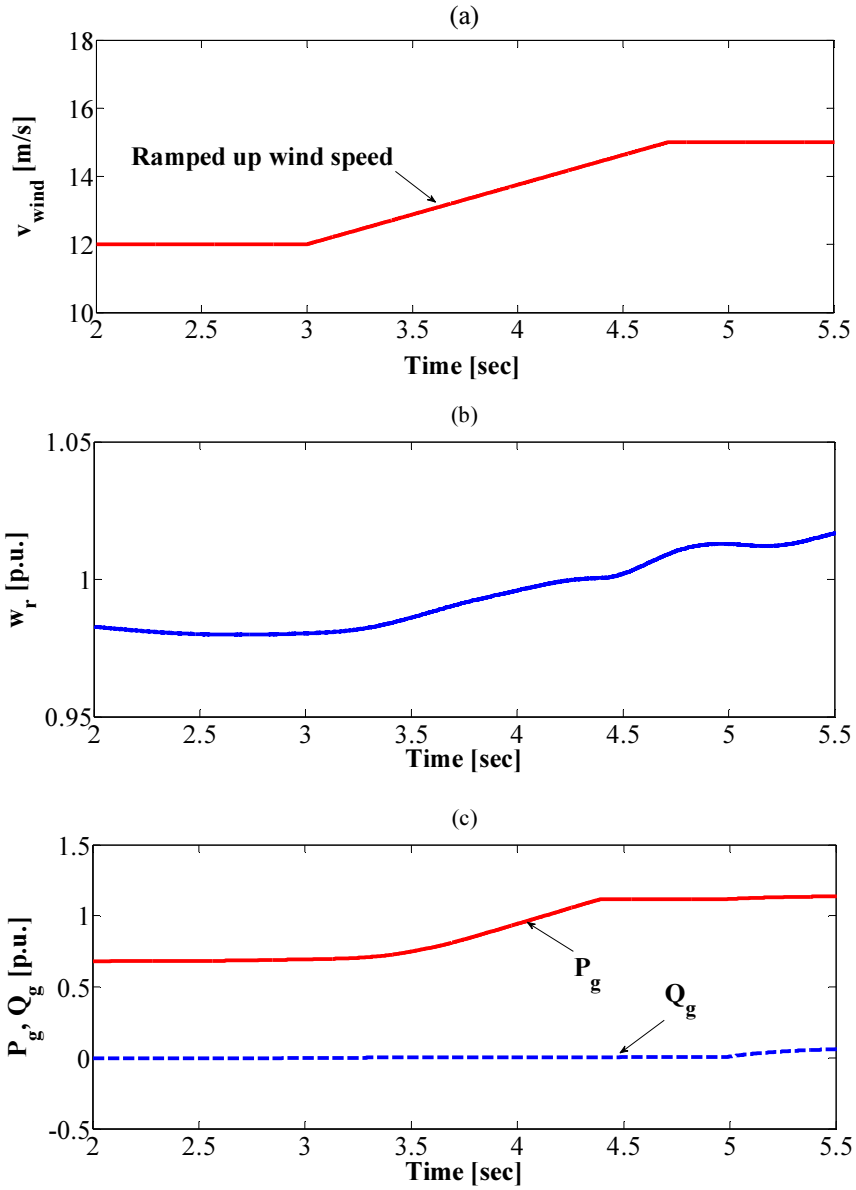

Figure 4-8 Simulation results under wind gusts. (a) Wind Speed of FCWGs. (b) Rotor speed of FCWGs. (c) Output power of FCWGs.

4.3.2 Transient performances under Q_g control

Figure 4-9 shows the detailed operation of the applied vector based PI controller subjected to a step change in the q-component of converter reference current, I^*_{qg}. When I^*_{qg} is step changed into 0.25 PU, the output reactive power, Q_g step changes accordingly. This confirms that the applied PI current controller effectively works in the Q control mode. The instantaneous current, I_{qg}, successfully keeps tracking the imposed I^*_{qg}; however, significant overshoot still occurs which is the typical transient characteristics of PI based controller [7]. Moreover, because both currents in the current regulator, I^*_{qg} and I^*_{dg}, are cross coupled, an increase in I^*_{qg} also increases the value of I^*_{dg}. This transient event also affects the DC link voltage, V_{dc}, which firstly drops to about 20 V from its nominal value of 1100 V. This voltage keeps oscillating for a few second before reaching its steady state. When the V_{dc} drops, the rotor speed, ω_r reduces due to the change in the DC link voltage. The electric power, P_g, firstly increases but then it follows the change of ω_r. This transient event has caused a voltage dip at the terminal (Bus 2), but the system can maintain the terminal voltage at about 1 p.u. without being disconnected from the grid.

4.3.3 Transient performances under network faults

Simulation results for voltage sag types A and C* are presented in Figure 4-10 and Figure 4-11, respectively. There are seven possible types of voltage sags as defined in [112-114]. The transient responses of wind turbine type 4 in riding through the fault have been evaluated by simulating type A and C* sags that refer to 3ϕ symmetrical sag in the grid and single-phase-to-ground at Bus 1 (see. Figure 4-7). Instead of applying type B sag, (i.e. single-phase to ground at PCC), type C* is chosen, as the type B unbalanced fault cannot occur at the terminal of wind farms. This is because the coupling transformer T_2 filters out the zero-sequence component in the secondary side (Bus 1 in Figure 4-7) once type B fault occurs.

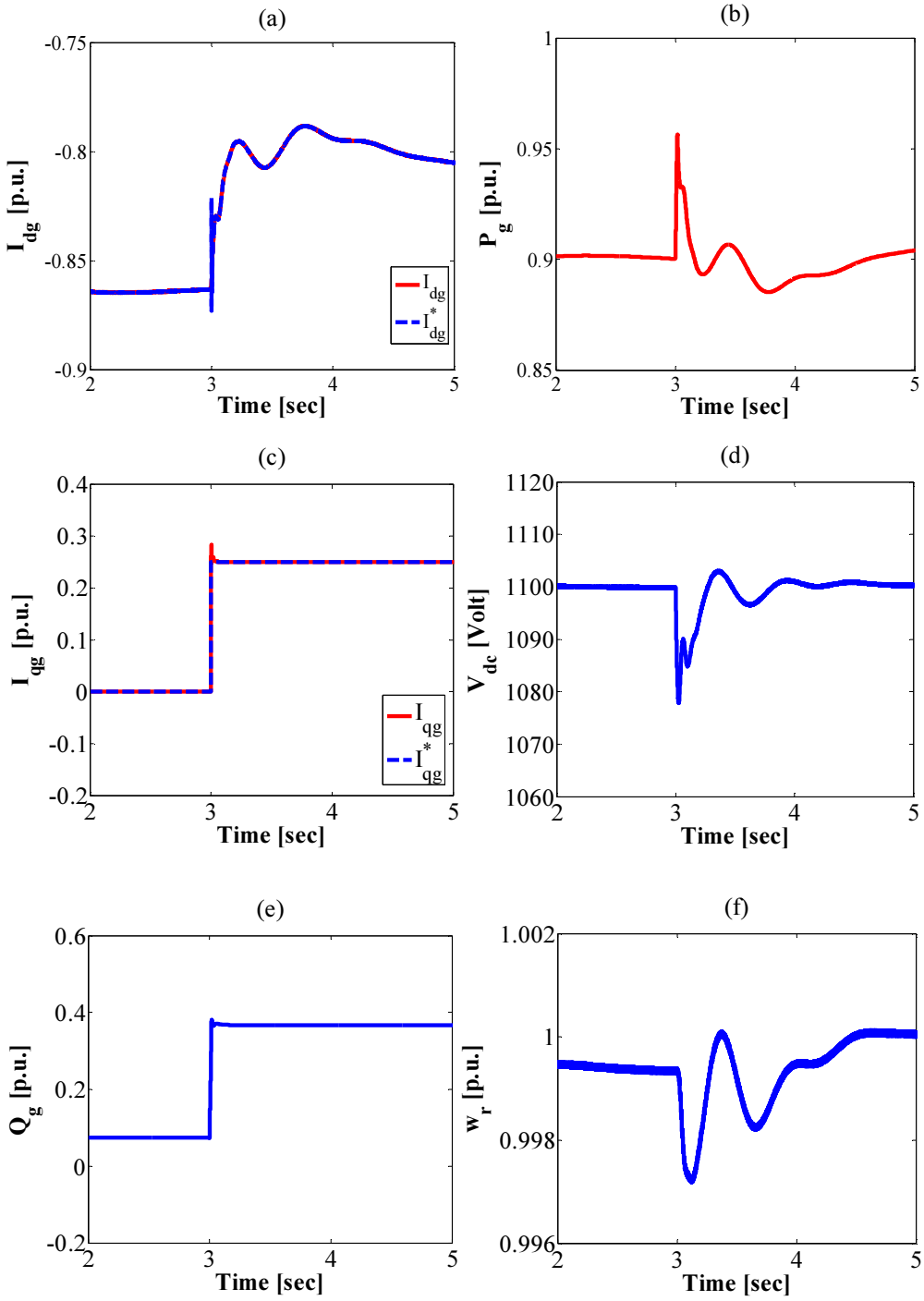

Figure 4-9 Simulation results for Q_g control. (a) Actual and reference *d*-current components of GSCs. (b) Active power output of FCWGs. (c) Actual and reference *q*-current components of GSCs. (d) DC-link voltage of FCWGs. (e) Reactive power output of FCWGs. (f) Rotational speed of FCWGs.

As can be seen in Figure 4-10, a 50% sag type A imposed in the grid has caused voltage drops in terminal of the machine. Then in Figure 4-11, passing through the YΔ transformer, the phase-to-ground fault in Bus 1 causes a voltage dip at the machine terminals. The voltage of faulted phase, V_a, remains zero due to the low impedance path between the faulted phase and the ground. Note that for both fault types A and C*, as the grid voltage drops, terminal voltage falls simultaneously. As a result, the P_g reduces from its steady state but Q_g can be maintained at 0 p.u.

During the faults, the MSC keeps delivering power normally but the GSC cannot transfer the power to the grid. As a result, the power surplus in the grid side inverter triggers the DC link capacitor to start charging causing V_{dc} to rise from its rated value (1100 V). When the DC-link voltage come close or surpass the tripping limit, the converter protective system reports abnormal operation causing the MSC to be blocked and remains on stand-by mode. On the other hand, the GSC can function as STATCOM to control the reactive power and the PCC voltage. But, the controllability of GSC is limited where its current cannot exceed its relay setting (i.e. 1.1 p.u.). This is part of the protection of the converter against the over currents and thermal over-loads. Usually, a chopper resistor is also applied in DC link to dissipate the excess power in the DC link as heat so that the FRT capability of the machine can be improved.

Notice that in Figure 4-10 and Figure 4-11, the DC link voltage is slowly discharged when the GSC starts delivering the electric power to the grid. Once the fault has cleared, the GSC keeps enabling the voltage regulator to control the reactive power injection to the grid. Thus, the grid voltage manages to quickly recover to 1.0 p.u.. The MSC is also activated right after the fault clearance so that the wind farms can continue supplying electric power to the grid. During the fault period, the overshoot in the DC link voltage, V_{dc}, depends on the superfluous power that is injected to the capacitor from the generator. Such that in this study, the simulated 3ϕ symmetrical sag has caused more severe effects to the DC link voltage as compared to the single-phase to ground fault.

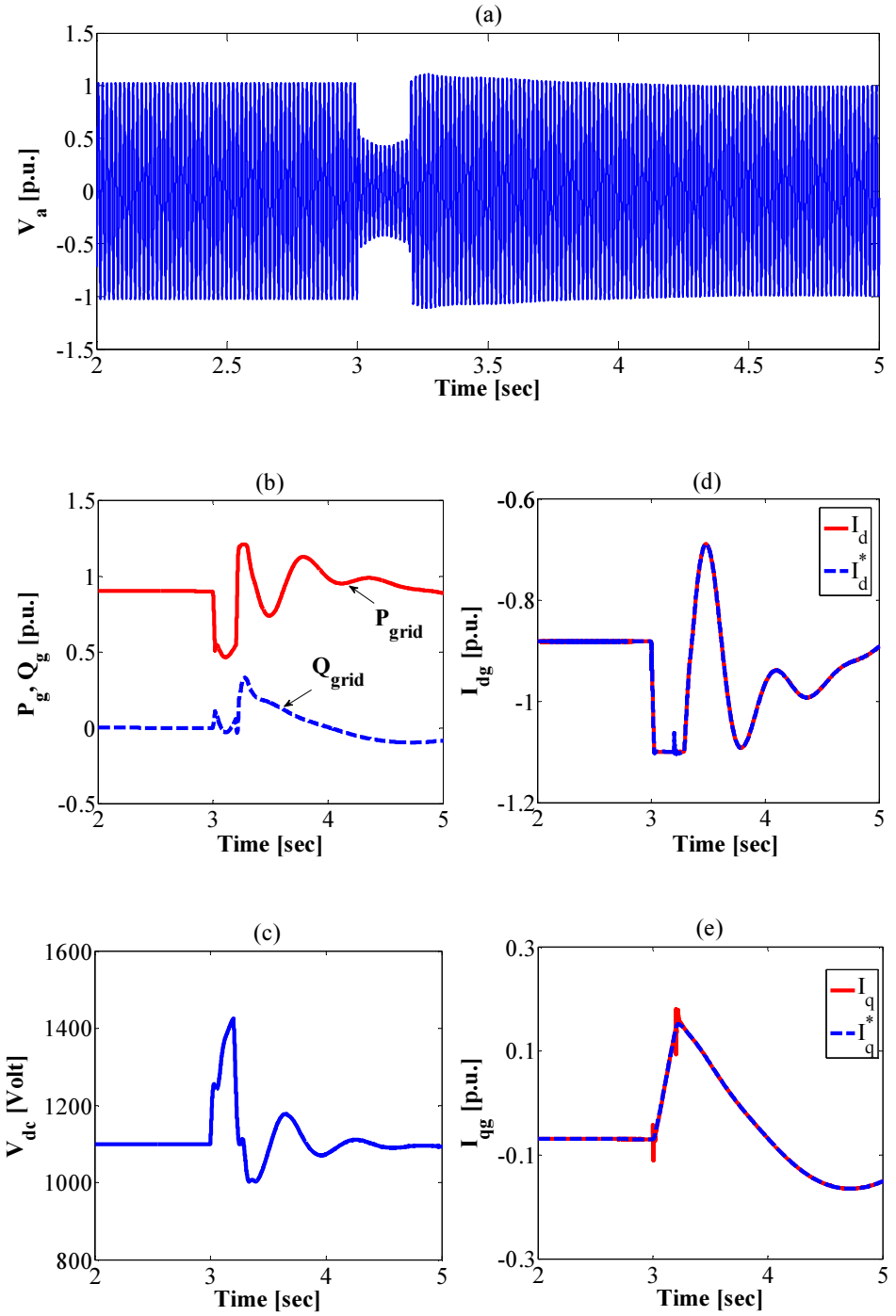

Figure 4-10 Simulation results for 3-phase-to-ground. (a) Terminal voltage (Phase A). (b) Output power of FCWGs. (c) The *d*-component of current controllers at GSC. (d) The DC-link voltage of FCWGs. (e) The *q*-component of current controllers at GSC.

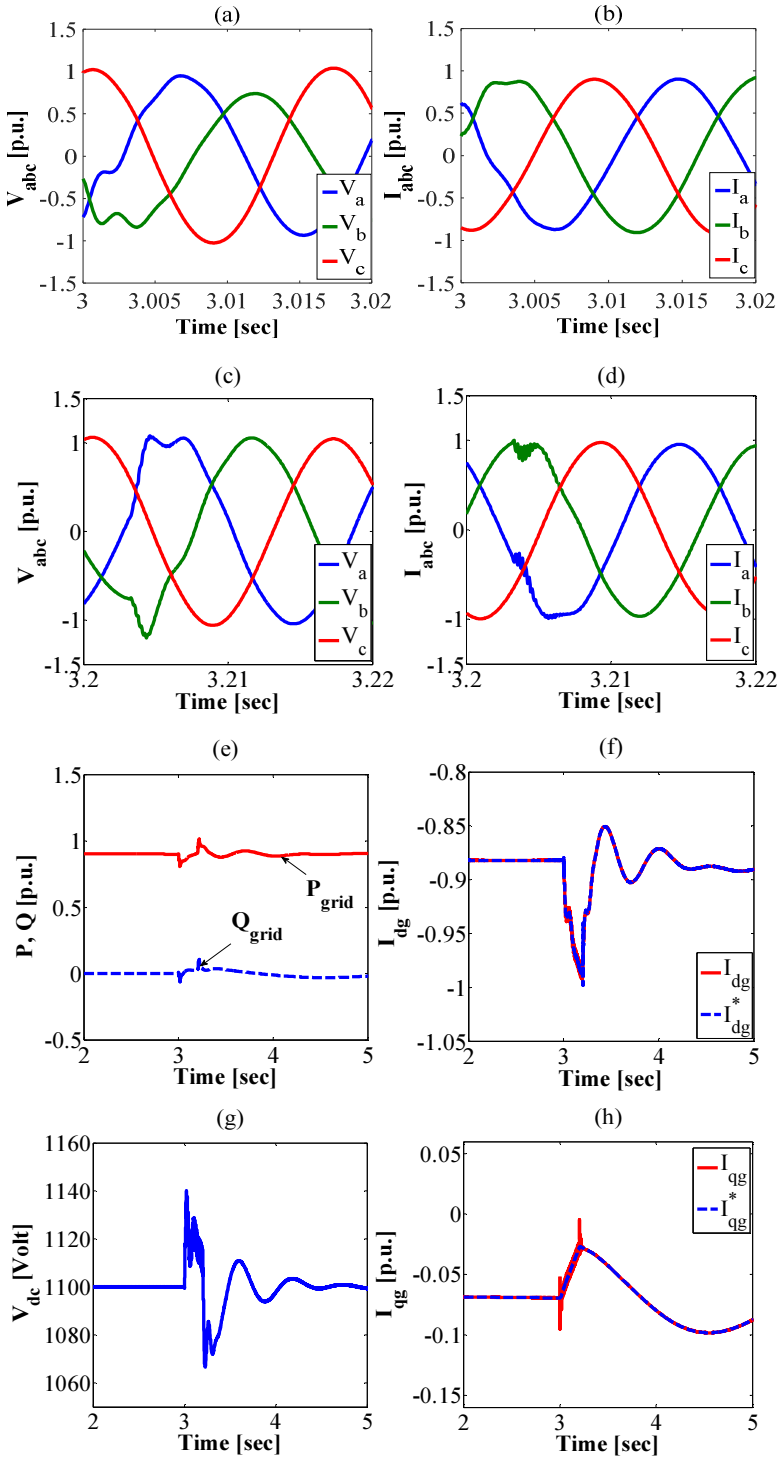

Figure 4-11 Simulation results for single phase to ground fault. (a-b) Terminal voltage and current (zoomed around fault instant). (c-d) Terminal voltage and current (zoomed around voltage recovery instant). (e) Output power. (f) *d*-components of converter currents. (g) DC-link voltage. (h) *q*-components of converter currents.

Based on simulation results, it is clear that the simulated full converter based wind turbine is able to ride through the fault and satisfy the WECC grid codes [92]. However, for both applied faults, large overshoots occurs in the PI-based inner controller when the instantaneous currents, I_{dq}, try to follow the imposed reference currents. If these overshoots are too large, then it can trip out the current protection of the system and might lead to the cascading failures, which is avoided in the operational of modern power system. Application of other control strategies in current regulator as suggested in [115] might improve the performance of the controller.

4.4 CONCLUSIONS

A thorough study on transient behaviour of FCWGs is reported in this chapter. Detailed analysis and representation of the machine is presented and simulations are performed under various voltage sag conditions. Theoretical and simulated results are in complete agreement. It is demonstrated that the pitch control of the machine is automatically activated in response to the wind gusts. The effect of step changing the *q*-component currents in the GSC to the reactive power control is also presented. It is shown that the wind farms can safely ride through the faults, satisfy the WECC grid codes, and also maintain the DC link voltage around its nominal value. Lastly, this study is merely focused on full converter based wind turbine technology using diode rectifier at the MSC and the PWM inverter at the GSC. The future work may be focused on PMSG based FCWGs applying back-to-back converters.

Chapter 5. Extended PQ Capability of Grid Connected Full Converter Wind Generation System

5.1 INTRODUCTION

In FCWGs, the generator is connected to the grid via power electronics. Utilization of power converter allows full control of active and reactive power outputs so that FCWGs has the ability to not only withstand during the fault but also provide reactive power support to the grid. Simulation results on Section 4.3.2 in Chapter 4. confirms that modification of reactive power control of FCWGs can be conducted at the GSC.

In this chapter, utilization of the GSC will be investigated in order to provide extended PQ capability of FCWGs. The GSC control will be assessed in order to temporarily increase maximum converter current during the fault. It has been shown in Chapter 3. that Australia applies the most stringent grid codes, both for western and eastern electricity market. AEMO has set certain reactive current support scheme. Therefore, 4 (four) possible control schemes for extending reactive power support of FCWGs will be investigated considering Australian grid codes (AEMO). This will be beneficial for both market operator and wind farms owner in designing proper control strategies such that the machines will not exceeding their current limit while meeting the network requirements.

Organization of this chapter will be as follow. Introduction of the chapter is provided in Section 5.1. Then, Section 5.2 discusses maximum current capacity of power converters. This includes the basic properties in designing the proposed control strategies to meet the Australian grid codes. Section 5.3 provides an in depth analysis on the proposed extended PQ control strategies for FCWGs, followed by simulation results on Section 5.4. Finally, Section 5.5 gives a brief remark of this chapter.

5.2 MAXIMUM CURRENT CAPACITY OF POWER CONVERTERS

Impacts on utilization of power converter by extending its PQ control have been shown in [3, 116, 117]. However, the design on reactive power prioritization over active power has not been explored yet. In addition to that, FCWGs has different control mechanism as compared to DFIGs which has been explained in [116]. This chapter is an expansion of previous work conducted in [117].

In Chapter 3. , it has been discussed that AEMO [86] demands the wind farms (WFs) to be capable of operation in the range from a lagging power factor of 0.9 to a leading power factor of 0.95. Moreover, the automatic access standard in AEMO also requires the generating units to operate within the range stated in Table 5-1.

Table 5-1 Voltage and frequency range in Australian grid codes.

Voltage		Frequency	
$\|V_{g,min}\|$	$\|V_{g,max}\|$	f_{min}	f_{max}
0.9 p.u.	1.1 p.u.	47.7 Hz	52.5 Hz

The aforementioned requirements must be put into consideration in determining maximum current capacity, I_{max}, of the GSC. It is important to make sure that active and reactive power requirements can be achieved within design range of I_{max}, including at the most critical operating conditions without exceeding the thermal limits of the GSC.

By omitting the scaling factors of Clarke's Transformation, the active and reactive powers in the synchronous frame can be defined as [109, 118]:

$$P_g = |V_g| I_{dg} \tag{5-1}$$

$$Q_g = |V_g| I_{qg} \tag{5-2}$$

where $|V_g|$ is the magnitude of grid voltage while I_{dg} and I_{qg} are the quadrature components of the GSC in the grid voltage-oriented frame. The current magnitude of GSC can be defined as:

$$|I| = \sqrt{I_{dg}^2 + I_{qg}^2} \tag{5-3}$$

By substituting equations ((5-1) and ((5-2) into ((5-3), then:

$$|I| = \sqrt{\left(\frac{P}{|V_g|}\right)^2 + \left(\frac{Q}{|V_g|}\right)^2} \tag{5-4}$$

In order the GSC to operate at its maximum current limit, the FCWGs are assumed to deliver rated values of active and reactive power while grid voltage at its minimum value. Since Australian grid codes requires rated capacitive/inductive reactive power of 0.395 [86], then Q_g = 0.395 p.u. while P_g = 1.0 p.u., and $|V_g|$ = 0.9 p.u. The total I_{max} achieved after substituting the aforementioned values into ((5-4) is 1.195 p.u. This value means that the GSC must operate such that its maximum current is about 19.5% larger than its rated active current in order to be able to provide the required reactive power support during the fault.

5.3 MODIFIED PQ CAPABILITY OF FULL CONVERTER BASED WTGS

In [86], AEMO set 4% reactive current injection in response to 1% voltage drop at the point of connection (PCC). In order to provide the required reactive power, there are four possible design schemes can be considered to provide the required support, i.e.

1. *Control Scheme A*: the conventional wind turbine control design, i.e. there is no reactive power support to the network during fault.
2. *Control scheme B:* modified control design to comply with Australian reactive power support requirements. This means that reactive component of the GSC current vector increases by 4% for each 1% reduction in the PCC voltage for voltage drops below 0.9 pu.
3. *Control scheme C*: modified control design to comply with Australian reactive power support requirements along with temporary overloading of the GSC. In this case, the maximum converter current is allowed to be 41% larger than its default (i.e. 1 p.u.) and active power is allowed to be prioritized than reactive power.

4. *Control scheme D*: quite similar to control scheme C by temporary overloading the GSC. But in contrast to Scheme C, the reactive power is allowed to be prioritized over active power after reaching certain voltage drop.

In all proposed schemes, the FCWGs are set to work at high wind speed (i.e. v_{wind} =15 m/s) and generate rated power to represent the most onerous condition happening in the WFs [3, 67, 112]. The following sections will briefly discuss the aforementioned control schemes.

5.3.1 Control scheme A

Following AEMO prerequisites [86], the FCWGs are required to work at the capacitive power factor of 0.95 and be able to provide reactive power capability of 0.395 under steady state condition. Figure 5-1 presents conventional PQ capability curve when the FCWG doesn't have capability to inject reactive power support during fault. There are two areas to be considered in this control scheme:

a. Area A (0.9 p.u. $\leq |V_g| \leq$ 1.0 p.u.) is the normal operating area where the FCWGs are required to deliver rated active power to the grid while at the same time also maintain their reactive power capability. Previously calculated that at rated active power output ($|V_g|$ = 1.0 p.u.) in order the FCWGs to provide 0.395 p.u. reactive power capability, the I_{dg} is set at 0.773 p.u. while I_{qg} = 0.305 p.u. As the grid voltage drop to 0.9 p.u., the I_{dg} and I_{qg} increase simultaneously to maintain rated power delivered into the grid.
b. Area B (0.0 p.u. $\leq |V_g| <$ 0.9 p.u.) is the fault area where terminal voltage of the machine beyond its normal range (Area A). As the voltage less than 0.9 p.u., the I_{qg} plunges to zero while I_{dg} increases until reaching its design limit (i.e. 1 p.u.) in order to maintain the rated active power output. As a result, the active power output reduces linearly following the voltage profile while reactive power output drop to zero.

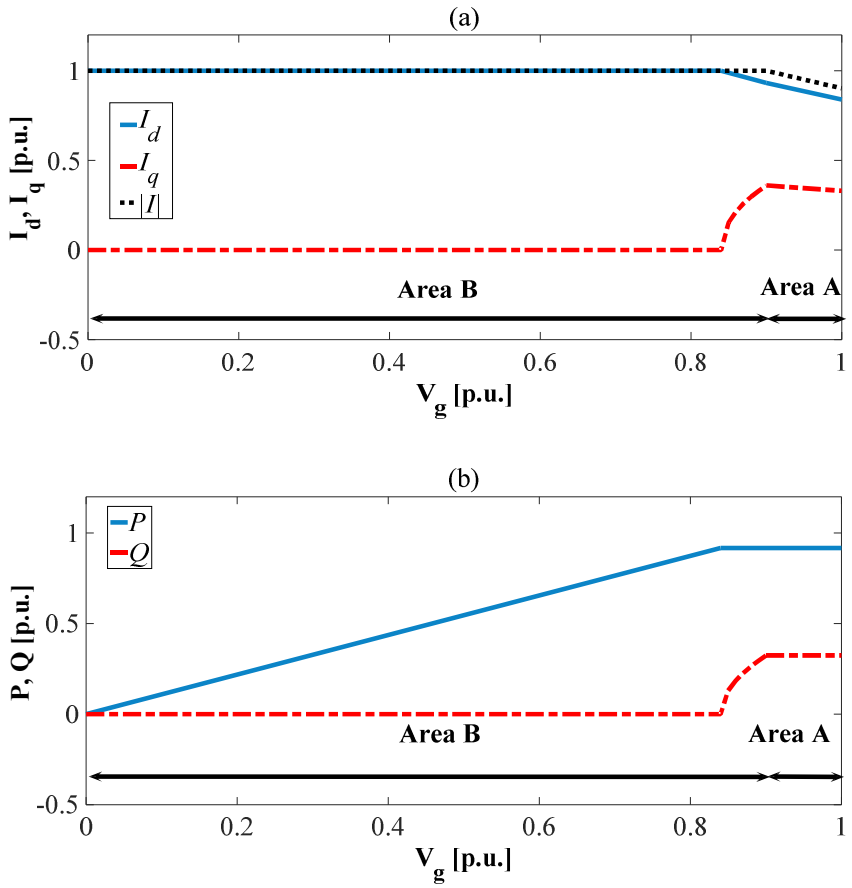

Figure 5-1 Representation of PQ curve capability for control scheme A. (a) Quadrature current components of GSC. (b) Active and reactive power output of FCWGs.

5.3.2 Control scheme B

Figure 5-2 illustrates modified control strategy when the GSC is equipped with auxiliary control such that FCWG has ability to provide reactive power injection during fault. There are three areas to be considered in this control strategy:

a. Area A (0.9 p.u. $\leq |V_g| \leq$ 1.0 p.u.) is a normal region which is similar to the conventional control scheme in Section 5.3.1.

b. Area B (0.75 p.u. $\leq |V_g| <$ 0.9 p.u.) is the area when the FCWGs are required to start injecting 4% reactive current component to compensate 1% voltage drop at the grid. As the result, the I_{qg} ramp up linearly from 0.4 p.u. at $|V_g|$ = 0.9 p.u. to 1.0 p.u at $|V_g|$ = 0.75 p.u. In contrast, I_{qg} will ramp down in order to maintain

maximum current converter, I_{max} = 1.0 p.u following Equation (5-3). This reactive power injection give impacts to partial reduction of active power delivered into the grid (P_g).

c. Area C (0.0 p.u. ≤ $|V_g|$ < 0.75 p.u.) is the area when the FCWGs maintain 4% reactive current injection all along. At $|V_g|$ = 0.75 p.u, the reactive current, I_{qg} reaches 1.0 p.u. and this condition will be maintained until grid voltage is at 0.0 p.u. On the other hand, starting from $|V_g|$ = 0.75 p.u, the I_{qg} drops to 0.0. p.u. Similarly, the active power, P_g, remains at 0.0 p.u. along the region; while reactive power, Q_g, will be reduced linearly following the voltage drop at the machine terminal.

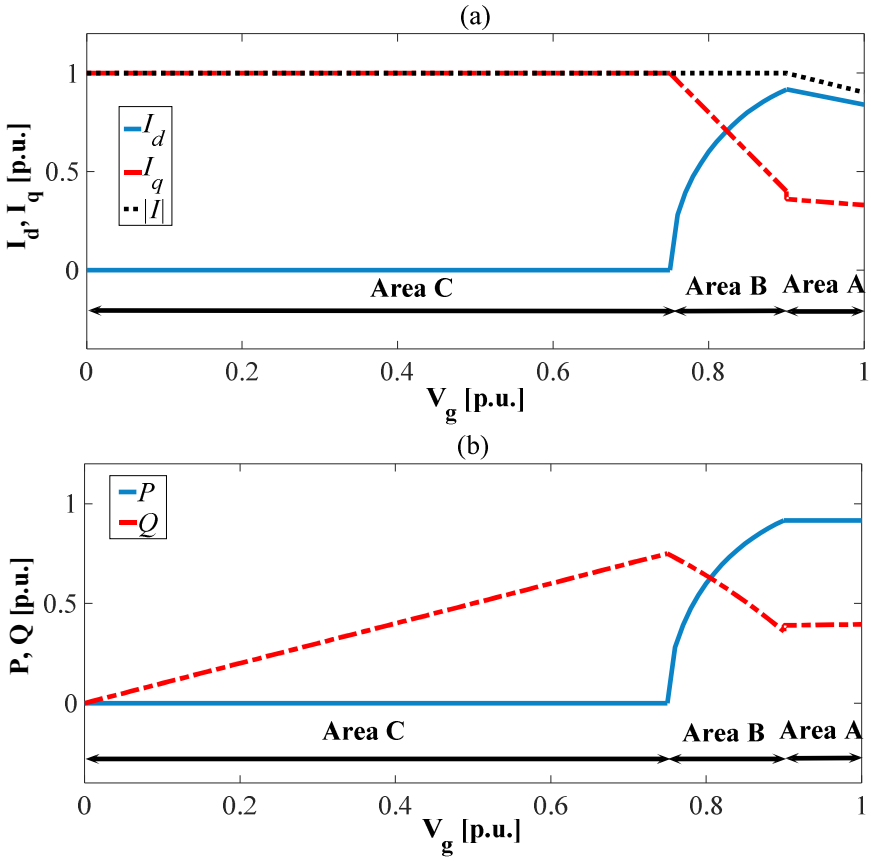

Figure 5-2 Representation of PQ curve capability for control scheme B. (a) Quadrature current components of GSC. (b) Active and reactive power output of FCWGs.

5.3.3 Control scheme C

Due to tremendous improvement in semiconductor technologies, the voltage source converters (VSCs) can be temporarily overloaded such that more active and/or reactive power delivered to the network. In recent wind turbine technology markets, Semikron Skiip Intelligent Power Module is designed to withstand up to 150% overloading within 20s [81] and the PM3100W power converter can withstand up to 1400V of V_{dc} during transient and 115% overloading of its nominal capacity for 10 seconds in every 60 second [80].

In this control scheme, the GSC is designed to temporarily exceed its maximum rated current to 1.41 p.u. such that it can deliver 1 p.u. active current component and 1 p.u. reactive current component consecutively. However, in this design, P_g is prioritized over Q_g. Figure 5-3 shows the diagram of modified scheme C with the following details.

a. Area A (0.9 p.u. $\leq |V_g| \leq$ 1.0 p.u.) is the normal operating area which is similar to the conventional scheme, explained in Section 5.3.1.
b. Area B (0.75 p.u. $\leq |V_g| <$ 0.9 p.u.) is quite similar to Scheme B in Section 5.3.2, i.e. when the FCWGs are obliged to provide reactive current injection with the slope of m = 4, following every 1% reduction of grid voltage. Power converter is allowed to temporary increased to 1.41 p.u. and by prioritizing active power than its reactive counterpart, the active current component, I_{dg}, is kept increasing until reaching 1.0 p.u. at $|V_g|$ = 0.75 p.u. By this way, the rated output active power of FCWGs can be maintained at 1 p.u.
c. Area C (0.0 p.u. $\leq |V_g| <$ 0.75 p.u.) is the area when both I_{dg} and I_{qg} are maintained at 1 p.u. as the converter current already reach its maximum, 1.41 p.u. Meanwhile, the output power, P_g and Q_g are reduced due to voltage drop at machine terminals.

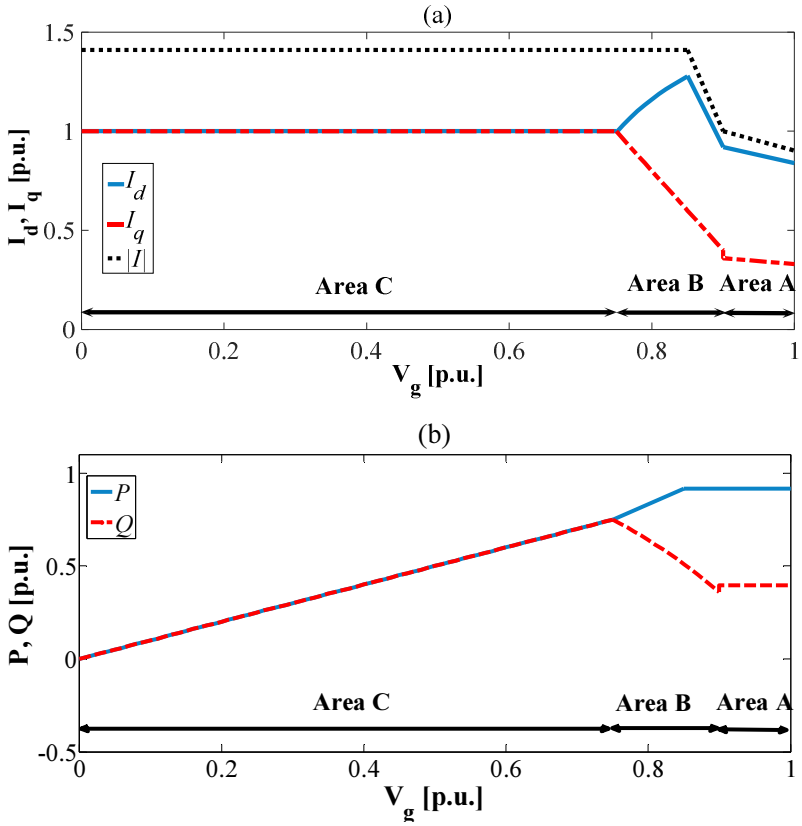

Figure 5-3 Representation of PQ curve capability for control scheme C. (a) Quadrature current components of GSC. (b) Active and reactive power output of FCWGs.

5.3.4 Control scheme D

Network requirements during faults will be different from one to another. Certain network condition such as those equipped with induction machine absorbs large reactive power in order to recover the air gap flux [5]. In order to deal with such condition, there should be a way to prioritize reactive power Q_g over its counterpart (P_g) when it is needed. Figure 5-4 depicts modified control scheme when reactive power is more prioritized than active power.

a. Area A (0.9 p.u. $\leq |V_g| \leq$ 1.0 p.u.) is the normal operating area which is similar to the conventional scheme, explained in the Section 5.3.1.

b. Area B (0.75 p.u. $\leq |V_g| <$ 0.9 p.u.) is similar to the modified scheme C in Section 5.3.3. Within this area, both active and reactive current are still within

the design limit while maintaining the 4% reactive current requirement set by AEMO.

c. Area C (0.0 p.u. ≤ $|V_g|$ < 0.75 p.u.) is the area when I_{qg} is more prioritized than the I_{dg}. Within this area, I_{qg} is allowed to be increased following the 4% reactive current requirement while I_{dg} is reduced such that the maximum current remains constant at 1.41 p.u. Consequently, reactive power output, Q_g, exceeds active power, P_g at Point (D, B) and Point (E, C). Point A is the condition when P_g and Q_g reach their equilibrium. Therefore, points (D, B) illustrate condition when 2% reactive power is injected into the network, while points (E, C) are for 4% grid requirement. Both output power, P_g and Q_g are decreased following voltage drop at machine terminals.

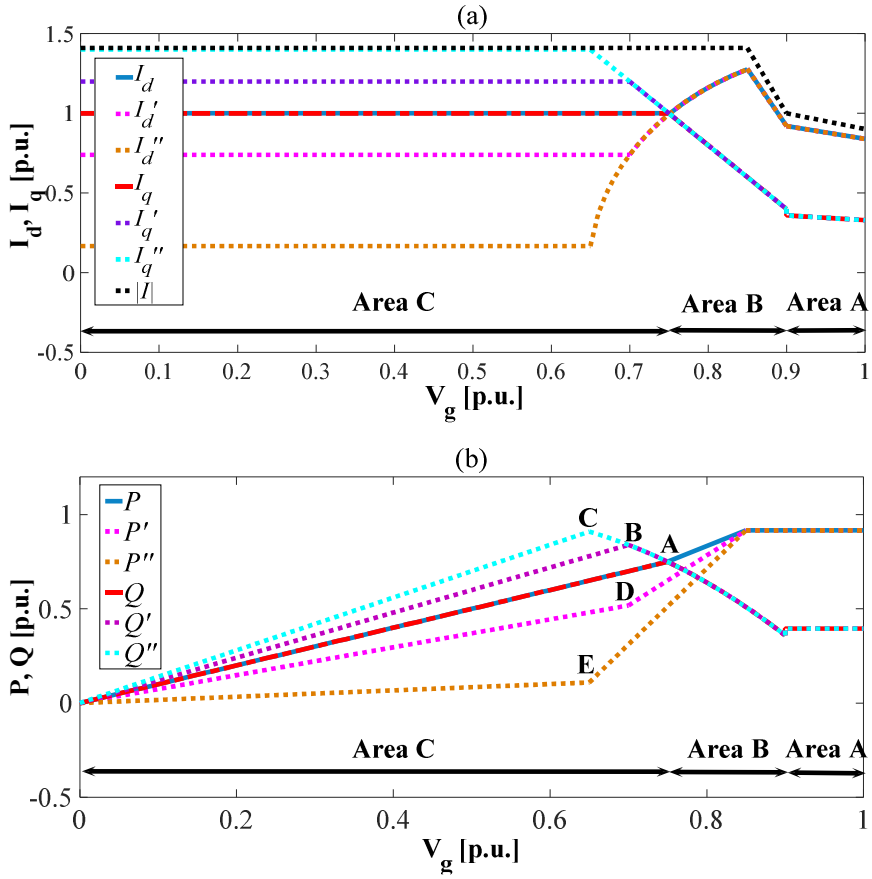

Figure 5-4 Representation of PQ curve capability for control scheme D. (a) Quadrature current components of GSC. (b) Active and reactive power output of FCWGs.

5.4 SIMULATION RESULTS

The simulation analysis is conducted using MATLAB/SIMULINK. Figure 5-5 shows the schematic of the simulated system. 2x1.5MW of FSIGs are connected to 5x2MW FCWGs at the common point B25 which is weakly connected to the grid through a 20 km transmission line.

Four types of control schemes have been considered in this study in order to see the ability of the FCWGs to allow reactive power injection during grid faults. For this purpose, the system will be subjected to voltage sag type A referring to three-phase symmetrical sag in the infinite bus [112, 113]. In addition, FRT capability of FSIGs is assessed by varying the fault duration as well as implementing the four proposed control schemes. A brief explanation of each case is presented in the following sections.

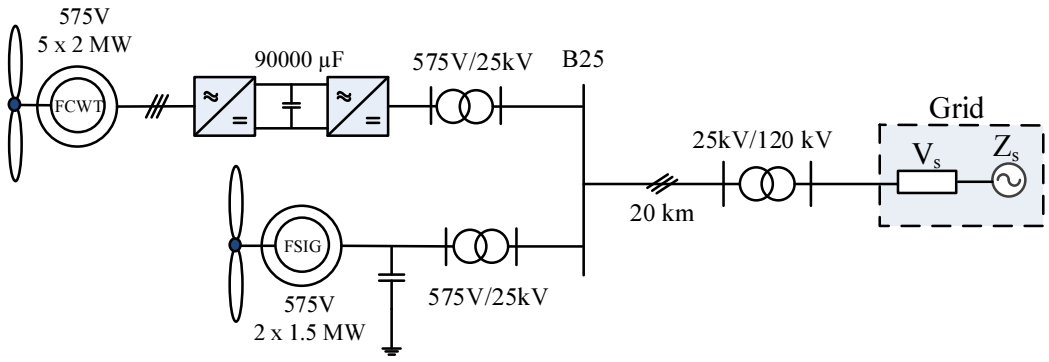

Figure 5-5 Schematic diagram of the simulated system.

5.4.1 PQ response of FCWGs

Response of FCWGs under type A sag is presented in Figure 5-6. As can be seen from Figure 5-6 (a-b), with Scheme A, FCWG is not equipped with reactive power supports. Therefore a 50% voltage sag at the grid will cause voltage drops at its terminal and as a result, the power delivered to the grid, P_g, reduces from its steady state. Response of wind generators with Scheme B are presented in Figure 5-6 (c-d).

Under normal condition, reactive power is maintained at 0 p.u. When the fault occurs, the wind generator must help the supply voltage restoration by injecting 4%

reactive current component for each 1% drop in the supply voltage amplitude. Accordingly, the I_{qg} component starts to increase linearly from 0.4 p.u. with the slope of 4.

In Scheme C, the GSC output current is allowed to temporarily increase to 1.41 times of its nominal capacity during the fault period (see Figure 5-6 (e-f)). It is not triggering substantial risk for semiconductor switches, since modern power converters are designed to tolerate temporary overloading. As an example, Semikron SKiiP® Intelligent Power Modules can resist maximum 150% overloading for period 20 s [81]. In Australian Grid Code [86], the system stability criteria specifies that the time for the amplitude of an oscillation to reduce by half ($|V_s|$ = 0.5 p.u.), should be maximum of 10 s. Therefore, the GSC can be safely overloaded by 41% during the requested fault period. It is worth to notice that during the 50% voltage sag, both I_{qg} and I_{dg} are maintained at 1.p.u. which confirms the schematic of the proposed control in Figure 5-3. Within this scheme, the active power P_g is allowed to stay within its rated value and consequently the reactive power Q_g can be maintained at 1 p.u. as its maximum value.

Lastly, Figure 5-6 (g-h), presents the results for proposed Scheme D which is in opposite to Scheme C for voltage 50% voltage sag. Based on Figure 5-4, the reactive power is allowed to dominate active power in order to help recovering network voltage stability. Therefore, when applied sag occurs, the reactive current component I_{qg} is increased while I_{dg} decreased which consequently cause reduction on active power output (P_g) of the FCWGs but a significant escalation of the reactive power output (Q_g).

In conclusion, for FCWGs, the GSC keeps enabling the voltage regulator to control the reactive power injection to the grid. Thus, the grid voltage manages to quickly recover to 1.0 p.u. The MSC is also activated right after the fault clearance so that the wind farms can continue supplying electric power at the rated value to the grid. In other word, for all four schemes, the FCWGs have the ability to ride through the fault.

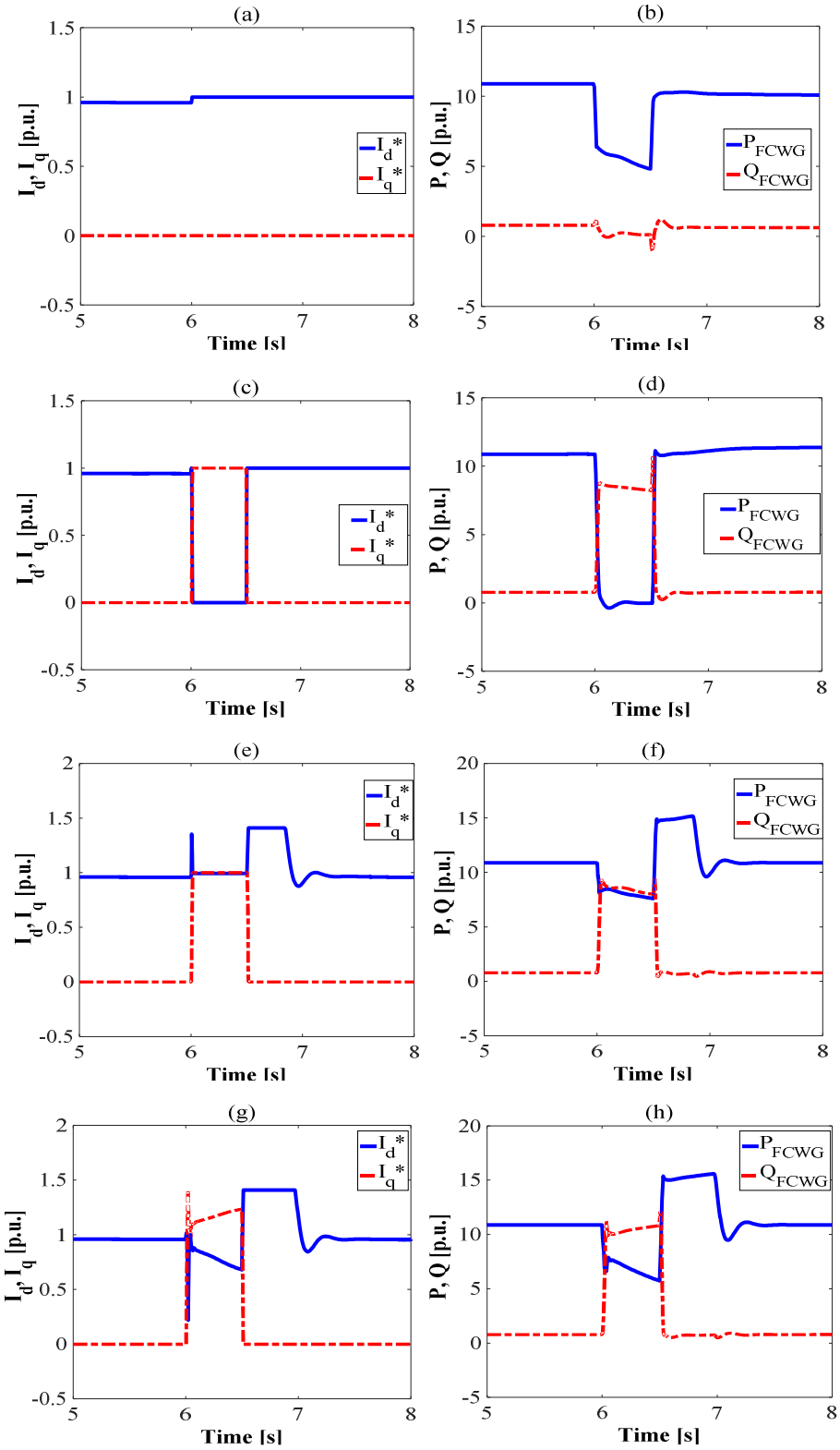

Figure 5-6 PQ Response of FCWGs. (a-b) Scheme A. (c-d) Scheme B. (e-f) Scheme C. (g-h) Scheme D.

5.4.2 Impacts of the proposed schemes to the nearby network

In Section 4.3.2, it has been shown that modification of the reactive power control of FCWGs is applied at the GSC by injecting certain amount of reactive power following the droop requirement from the transmission operator. In the case of fault, the voltage at the terminal drops causing reduction of the active power delivered to the grid. The power converter has maximum current and recent technologies allow its maximum current to be extended beyond its rated limit for several seconds [80, 81]. When fault occurs, it is important for transmission operator to determine either to safe the network stability or maintain the active power delivered to the network. This becomes very crucial for network connecting the induction machines as shown in the simulated system (Figure 5-5) and Figure 5-7 shows voltage profiles at point of connection for the four different control schemes.

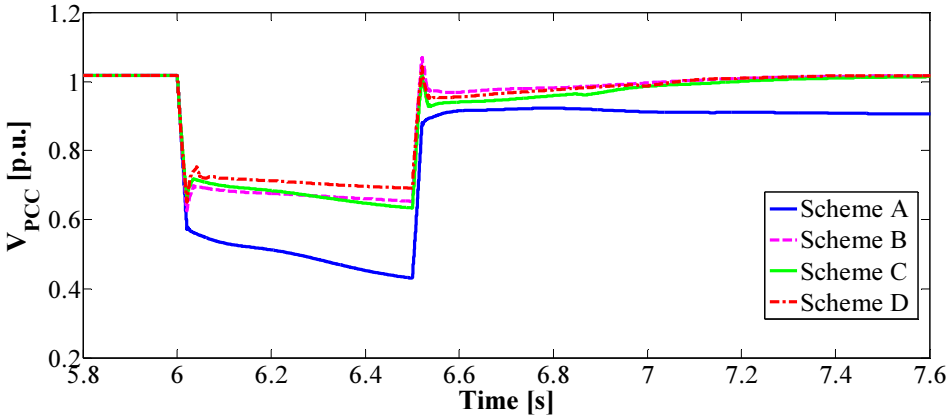

Figure 5-7 Voltage profiles at point of connection (PCC).

From the aforementioned figure, it can be clearly seen that it is necessary to provide reactive power support during the fault. In the case of no reactive support from FCWGs (Scheme A), there is a significant voltage drop at PCC after fault clearing. This is due to voltage drop at FSIGs terminals lead to excessive consumption of reactive power. Therefore, as the fault is cleared, they cannot recover to their steady state leading to the voltage instability at the PCC. Such trend does not occur when modified reactive power support is applied to FCWG, i.e. Scheme B, C and D. However, the best voltage profile is achieved when reactive power is prioritized over

active power (Scheme D). Details about FRT capability improvement of FSIGs for the proposed schemes are presented in the following section.

5.4.3 Impact to the FRT Capability of FSIGs

It has been explained in Section 2.3.1 that there are some FSIGs that are still operating and having low FRT capability. Dynamic stability of FSIGs highly depend on their ability to maintain slip below the critical limit. Figure 5-8 shows the induction machine torque–slip characteristics given variable voltage at terminal of the generator [119, 120]. The following swing equation [121] also explains the instability phenomena at FSIGs following the network fault:

$$\frac{ds}{dt} = \frac{1}{2H}(T_e - T_m) \qquad 5\text{-}5$$

where s denotes the rotor slip and H is the inertia constant of the machine; while T_e and T_m represent electromagnetic and mechanical torque accordingly.

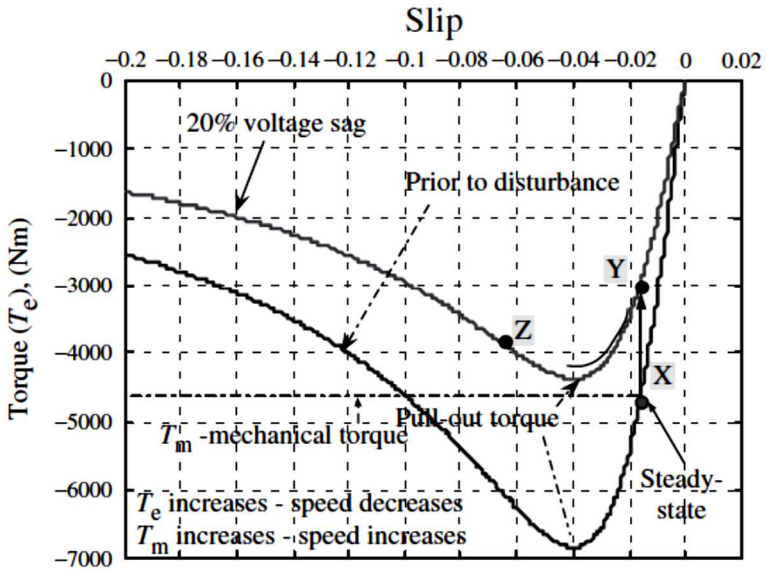

Figure 5-8 Induction machine torque–slip characteristics for variations in generator terminal voltage [119, 120].

When the network fault occurs, the voltage at machine terminal will suddenly drop which lead to a significant reduction of electromagnetic torque (T_e) and output power production (P_g). However, the turbine remains rotating causing an almost constant

production of mechanical torque (T_m). As a result, the generator accelerates and causes an increase of the rotor slip which leads to reactive power absorption from the network. If the machine keeps increasing its acceleration, it will absorb large reactive power in order to recover the air gap flux [5]. Otherwise, large difference between electromagnetic and mechanical torques can lead to the instability of the machine. If reactive power cannot be fulfilled, then machine should be disconnected from power system because it can also exacerbate the voltage stability by absorbing reactive power from the network. Recent grid codes prevent the disconnection of the wind farms as it can lead to the cascading failures in the system.

The use of induction machines causes the FSIGs to have simple construction and low cost maintenance as compared to the variable speed wind turbines. However, this type of machine consumes reactive power significantly for its excitation and rotor speed reduction during the fault. Figure 5-9 shows the effect of fault duration to FRT capability of FSIGs connecting to FCWGs.

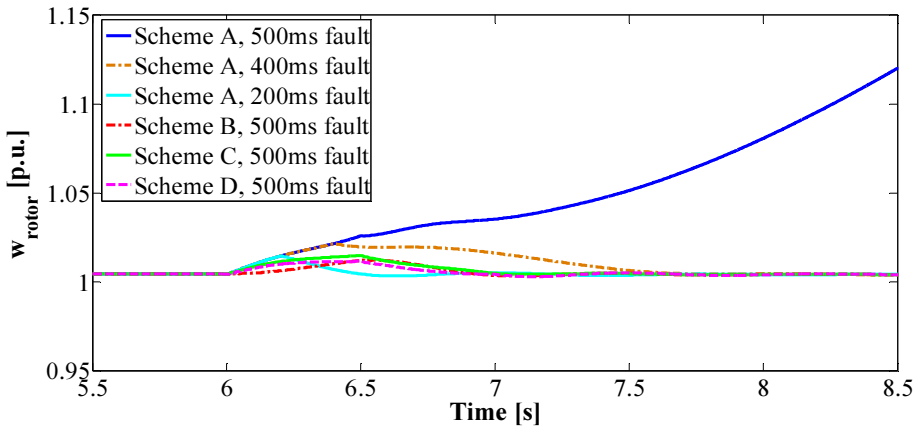

Figure 5-9 Rotor speed of FSIGs for different fault durations and schemes complying with Australian grid codes.

In the case of no reactive power support from FCWGs (Scheme A), FSIGs can only withstand to fault after duration of less than 500 ms. However, FSIGs start losing its synchronism to the network when the fault is sustained to 500 ms. As expected, for fault duration 200 ms, the FSIGs can recover to its stability sooner as compared to 400 ms fault duration. Moreover, when the FCWGs provide reactive power support

to the network (Scheme B, C, and D), FSIGs can withstand during 500 ms fault duration. This is confirmed by the rotor speed of FSIGs that remains in synchronism with the network.

Regarding the FSIGs, prioritization of Q over P in reactive power control of FCWGs causes a less rotor speed during the fault onset in both implemented grid codes (Figure 5-9). This confirms that within a network with FSIGs, it is important to prioritize reactive power support in order to maintain the stability of the network as well as reduce the tear and wear of the aforementioned machines. For more clarity, Figure 5-10 also presents PQ response of FSIGs connecting to FCWGs complying with Australian grid codes.

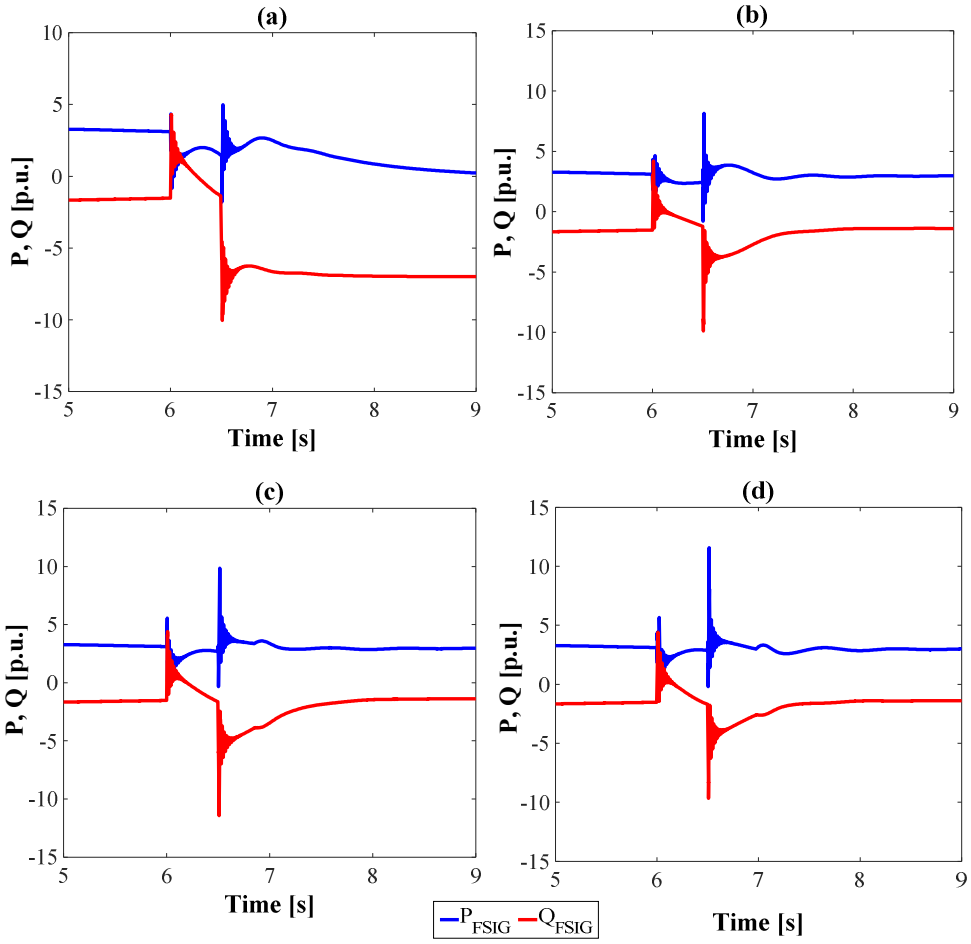

Figure 5-10 Output of FSIGs for different schemes. (a) Scheme A. (b) Scheme B. (c) Scheme C. (d). Scheme D.

It has been explained before that application of control scheme A into FCWGs cannot help to improve FRT capability of the FSIGs. The FSIGs go offline indicated by active power output drop to zero at t = 9s. Meanwhile, the FSIGs are already connected with typical reactive power compensator next to them. As for other schemes, the FSIGs can regain its steady output power once the fault is cleared.

5.5 CONCLUSION

Impacts of four different designs of FCWGs in providing reactive power support to its nearby grid have been investigated. Simulation studies confirm that FRT capability of FSIGs can be improved if Australian grid codes are implemented to enhance the capability of FCWGs. It is shown that for certain fault periods, the FSIGs cannot remain synchronism with the grid. However, their FRT performance can be improved after being connected to FCWGs with extended reactive power support. Prioritization of real power over reactive power and vice versa will determine the amount of reactive power injected into the grid at PCC and also received at terminal of FSIGs.

Chapter 6. Impacts of Grid Compliant Full Converter Wind Generation Systems on Weak Networks

6.1 INTRODUCTION

In Chapter 5, three different control schemes in compliance with the Australian grid codes are investigated. The simulation results on the hypothetical power system shows that the proposed control schemes can improve the voltage stability of the adjacent grid while providing reactive power support during fault conditions.

High penetration of distributed generation scattered all over the network is accompanied with installation of numerous transformers and long transmission lines in order to interconnect generations to the loads. WTs are commonly installed in coastal areas to provide strong and steady wind speed. However, the locations of the installed WTs are also far away from the load and the rest of the network. This implies more impedance of the transmitting lines leading to a weaker bus. In some cases, the electrical grids are not initially constructed to be connected with the new installed WTs. So that, energy transmission from the new installed WTs will cause more burden into the networks, particularly during the fault. Therefore, it is important to investigate the impacts of FCWGs on the stability of the weak grid.

There are three possible causes of weak grid condition [122]: (1) intentional separation; (2) islanding from the grid; and (3) grid faults or unintentional islanding. This chapter will investigate the impacts of grid compliance FCWGs into the practical weak grid due to faults (unintentional islanding). The chapter will be organized as follow. Section 6.2 will describe the characteristic of weak grid based on available literatures. Section 6.4 will concisely describe the simplified practical weak network for testing the proposed control schemes, explained in Chapter 5. Simulation results will be presented in Section 6.5, concerning on the impact of

FCWGs with the proposed control schemes on enhancing the stability of adjacent network during fault onset. Finally, Section 6.6 will provide a conclusion of this chapter.

6.2 DEFINITION OF WEAK GRID

The grid is an interconnected power network that delivers electric power from source to the load through transmission and/or distribution lines. It is generally characterized by an alternating voltage source V_g and an internal impedance Z_S. The grid impedance is the total impedance of the whole components including transformers and line impedances. The impedance value is highly determined by the physical characteristics of the components, such as material and size.

The stiffness of the grid refers to the ability of the grid to maintain its stability during the fault onset, without or with the renewable energy resources such as wind turbines. In wind turbine connection, there are two parameters commonly used for determining the stiffness of the grid including short circuit ratio (SCR) and the X/R ratio. SCR can be defined as [123]:

$$SCR = \frac{SCC}{S_{WT}} = \frac{V_g^2}{Z_{weak} \cdot S_{WT}} \tag{6-1}$$

where Short Circuit Capacity (SCC) is the amount of power flowing to the appointed point during fault onset; S_{WT} is the rated power of wind turbine; V_g is the grid voltage; and Z_{weak} is the impedance of the grid. If SCR < 10, then the grid is categorized as a weak network [123, 124].

Following its name, the X/R ratio is the ratio of inductive part (X) and the ohmic part (R) of the grid impendance Z_S. The weak grid typically has X/R < 0.5 [123].

6.3 ANALYTICAL MODEL OF WEAK GRID CONNECTION

According to [113], the voltage divider model shown in Figure 6-1 can be used to calculate sag magnitude in radial system. In Figure 6-1, Z_S is the source impedance at the PCC while Z_F is the impedance between the PCC and the fault. Based on Figure

6-1, the PCC is the feeding point for both fault and the load. From perspectives of wind turbine connection to the weak grid, PCC is the point in which both wind turbine and the fault are linked.

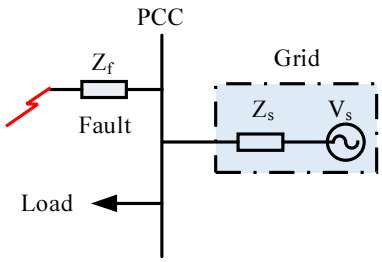

Figure 6-1 Voltage divider model for a voltage sag.

The voltages at the PCC and equipment terminals can be calculated as [113]:

$$V_{sag} = \frac{Z_F}{Z_S + Z_F} E \tag{6-2}.$$

The pre-fault voltage at the PCC is assumed to be 1 p.u., such that E is set to 1 p.u. Thus:

$$V_{sag} = \frac{Z_F}{Z_S + Z_F} \tag{6-3}.$$

Based on Equation (6-3), when Z_F becomes smaller (i.e. the fault location is closer to the load), the voltage sag will be deeper. Similar trend also happen when Z_S becomes larger as in the case of the weak grid.

If $Z_F = zd$, the sag magnitude as the function of the distance to the fault can be stated as [113]:

$$V_{sag} = \frac{zd}{Z_S + zd} \tag{6-4}$$

where z is the impedance of the feeder per unit length while d is the distance between the fault and the PCC.

6.4 PRACTICAL TEST SYSTEM

In this chapter, the performance of the proposed grid code compliant FCWGs (explained in Chapter 5. by using 29 bus test system of Figure 6-2 developed in Matlab/Simulink [125]. The test system comprises of 7 machines (based on synchronous generators), 6x1.5 MW wind farm (based on asynchronous generator), and various buses, e.g. load bus and swing bus. Table 6-1 shows voltage level of each bus within the test system. The test system generally consists of two main areas, i.e. North West Network and North East Network connected to each other through a 735 kV transmission network having series and shunt compensation at selected locations. A load and 6x1.5 MW wind turbine are also connected along the 735 kV transmission lines.

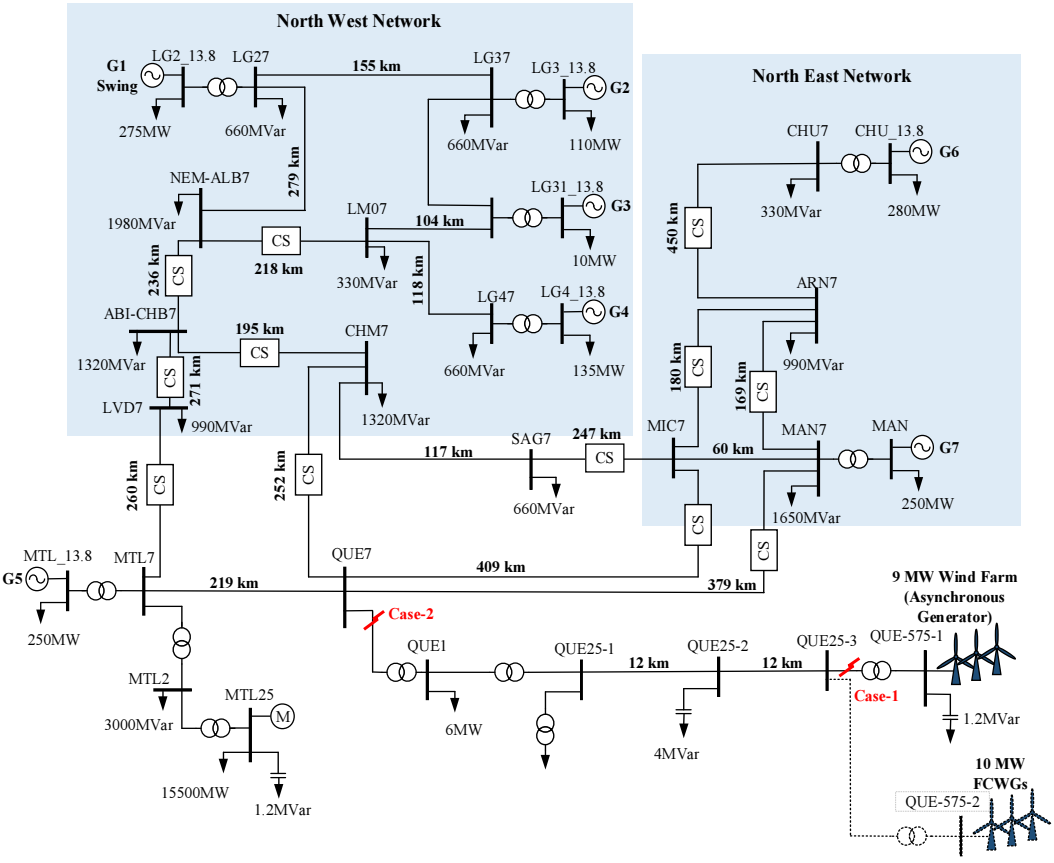

Figure 6-2 Practical test system [125].

Table 6-1 Voltage level of each bus of the test system.

Bus Name	Nominal Voltage	Bus Name	Nominal Voltage	Bus Name	Nominal Voltage
QUE1	120kV	MAN7	735kV	LG47	735kV
QUE1_25_1	25kV	MAN_13.8	13.8kV	LG47_13.8	13.8kV
QUE1_25_2	25kV	ARN7	735kV	LG31_13.8	13.8kV
QUE1_25_3	25kV	CHU7	735kV	LG37	735kV
QUE_575	575 V	CHU7_13.8	13.8kV	LG37_13.8	13.8kV
QUE7	735kV	LVD7	735kV	LG27	735kV
MTL7	735kV	CHM7	735kV	LG2_13.8	13.8kV
MTL_13.8	13.8kV	ABI_CHB7	735kV	LMO7	735kV
SAG7	735kV	NEM_ALB7	735kV	MIC7	735kV

A series of simulation has been conducted to investigate performance of the FCWGs with the proposed controller during selected faults at 2 (two) various location. Table 6-2 shows detail description of testing scenarios for the simulation.

Table 6-2 Description of test scenarios.

No	Fault Locations	Description	Scenarios
1	Bus QUE25-3 (Case 1)	Type-A fault at the PCC, i.e. 3ϕ-g fault (symmetrical fault).	1. Initial condition, only FSIGs are installed in the network 2. Both FSIGs and FCWGs with Scheme B are installed in the network 3. Both FSIGs and FCWGs with Scheme C are installed in the network 4. Both FSIGs and FCWGs with Scheme D are installed in the network
2	Bus QUE1 (Case 2)		
3	Bus QUE25-3 (Case 1)	Type-C fault at the PCC, i.e. ϕ-ϕ fault (unsymmetrical fault)	
4	Bus QUE1 (Case 2)		

According to [112], there are 7 possible faults in the network, however only type A and type C affect the wind turbine terminals. The type A fault cannot be affected by transformer configuration. Therefore, the type A appears inside the wind farm wherever the fault is located. The type B and type E cannot propagate to the wind turbine due to the zero sequence components. In addition, type D, type F and type G can only be observed when the transformer parameters are in consideration. Since transformer parameter is beyond the scope of this research, the type D, type F and type G will not be simulated.

6.5 SIMULATION RESULTS

6.5.1 Case 1 – Faults at Line Connecting Bus QUE25-3 and FSIGs

Two faults of type A and type C with durations of 200 ms are applied to the line connecting the Bus QUE25-3 and the FSIGs. FCWGs with the proposed control schemes are also connected to the Bus QUE25-3.

The distance of the fault location with the FCWGs will determine the level of voltage drop at its terminal and simultaneously determine the amount of reactive power injected into the network. When the fault occurs at the line connecting Bus QUE25-3 and FSIGs, the voltage level at Bus QUE25-3 drops simultaneously. Since the FCWGs are tied to the Bus QUE25-3 through transformer, the voltage at FCWG terminals drops accordingly. As the results, the FCWGs automatically activate its controller to provide the required reactive power. The voltage profile of the PCC (i.e. Bus QUE25-3) as shown in Figure 6-3a and Figure 6-3b confirm that the grid compliance FCWGs successfully provide reactive power support to the network such that voltage profile at the PCC can be improved.

FSIGs are also connected to the Bus QUE25-3 through a transformer. Figure 6-4 shows the rotor speed of the FSIGs during fault and after fault clearance for both type A and type C faults. When there is no FCWGs installed, the applied faults cause the induction motor to accelerates and loose its synchronism during the 200 ms type-A fault (Figure 6-4a). Figure 6-4a and Figure 6-4b confirm that FRT capability of adjacent FSIGs can be improved by applying FCWGs with the proposed schemes. This can be achieved due to the sufficient reactive power which is available to help the induction machine to restore back to the normal condition during and after faults.

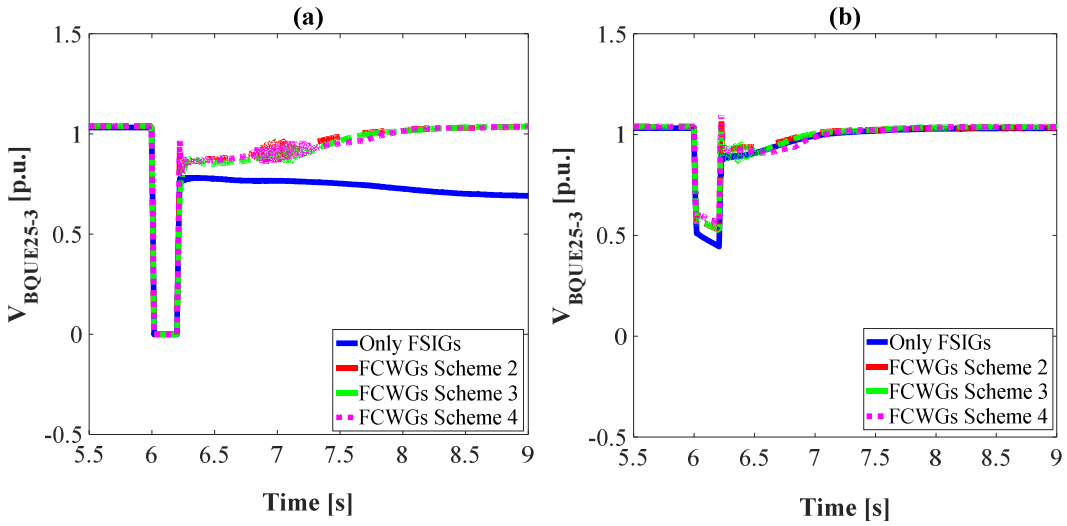

Figure 6-3 Voltage profile of the adjacent buses during faults at line connecting the Bus QUE25-3 and the FSIGs: (a) symmetrical fault; (b) unsymmetrical fault.

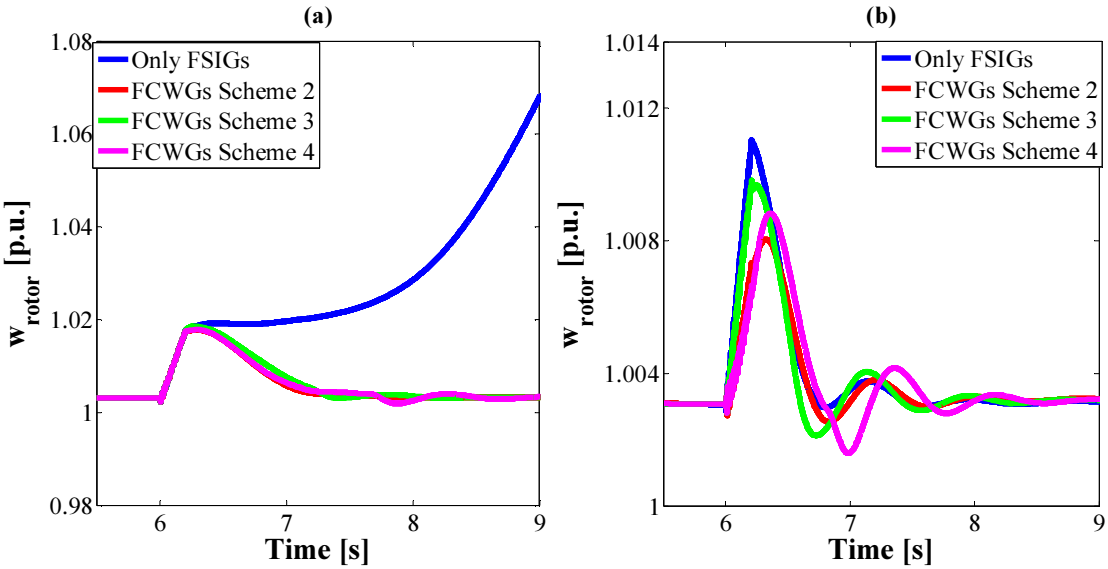

Figure 6-4 Rotor speed of FSIGs during fault at faults at line connecting the Bus QUE25-3 and the FSIGs: (a) selected symmetrical fault; (b) selected unsymmetrical fault.

Based on Figure 6-2, the nearby loads are located at the Bus QUE1. Under normal condition, these loads are supplied by the FSIGs which is the nearest as compared to other generation systems. During the faults, the load profile remains constant as the loads have power transferred from the rest of the testing network. Therefore when the voltage at PCC drops to zero during symmetrical fault (Figure 6-3a), the load can be fully supplied as normal condition.

6.5.2 Case 2 - Faults at Line Connecting Bus QUE7 and Bus QUE1

It is shown in Figure 6-2, the line between Bus QUE7 and Bus QUE1 is a critical line as it connects both the 6MW load and the wind turbines. A fault at this line can lead to unintentional islanding of the load and the wind farms from the rest of the network. Two faults of type A and type C with durations of 200 ms are applied to investigate the impact of the FCWGs with the proposed control schemes.

Figure 6-5 and Figure 6-6 depict voltage profiles of the connecting buses respectively. During fault onset, the connecting Bus QUE7 and QUE1 experience the worst voltage drop. For example, in the case of type A fault, the voltage of the aforementioned buses drops to zero. As the result, the adjacent Bus MLT7 and Bus QUE25-3 also simultaneously experience voltage drop. The severity of the voltage drop varies for both Bus MLT7 and Bus QUE25-3 as the distance from the fault location are 219 km and 24 km respectively. For both applied faults, the grid compliance FCWGs can improve the voltage profiles of Bus QUE25-3 which connects the wind farms to the grid (Figure 6-5d and Figure 6-6d). Again, the amount of reactive power support provided by FCWGs depend on the voltage drop at its terminals.

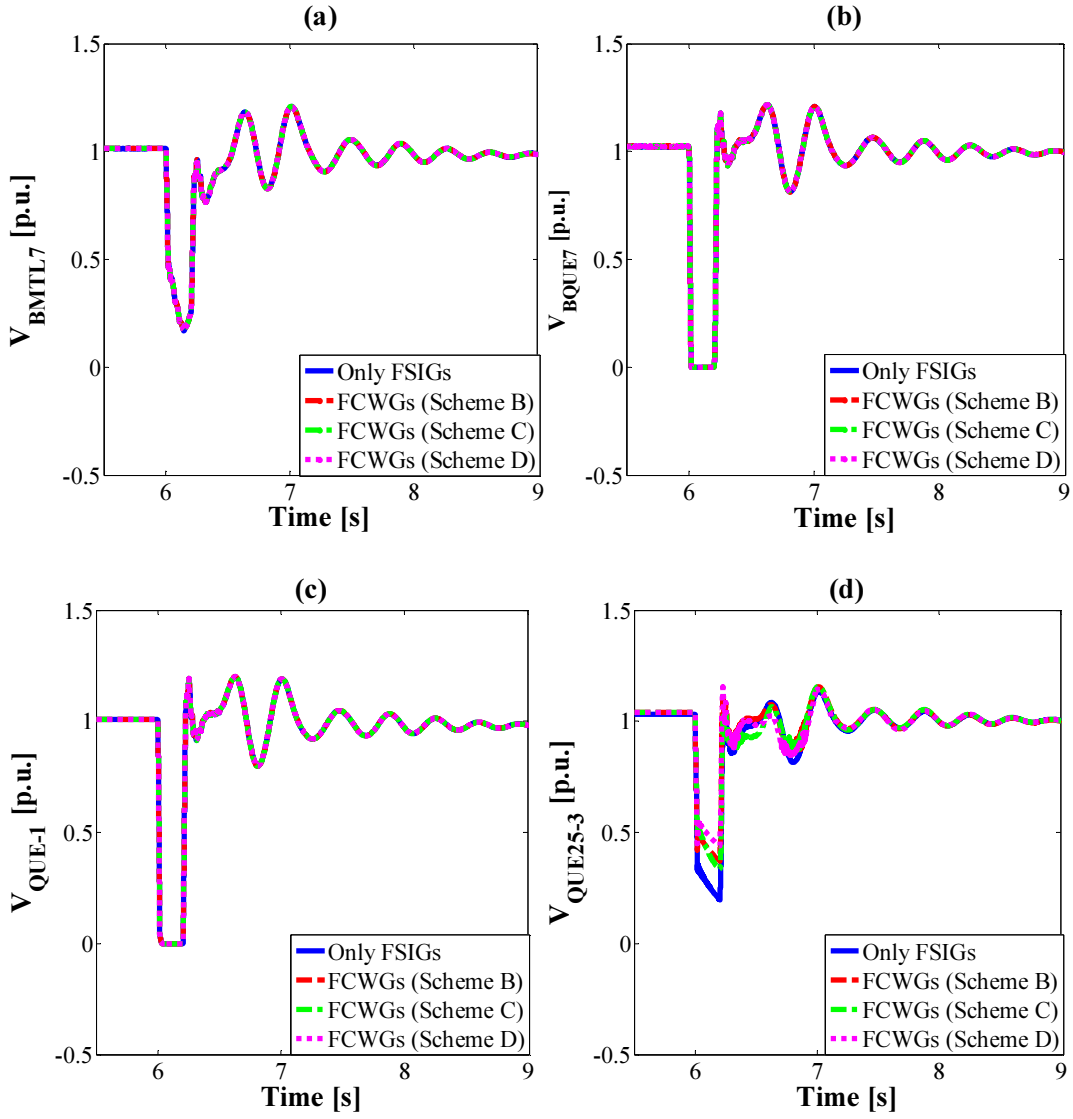

Figure 6-5 Voltage profile of the adjacent buses during symmetrical fault at Bus QUE7: (a) Bus MTL7; (b) Bus QUE7; (c) Bus QUE1; (d) Bus QUE25-3.

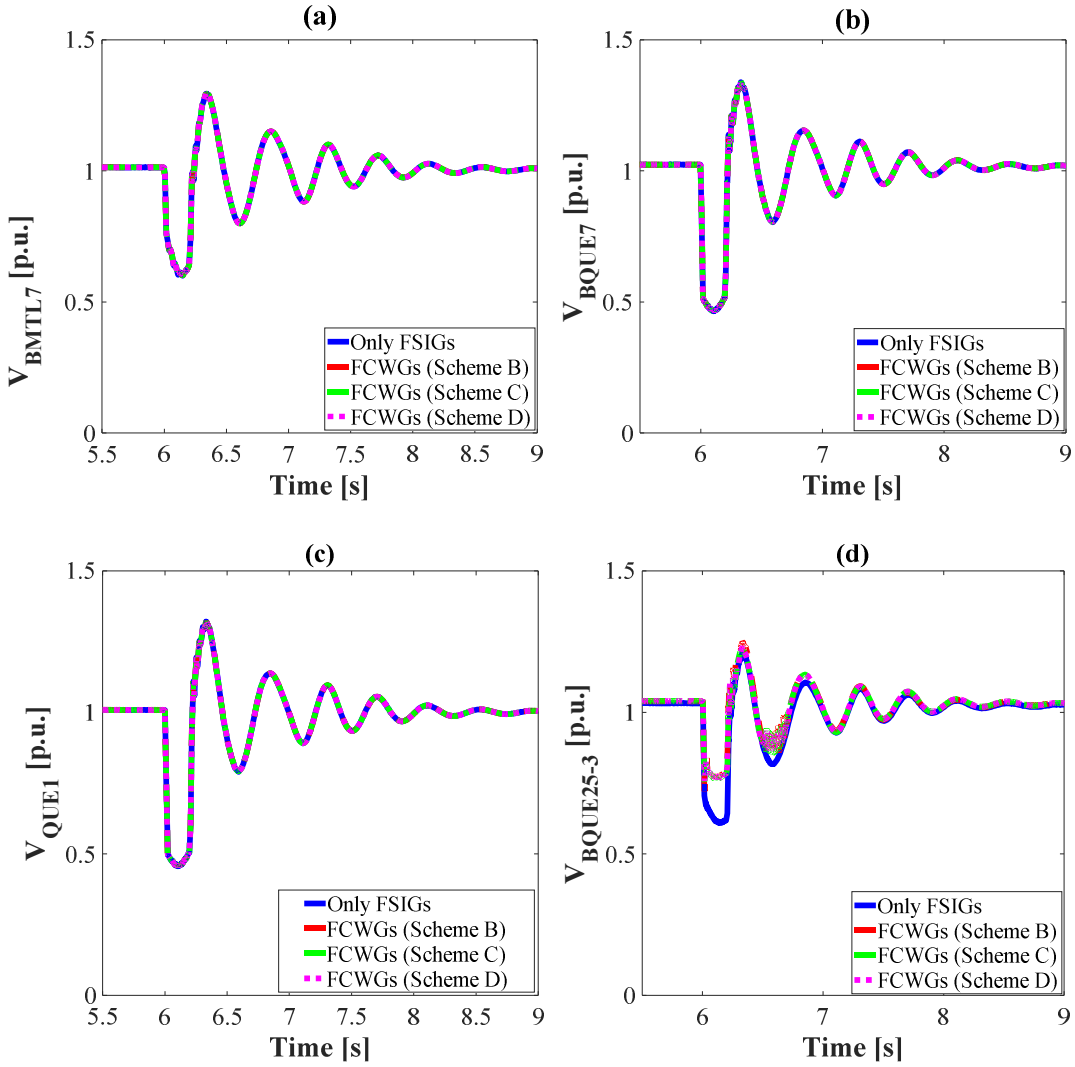

Figure 6-6 Voltage profile of the adjacent buses during unsymmetrical fault at Bus QUE7: (a) Bus MTL7; (b) Bus QUE7; (c) Bus QUE1; (d) Bus QUE25-3.

6.6 CONCLUSION

The integration of FCWGs equipped with the proposed grid code compliant control schemes has been investigated. Simulations results of a practical weak network confirmed that the FCWGs with the proposed control scheme can significantly improve the stability of the adjacent network during applied symmetrical (i.e. type A) and unsymmetrical (i.e. type C) faults. Location and the distance of the fault from the FCWGs will significantly affect the amount of reactive power injected into the

grid. Therefore, it is important to install FCWGs with the enhanced PQ support near the critical points within the weak grid.

Chapter 7. Enhanced Reactive Power Allocation of Full Converter Wind Generation System

7.1 INTRODUCTION

In previous chapters, it has been shown that FCWGs have the ability to withstand faults while providing reactive power support to the grid and GSC is fully responsible to manage the active and reactive power exchange with the network. Regarding FRT capability of wind farms, grid codes such as in Australia [86, 87] require the wind generators to remain grid connected considering the voltage profiles at PCC. In order to fulfil these requirements, wind turbines are expected to provide particular reactive current droop control following any voltage drop at the common point.

There are various source of reactive power in the network, however only a few researches have focused on the coordination control among these reactive power sources within the wind farms [126, 127]. Due to the intermittent nature of wind power, the output powers of WTGs located in the same wind farm are not the same due to the variations in their wind speeds. It is shown in [127] that coordinated control among wind turbines with different levels of wind speed can determine the total reactive power allocation to the network. However, this reference does not explore the implications of grid codes in the allocation of reactive power among dispersed FCWGs. In addition, most of the published work is focused on DFIGs that have different PQ control strategies compared to FCWGs.

This chapter investigates reactive power allocation of FCWGs with different wind speeds in order to comply with the Australian and Danish Grid Codes. The approach uses voltage drops at PCC and the wind speeds to define a power index for PQ control of FCWGs.

In order to achieve the aforementioned objectives, this chapter is constructed based on the following direction. Section 7.1 provides explanation about the objectives as well as organization of the chapter. Then, Section 7.2 gives a brief explanation about PQ capability of applied FCWGs. Basic concept of proposed power index for extended PQ support of FCWGs is explained in Section 7.3. Simulation results to confirm the aforementioned concept is presented in Section 7.4. Finally, Section 7.5 concludes the whole content of the chapter.

7.2 *PQ* CAPABILITY OF FULL CONVERTER BASED WTGS

Figure 7-1 show the simplified configuration of FCWG investigated in this study including its controllers both at machine and grid side. The machine side controller responsible to maximize power produced by the generator while the grid side controller manages the active and reactive power exchange with the grid. Further details about the applied controllers are explained in Chapter 4.

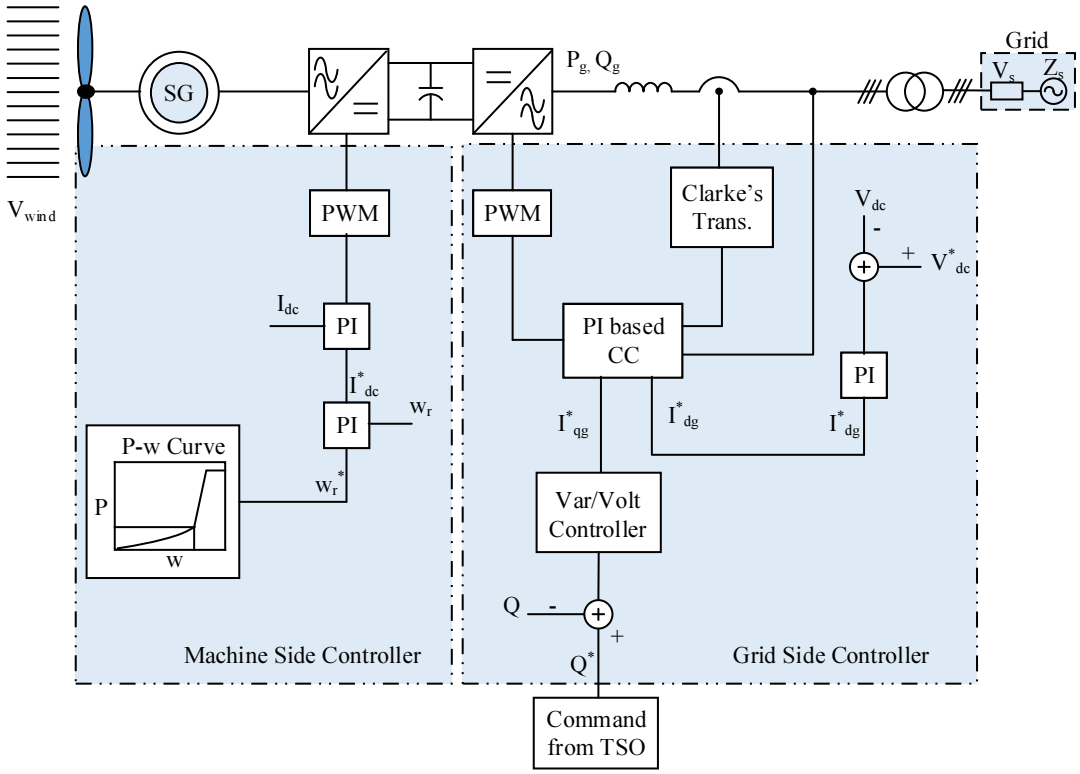

Figure 7-1 Simplified schematic diagram of simulated FCWG.

Since the GSC is in charge of delivering power to the network, the operational limit of the converter needs to be carefully considered when modifying PQ control of WTGs particularly under the most onerous conditions. These limiting factors include $I_{c,max}$, $V_{c,max}$ and $V_{dc,max}$ [118, 128]. By neglecting the scaling factors of Clarke's Transformation, the delivered P and Q to the grid in the synchronous frame are [109, 118]

$$P_g^2 + Q_g^2 = \left(\left|V_g\right| I_{dg}\right)^2 + \left(\left|V_g\right| I_{qg}\right)^2. \tag{7-1}$$

If converter losses are neglected, the powers at the DC and AC sides will be equal and

$$P_g = \left|V_g\right| I_{dg} = V_{dc} I_{dc}. \tag{7-2}$$

Based on Equation (7-2), $V_{dc,max}$ can be controlled by adjusting its d-axis current component. Meanwhile, the amplitude of converter current can be defined as Equation (5-3). The $I_{c,max}$ is defined at the minimum value of $V_{g,}$ while both P_g and Q_g are within their rated values:

$$\left|I_{c,\max}\right| = \frac{\sqrt{P_g^2 + Q_g^2}}{\left|V_{g,\min}\right|}. \tag{7-3}$$

7.3 POWER INDEX FOR EXTENDED *PQ* SUPPORT OF FCWGS

In this section, reactive power allocation method for properly distributing reactive current injection among wind turbines is explained. This method carefully calculate the power index based on the rated active power produced considering the actual wind speed. Determination of power index for extended PQ support of FCWGs is using the following steps:

- Step 1- Defining a power index as follows:

$$M_i = \frac{\frac{1}{N}\sum_{j=1}^{N} P_j}{P_i}; \quad i = 1,.....N \tag{7-4}$$

where N is the total number of FCWGs, M_i is the power index of FCWG number i and P_j is the active output power of the j^{th} FCWG.

- Step 2- Adjusting the machine side and grid side reference currents:

$$\hat{I}^*_{dc,i} = \frac{M_i}{\sum_{j=1}^{N} M_j}(I^*_{dc,i}); \quad i = 1,.....N \tag{7-5}$$

$$\hat{I}^*_{qg,i} = \frac{M_i}{\sum_{j=1}^{N} M_j}(I^*_{qg,i}); \quad i = 1,.....N \tag{7-6}$$

where I^*_{qg} is reactive current set at the GSC as demanded by the grid codes during faults, I^*_{dc} is the rated dc current at the machine side controller for the corresponding wind speed, and M_i is the index of reactive power allocation for corresponding FCWGs.

7.4 SIMULATION RESULTS

Simulation analysis is conducted using MATLAB/SIMULINK. Figure 7-2 shows the schematic of the simulated system. 6 x 2 MW of FCWGs are connected to the common point B25 which is connected to the grid through a 20 km transmission line. Each wind turbine has different wind ratings as presented in Table 7-1.

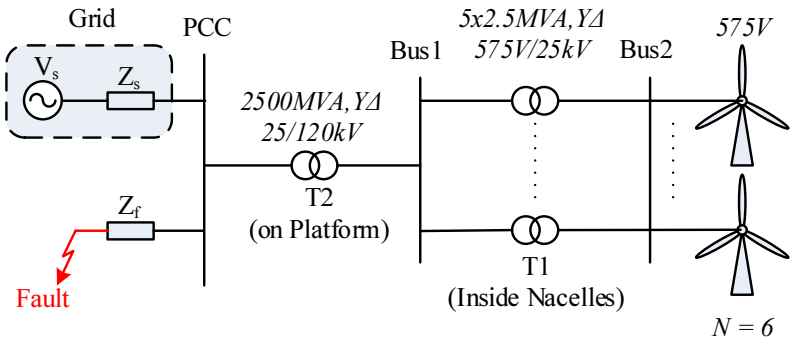

Figure 7-2 Schematic diagram of the simulated system.

Table 7-1 Wind speed level of each FCWG.

Wind Turbines	Wind Speed (m/s)
FCWG 1	16
FCWG 2	14
FCWG 3	12
FCWG 4	10
FCWG 5	8
FCWG 6	6

In order to evaluate performance of the proposed reactive power allocation method, two main objectives are included in the simulation. (1) To investigate the FRT capability of FCWGs after being subjected to Types A and F faults. Voltage sag types A and F refer to three-phase symmetrical sag in the grid and double-phase-to-ground fault at Bus 1 consecutively [112, 113]. This also includes their voltage profiles at the DC link during fault event for two different grid requirements, i.e. Australian [86] and Danish grid codes [89]. (2) To assess the PQ responses of the FCWGs complying with Australian codes during the aforementioned faults.

7.4.1 Fault ride through response of FCWGs

Figure 7-3 shows the voltage profiles at PCC for the applied faults with and without reactive power allocation from FCWGs while Figure 7-4 presents a comparison of DC link voltage profiles for different reactive power droop requirements under different wind ratings. According to Figure 7-3, for both types A and F faults, FCWGs with reactive power allocation is significantly improving the voltage profile at PCC. In addition, the type F fault is causing more severe voltage drops since it is located closer to the FCWGs.

As FCWGs are connected to the network through the GSC, it is important to consider the operational limit of power converter in any condition particularly during fault onset. These limiting factors include maximum current of converter (I_{max}), maximum converter voltage ($V_{c,max,}$) and the maximum DC link voltage ($V_{dc,max}$) [118, 128].

The typical power converters for FCWGs such as Semikron Skiip Intelligent Power Module [81], set the $V_{dc\text{-}max}$ to about 1.25 p.u. The results in Figure 7-4 confirm that the FCWGs are able to safeguard their DC links within their limits for both droop requirements.

Normally, application of protection equipment such as braking resistor [107] can help the FCWGs to get rid of the excessive voltage in the DC link during the fault. With the proposed reactive power allocation, the wind farm owner can reduce the need of such protection equipment while also reducing the wear and tear of the power converter.

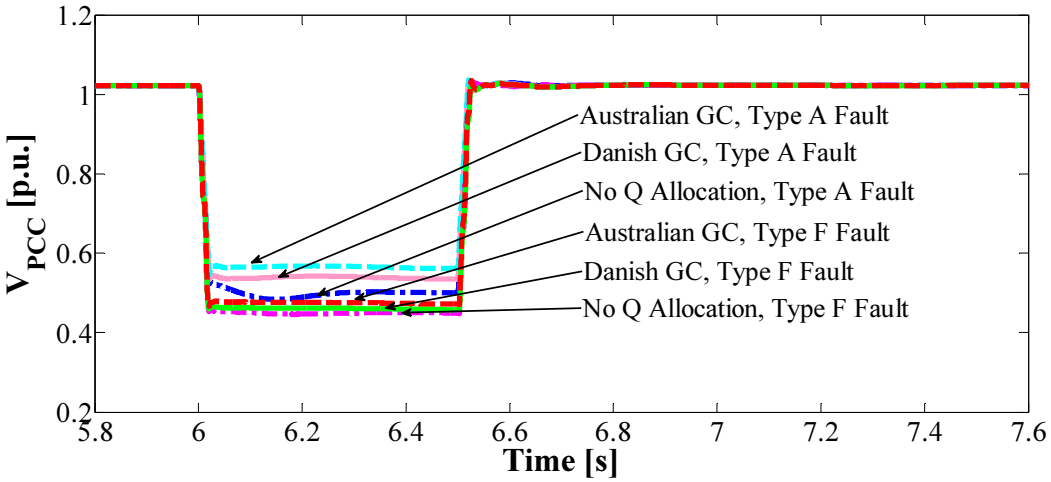

Figure 7-3 Voltage profiles at PCC (B25).

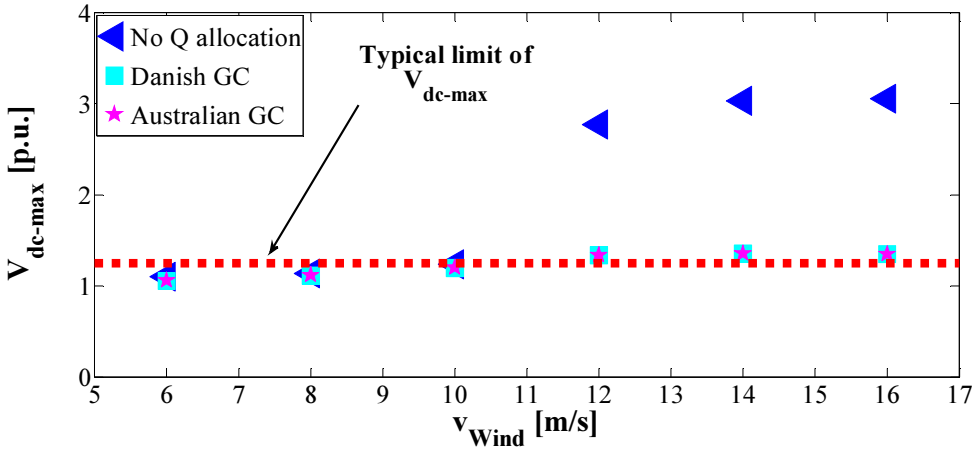

Figure 7-4 DC-link voltage profiles.

7.4.2 *PQ* response of FCWGs

Figure 7-5 presents the PQ response of the FCWGs complying with Australian grid codes during type A fault, while the results for type F is presented in Figure 7-6. As can be seen from Figure 7-5, a 50% sag type A imposed in the grid has causes a voltage drop at the terminal of FCWGs. Passing through the YΔ transformer shown in Figure 7-2, the type F fault in Bus 1 causes a voltage dip at the machine terminals as well. It is worth to notice that as the grid voltage drops, the terminal voltage of the connecting FCWGs drops accordingly. As a results, the output power of FCWGs, P_g, reduces from its rated value. Then, based on the power index calculations of Equations (7-4), (7-5), and (7-6), different levels of Q^* are allocated to each FCWG. This control approach allows the wind turbines with lower wind speeds to contribute more in the reactive power support to the network. As can be seen from Figure 7-5 and Figure 7-6, FCWGs with 6 m/s wind rating can inject more reactive currents, I_{qg}, as compared to FCWGs with at 15 m/s wind level. Similar trend is also found for other FCWGs with different wind rating.

In the simulated cases, Australian and Danish grid code has been implemented as an example of introducing the grid codes in the proposed Q control. However, this Q allocation method can also be applied in other grid environment. It is worth mentioning that the amount of injected reactive current component, I_{qg}, will also depend on the rating of the machine. In the simulations of this paper, FCWGs are assumed to have the same rating but working on different level of wind speed. Consideration of different machine ratings within the wind farms is an interesting topic to explore in the future.

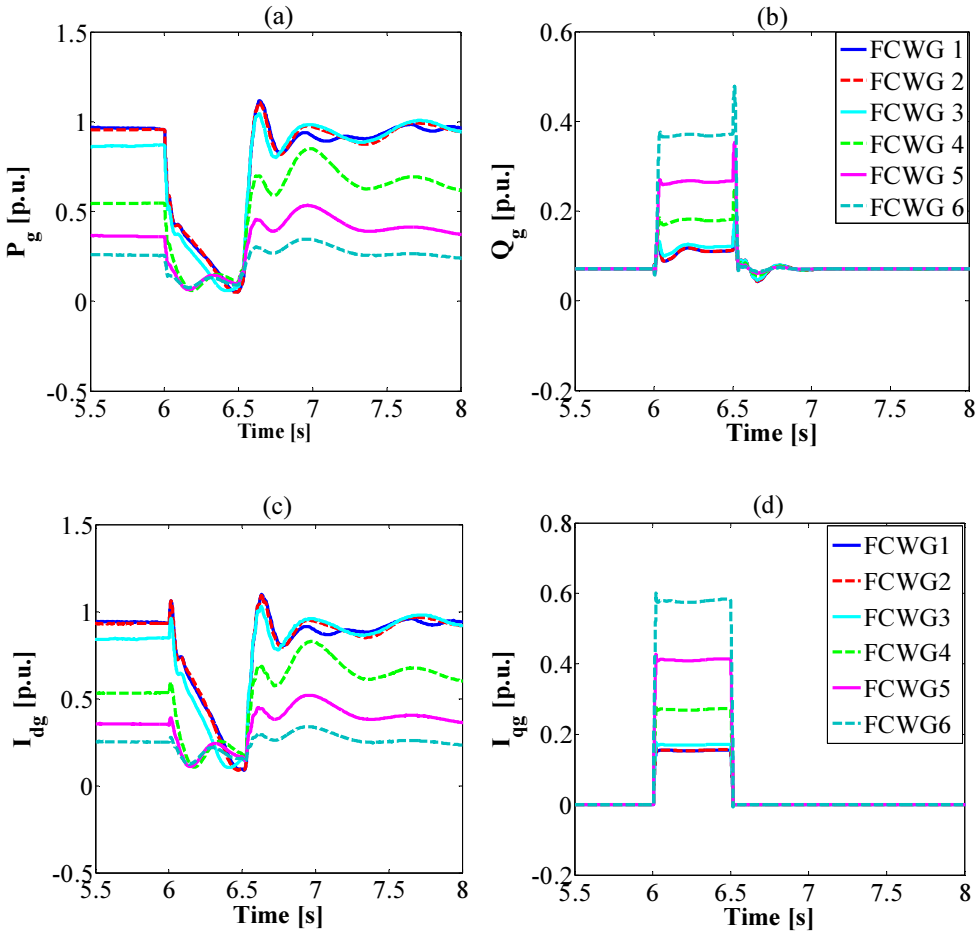

Figure 7-5 *PQ* response of FCWGs complying with Australian grid codes for Type A Fault. (a) Active power output. (b) Reactive power output. (c) Active current component of GSC. (d) Reactive current component of GSC.

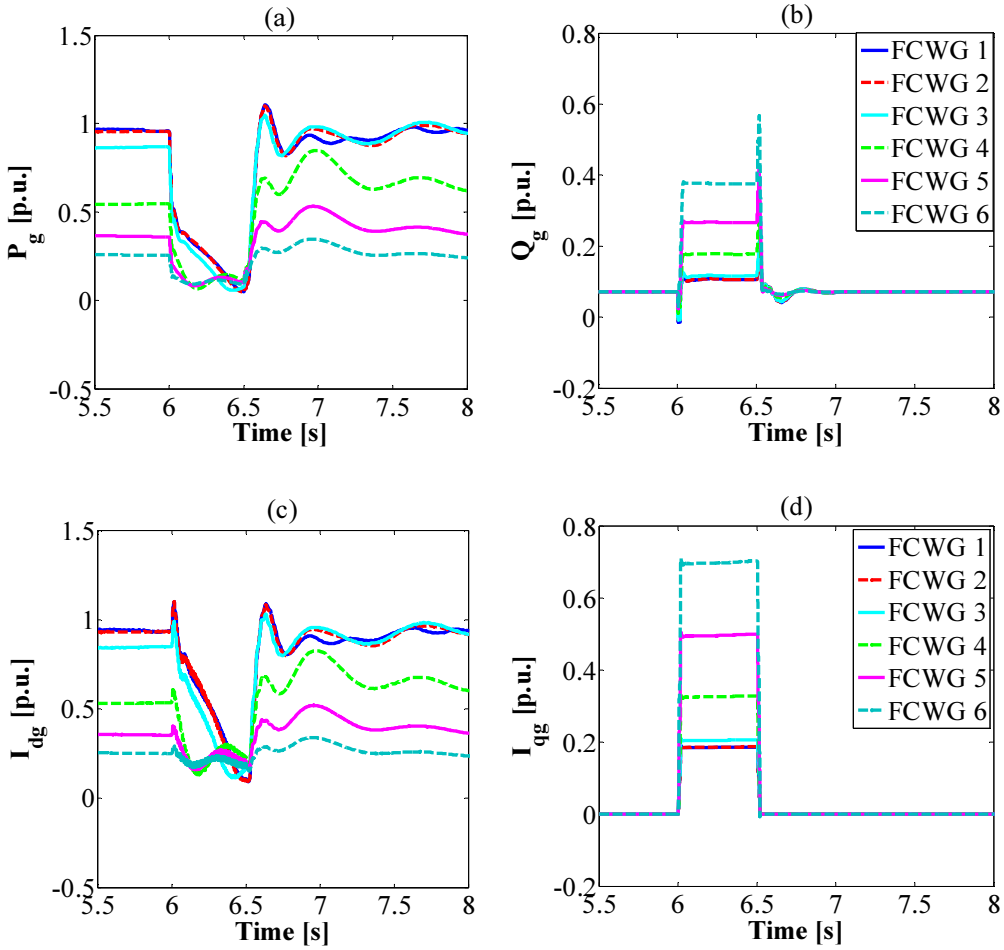

Figure 7-6 *PQ* response of FCWGs complying with E.ON Netz grid codes for Type F Fault. (a) Active power output. (b) Reactive power output. (c) Active current component of GSC. (d) Reactive current component of GSC.

7.5 CONCLUSIONS

The simulation results confirm that the FRT capability of FCWGs with different wind speeds within a wind farm can be improved by implementing a power index based reactive power allocation technique. Simulation results indicate that with the proposed control approach the FCWGs can safely withstand both balance and unbalanced faults. This is done through the proposed index scheme that requires the FCWGs with lower wind speeds to inject more reactive power as compared to machines working with higher wind speed levels. Furthermore, the proposed reactive power allocation

can also comply with the Australian and Danish Grid Code. This can be seen by the improvement in voltage profiles at PCC during fault onset. In addition, the DC-link voltage can also be maintained within their safety limits. Finally, the proposed technique will reduce the wear and tear at the DC link and the need for protection equipment such as braking resistor at GSC of FCWGs.

Chapter 8. Supervisory PQ Control of Full Converter based WTGs

8.1 INTRODUCTION

Simulation results in Chapter 5 confirms that utilization of larger converters considering Australian grid codes [86] in FCWGs can improve the voltage profile at PCC. Temporary overloading of the converter during the fault will enhance the reactive power capability such that wind turbine can support the stability of the nearby grid. Most studies on utilization of power converter such as [3, 116] considers wind turbines as aggregate models such that lack of coordination among them and the wind speed is only presented at its nominal value. Consideration of different wind speed levels in control of FCWGs to provide reactive power support is a challenging subject that has not been explored yet in the literature. In FCWG, the wind speed determines the active current component of the GSC that can be controlled to regulate the amount of reactive power injection to the grid.

Furthermore, research on FRT capability of the wind farms are mostly focused on improving the performance of individual power converters [39, 107, 116] without paying much attention to the centralized control schemes considering power converter capacity of each wind turbine. Meanwhile, it is more susceptible and cost efficient to do modification at the central level as compared to the individual units; particularly for wind turbines that are still relying on conventional control mechanisms. It is worth to notice that even within the same wind farm, power produced by each wind turbine may be different and depend on the wind variations. It is shown in Chapter 7 that coordinated control among wind turbines with different active power production can determine the total reactive power allocation of FCWGs

to the network. Nevertheless, limited current rating of the GSC contributes to minimum active and reactive power injected during the fault.

This chapter proposes a new supervisory active and reactive power control (SPQC) that considers the individual FCWG wind speeds within the wind farm to improve the overall reactive power support to the network. The main idea is for the wind turbines that are delivering less active power to inject more reactive power or temporarily increase their current ratings such that FCWG is able to help the nearby generators and loads to recover during severe fault conditions while working under safe operating area. The control command is centralized at the common point and the SPQC is independent of the wind turbine technology. Therefore, the proposed method may also be applied to other types of variable speed wind turbines. As for each FCWG, the proposed control modifications are performed at the GSC without any changes imposed on the MSC. Lastly, this research is focused on the transient analysis of FCWG therefore the impact of the communication equipment is negligible.

The above-mentioned objectives are achieved by implementing a new SPQC. In Section 8.2, the overall control scheme of the proposed SPQC is explained. In Section 8.3, simulation results are presented to validate the proposed control scheme. Lastly, Section 8.4 provides final statements about the proposed SPQC.

8.2 PROPOSED SUPERVISORY PQ CONTROL SCHEME

8.2.1 Overall SPQC control scheme

The capability of the power converter can be extended to accommodate more active and/or reactive power delivered to the network. Modern power converter are mostly designed to temporary allow such control strategies as explained in Sections 5.3.3 and 5.3.4. The basic formulas for calculating PQ capability of FCWGs is presented in Section 7.2.

The proposed SPQC scheme consists of two main parts including the master control unit (MCU) located at PCC (Figure 8-1) and the SPQC units of each FCWG within

the appointed network (Figure 8-2). The master controller is configured using the following steps:

1) MCU monitors the per-unit voltage as well as each FCWG's instantaneous P output considering the wind speed during the normal and faulted operating conditions. In addition, I_{dg} is also recorded.
2) MCU utilizes the look up table that indexes the per-unit voltage at PCC as well as the post and pre-fault loading at each FCWG. Details about the look up table are explained in Section 8.2.2.
3) In the case of fault, MCU is enabled to dispatch $\hat{I}_{qg}^{*}$ signals among the FCWGs.

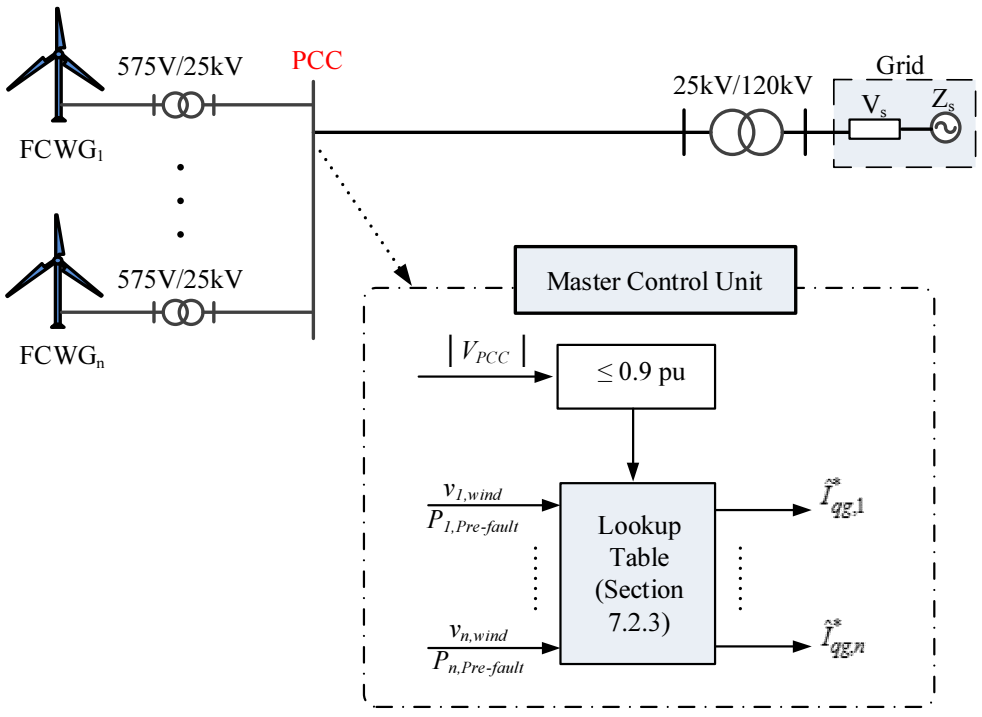

Figure 8-1 The MCU of the proposed SPQC scheme.

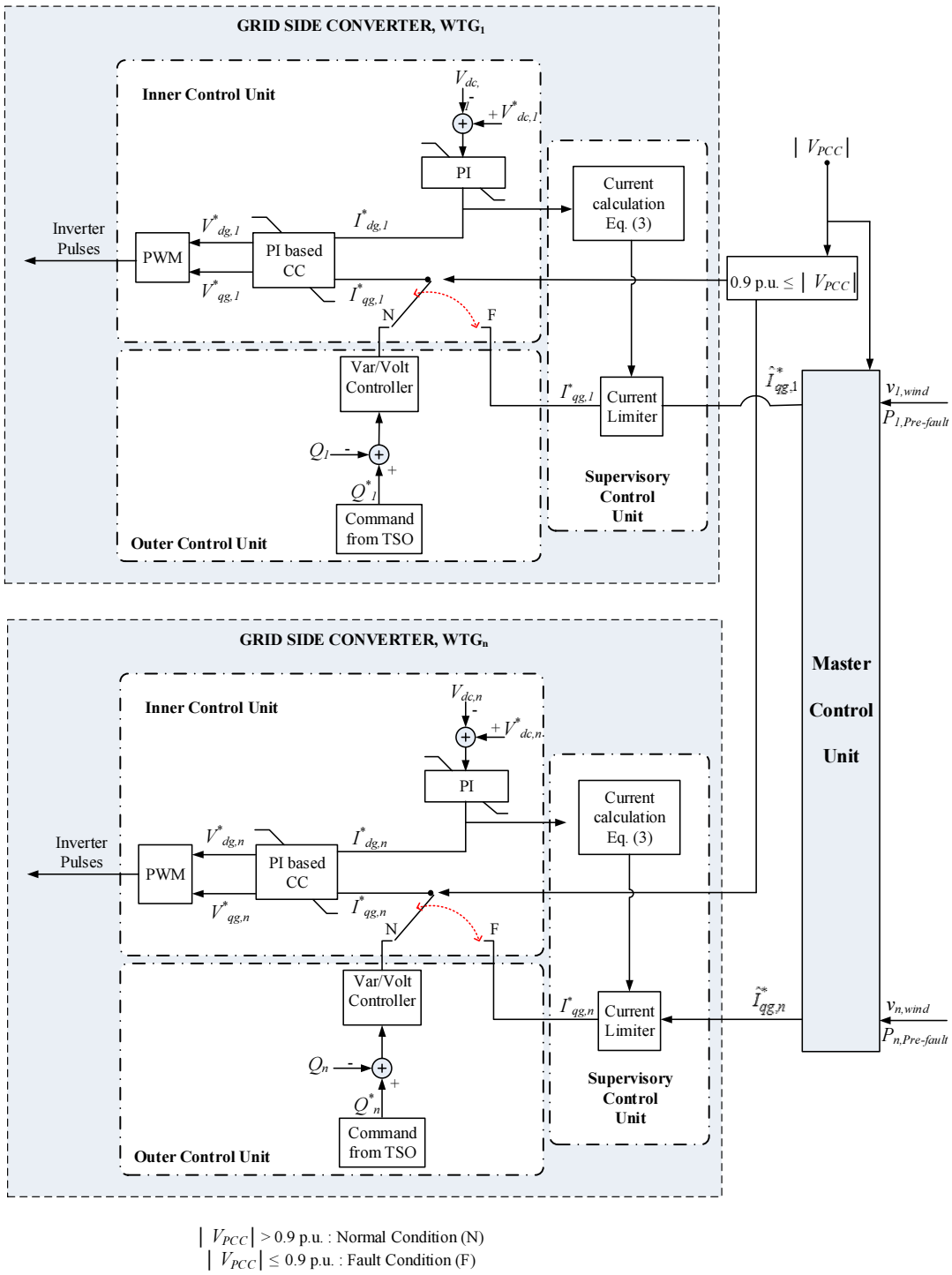

Figure 8-2 The proposed SPQC unit at the GSC of each FCWG.

For the purpose of this research, the WTG type 4 model with volt/var control at GSC based on [104, 105] is implemented. Data received from MCU ($\tilde{I}^*_{qg}$) are then fed into SPQC unit of each FCWGs. Salient properties of the proposed SPQC are as follows:

1) The active and reactive power produced by the machine is calculated using Equation (7-1) and then compared to their command values. The optimal power-speed curve dictates the active power command signal, P^* [104, 105] and the reactive power command Q^* signal depends on requirement stated in the grid codes. As an example, the Australian network authority requires the power factor to be between 0.93 capacitive and 0.93 inductive [129].

2) Using Clarke's transformation, the measured three phase signal is projected into the space vector domain.

3) During normal operation (0.9 p.u. < $|V_g|$ < 1.1 p.u.), the I^*_{qg} and I^*_{dg} signals are calculated from the error signals of ΔP_g and ΔQ_g feeding to the PI compensators. However, if the supply voltage drops below 0.9 p.u., then the I^*_{qg} data from MCU is fed to the current control loop at the GSC of each machine.

4) In the case of fault, the control block for the direct quadrature component remains similar to normal condition. However, the I^*_{dg} will be somehow increased to compensate for the voltage drop received at the generator terminal. Therefore, this available I^*_{dg} signal is sequentially fed into the current prioritization block to calculate the available amount of I^*_{qg} using (3). The available I^*_{qg} signal is then matched with $\hat{I}^*_{qg}$ signal from MCU in the current limiter block before it is fed into the current controller unit (Figure 8-2). It is worth to notice that, the maximum capacity of the power converter will also determine the maximum allowed level of the injected I^*_{qg}.

5) Lastly, the error signal calculated from GSC current vector and its references is fed to the PI-based current controller to produce the switching

gate signals for the aforementioned converter.

8.2.2 Look up table

Figure 8-3 shows the baseline data that includes the actual $V_{dc,max}$ as a function of the default active power output ($P_{Pre\text{-}fault}$) for different voltage sags. This data represent the condition of FCWGs at different wind speed (6m/s – 25m/s) when experiencing 50% voltage sag for 500ms.

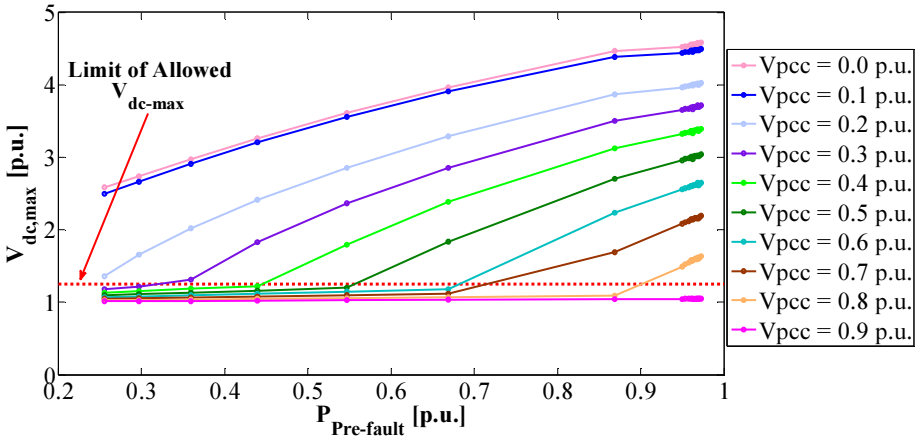

Figure 8-3 Baseline data for determining the look up table data.

In this figure, the red-dashed-line shows the limit of allowed maximum DC link voltage to avoid the failure at the power converter. Typically it is 25% higher than the rated DC link voltage [116, 130]. For the sake of clarity, Table 8-1 depicts the selected critical points of the DC link voltage during the aforementioned fault condition. These points are arranged based on the severity of the fault and Table 8-1 only shows the closest value to the limit of $V_{dc,max}$. In Figure 8-3, as the voltage sag falls below 30%, the DC link voltage exceeds the 1.25 p.u. in any wind speed level. Therefore Table 8-1 only presents data for voltage sags larger than 0.3 p.u.

Based on the DC link voltage profile, the look up table data for determining I^*_{qg} (Figure 8-5) is constructed. Figure 8-4 illustrates several possible strategies to be considered in relation to mapping the $V_{dc,max}$ and I^*_{qg} while Table 8-2 summarizes these aforementioned strategies.

Table 8-1 Selected critical point for $V_{DC\text{-}Link} \leq 1.25$ p.u.

V_{PCC} [p.u.]	$P_{Pre\text{-}fault}$ [p.u.]	$V_{DC\text{-}Link}$ [p.u.]
0.3	0.2971	1.2128
0.4	0.4394	1.2238
0.5	0.5469	1.2001
0.6	0.5469	1.1442
0.7	0.6687	1.119
0.8	0.8688	1.0929
0.9	0.9727	1.049

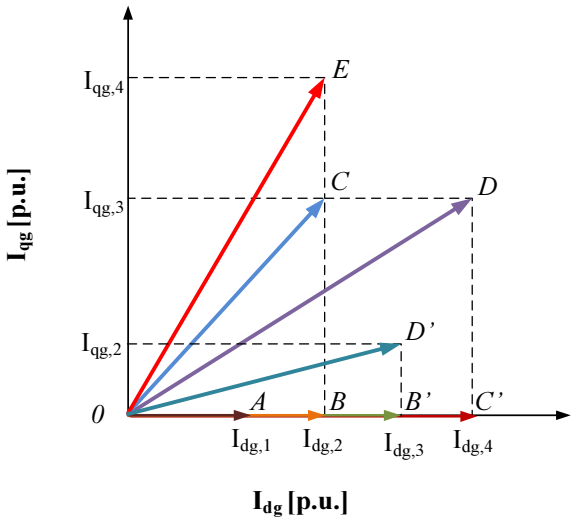

Figure 8-4 Illustration of possible strategies (A - E, B' - D') in determining I^*_{qg} for look up table data.

Table 8-2 Possible applied strategies in the proposed SPQC

Strategy	**Description**
A	$I_{dg} \leq I_{c,max}$; $I_{qg} = I_{qg,1} = 0$ p.u. ; $V_{dc,max} = 1$ p.u.
B	$I_{dg} \leq I_{c,max}$; $I_{qg} = I_{qg,1} = 0$ p.u. ; $V_{dc,max} \leq 1.25$ p.u.
C	$I_{dg} \leq I_{c,max}$; $I_{qg} = I_{qg,3}$; $V_{dc,max} \leq 1.25$ p.u.
D	$I_{dg} \geq I_{c,max}$; $I_{qg} = I_{qg,3}$; $V_{dc,max} = 1.25$ p.u.
E	$I_{dg} \leq I_{c,max}$; $I_{qg} = I_{qg,4}$; $V_{dc,max} = 1.25$ p.u.
B'	$I_{dg} = I_{c,max}$; $I_{qg} = I_{qg,1} = 0$ p.u. ; $V_{dc,max} \leq 1.25$ p.u.
C'	$I_{dg} \geq I_{c,max}$; $I_{qg} = I_{qg,1} = 0$ p.u. ; $V_{dc,max} = 1.25$ p.u.
D'	$I_{dg} = I_{c,max}$; $I_{qg} = I_{qg,2}$; $V_{dc,max} = 1.25$ p.u.

The following points should be considered in selecting the proper strategy:

- ***For wind speeds causing*** $\hat{I}^*_{dg}$ ***<*** $I_{c,max}$ ***(i.e 1.1 p.u.) and*** $V_{dc,max}$ ***(during fault) < 1.25 p.u.-*** Under normal operating condition, FCWGs are working on unity power factor (Figure 8-4) therefore the direct and quadrature current components are under Strategy A and moved to Strategy B on the occurance of the fault. With $I_{dg,2} < I_{max}$, the wind turbine has available capacity to inject reactive current component, $I_{qg,2}$ (Strategy C). The GSC applies the voltage oriented control scheme and the active current component I^*_{dg} is generated by the PI-based voltage controller. $V_{dc,max}$ determines the condition of I^*_{dg}, based on the following formula [109]:

$$P_g = \frac{3}{2} V_{dg} I_{dg} = V_{dc} I_{dc} \tag{8-1}$$

Since the allowed limit of $V_{dc,max}$, is set to 1.25 p.u., then the real current component can be increased to $I_{dg,4}$ (Strategy D) considering that the ratio of $\frac{\Delta I_{dg}}{\Delta V_{dc}}$ remains constant. Therefore, the formula for ratio calculation is:

$$\frac{\Delta I_{dg}}{\Delta V_{dc}} = \frac{I_{dg,2} - I_{dg,1}}{V_{dc,\max 2} - V_{dc,\max 1}} = \frac{I_{dg,3} - I_{dg,2}}{V_{dc,\max 3} - V_{dc,\max 2}}. \tag{8-2}$$

However, due to low wind speed, the maximum real current component to deliver during fault is $I_{dg,2}$. Therefore using Equation (5-3), the operating point of the wind turbine within this range of speed is set to Strategy E.

- ***For wind speeds causing*** $\hat{I}^*_{dg}$ ***to reach*** $I_{c,max}$ ***(i.e 1.1 p.u.) but*** $V_{dc,max}$ ***(during fault) < 1.25 p.u.-*** This case is similar to the previous condition with the working point under normal condition set to strategy A (Figure 8-4) and then switched to Strategy B' when the fault occurs. Using Equation (5-3), the reactive current component can be increased to $I_{dg,4}$ to be able to reach the limit of $V_{dc,max}$ (Strategy C'). However, the maximum real current component to deliver is $I_{dg,3}$ which is similar to the I_{max}. Therefore, the amount of reactive current to inject during fault is $I_{qg,2}$ (Strategy D').

- ***For wind speeds causing*** $\hat{I}_{dg}^{*}$ ***to reach*** $I_{c,max}$ ***(i.e 1.1 p.u.) and*** $V_{dc,max}$ ***(during fault)*** $\geq$ ***1.25 p.u.-*** For this case, as the fault occurs, the limit of $V_{dc,max}$ has been reached or exceeded. Therefore there are three possible actions to take; (i) do not inject any reactive current, (ii) sacrifice a small amount of active power produced from the wind turbine following the requirements from the referenced grid codes based on (5) and (iii) applying additional protection equipment such as braking chopper etc. Since this research is aimed to maximize the amount of active power delivered to the network then the first option is chosen. In other word, active power is prioritized over reactive power.

Figure 8-5 shows the reactive current components command as the output of the look up table at the MCU during fault for different wind ratings.

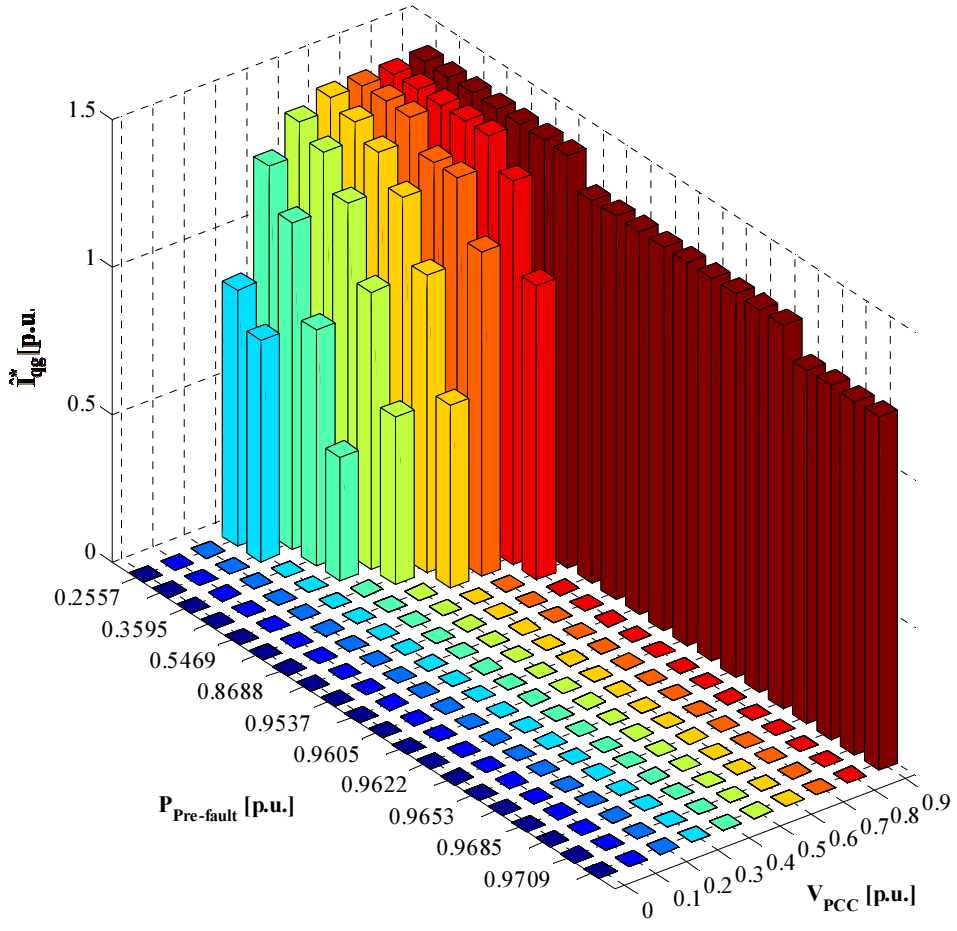

Figure 8-5 The output of look-up table at MCU.

As can be seen, the amount of $\tilde{I}_{qg}^{*}$ will be varied based on the severity of the sag at PCC (V_{PCC}) as well as the wind speed which is proportional to the pre-fault FCWGs output power $P_{Pre\text{-}fault}$. For example, with 10% sag, the wind turbines with less wind speed take over more responsibility in injecting reactive power. As the voltage drops to 0.5 p.u., a set of wind turbines with higher wind speeds are no longer required to inject reactive power in order to prevent converter DC link voltage violations.

8.3 SIMULATION RESULTS

The transient response of the proposed SPQC scheme has been investigated by running various scenarios using MATLAB/Simulink. Figure 8-6 shows the schematic diagram of the simulated system and the details of machine parameters are presented in the Appendix A. A 5km transmission line and a step up transformer connect the set of five 2.0-MW FCWGs with different levels of wind speed to the medium-voltage bus (B25). Table 8-3 shows wind speed profiles for each FCWG. A 20km transmission line connects the distribution feeder (B25) and its local load to the main grid (B120). A type A1 fault [112] is applied at the grid and cleared after 500ms for four different cases presented in Table 8-4. Detailed simulations are performed to examine the FRT capabilities of FCWG with the proposed SPQC at different levels of wind speed, as well as its positive impacts on the nearby grid.

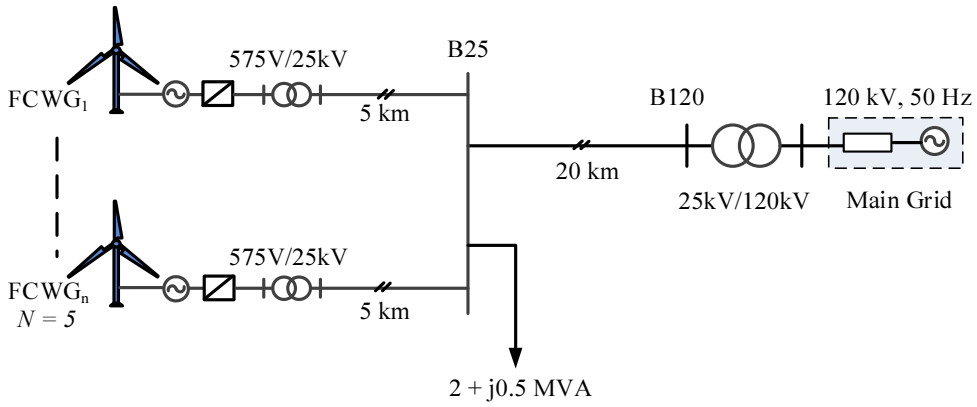

Figure 8-6 Schematic of the simulated system.

Table 8-3 Wind speed level of each FCWG.

Wind Turbines	Wind Speed (m/s)
FCWG 1	14
FCWG 2	12
FCWG 3	10
FCWG 4	8
FCWG 5	6

Table 8-4 Simulated case studies.

Case	Definition
Case 1	Without SPQC and rated I_{max}
Case 2	Without SPQC and increased I_{max}
Case 3	With SPQC and rated I_{max}
Case 4	With SPQC and increased I_{max}

8.3.1 FRT response of FCWG

Most grid codes require the wind farms to remain scheme intact during the fault as well as to contribute to the stability of the network, during fault and afterwards. Thus, it is compulsory for the wind turbine to operate within its safety range while maximizing its potentials. The proposed SPQC is aimed to gain these two main objectives.

As discussed in the previous section, the SPQC is activated on the occurrence of the fault in the network. Figure 8-7 depicts the output of MCU for the applied faults of Cases 3 and 4 to show PQ responses of each FCWG. When a sensor at MCU detects 50% voltage sag at PCC, SPQC is activated to send commands to each FCWG in order to request a certain amount of reactive power based on their individual actual wind speeds. Figure 8-7 (a and c) show the output of MCU for rated I_{max} and increased capacities, respectively. Note that based on Figure 8-7, the FCWG with the lowest wind speed (i.e. 6m/s) can afford up to 1.4 p.u. of I^*_{qg} to respond 0.5 p.u. voltage drop, while for higher levels of wind speed, MCU sends lower I^*_{qg} signals. Since Case 4 allows for a larger current capacity during the fault; therefore, more reactive power demand can be injected by each FCWG. Figure 8-7 (b and d) consecutively shows I^*_{dg} at each GSC of FCWG for Case 3 and 4, respectively.

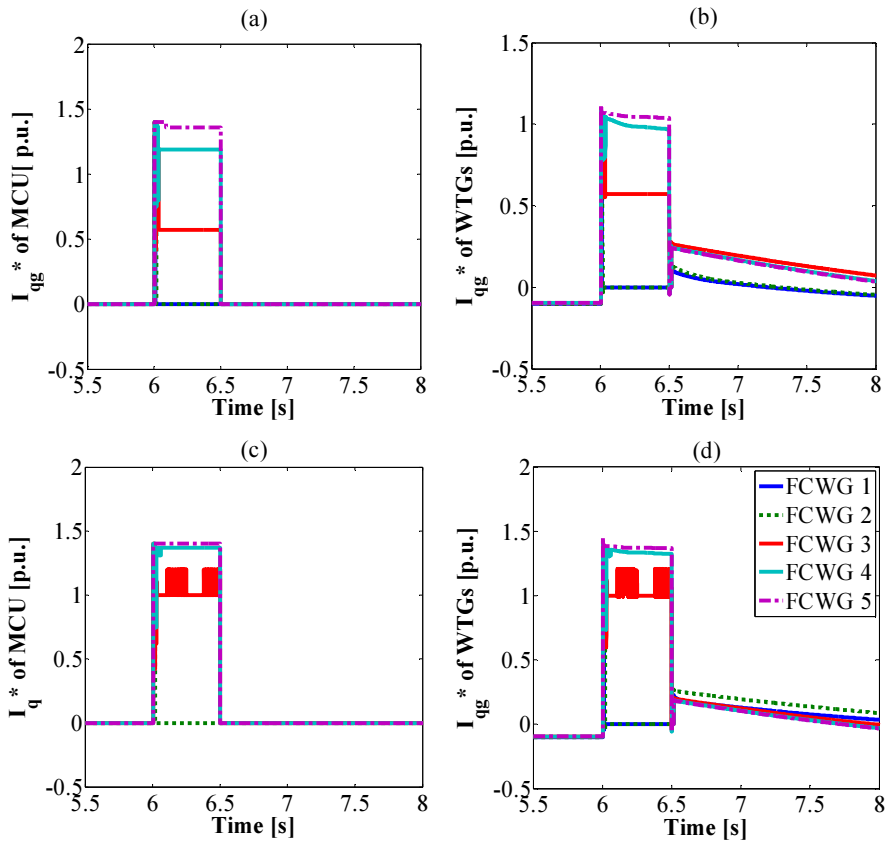

Figure 8-7 Reactive power current components for Case 3. (a) I^*_{qg} as output of MCU. (b) I^*_{qg} as output of FCWGs. Reactive power current components for Case 4. (c) $I_{qg}{}^*$ as output of MCU and (d) I^*_{qg} as output of FCWGs.

In the process of stabilizing the network, the wind turbine is also required to have decent level of protection scheme to safeguard its converter from overloading that may lead to an excessive DC link voltage. As shown in Figure 8-8, with Case 4 the DC link voltage can be maintained below its limit (1.25 p.u.) as compared to other cases. However, for FCWGs with wind speed above their nominal values (i.e.14m/s), the DC link voltage is slightly above its limit. This is due to the duration of the fault causing the MSC to keep generating power while the GSC is only able to deliver certain amount of power to the grid. As a result, there is an excessive power produced causing an increase in the DC link voltage. There are several options to tackle this problem:

(i) Implementing a responsive control scheme that realizes the instantaneous power transfer during the fault [39, 79, 116]

(ii) Applying protection equipment such as braking resistor [107].

Prioritization of active power over reactive power or vice versa will depend on the requirements set by the TSO. Since the scope of this study is to maximize the amount of active power delivers during the fault, the impact of grid codes requirement is not shown here.

It is also important to keep in mind that in maintaining the DC link voltage within its safety range, the wind turbine also needs to have a proper internal control system that ensures the power produced is similar to the power delivered to the network. In this simulation, modification is only applied at the outer control part without modifying the inner control part. However, there are significant reductions in the excessive DC link voltage during fault when the proposed SPQC is implemented as shown in Figure 8-8.

Figure 8-9 presents the active and reactive power distribution over FCWGs having different levels of wind speed. Both in Case 3 and Case 4 when SPQC is applied, the active power recovers back to stable region faster as compared to the Case 1 and Case 2 with conventional control scheme.

It is interesting to see that for FCWGs with wind speed of 10, 8 and 6m/s, the produced active power (P_g) tends to reach its normal state while for the other two FCWGs (12 and 14m/s), the steady P_g during fault is reached only for Case 4. Based on these results, the proposed SPQC can improve the amount of active and reactive power support such that the FCWGs support the stability of the adjacent network during and right after fault clearance.

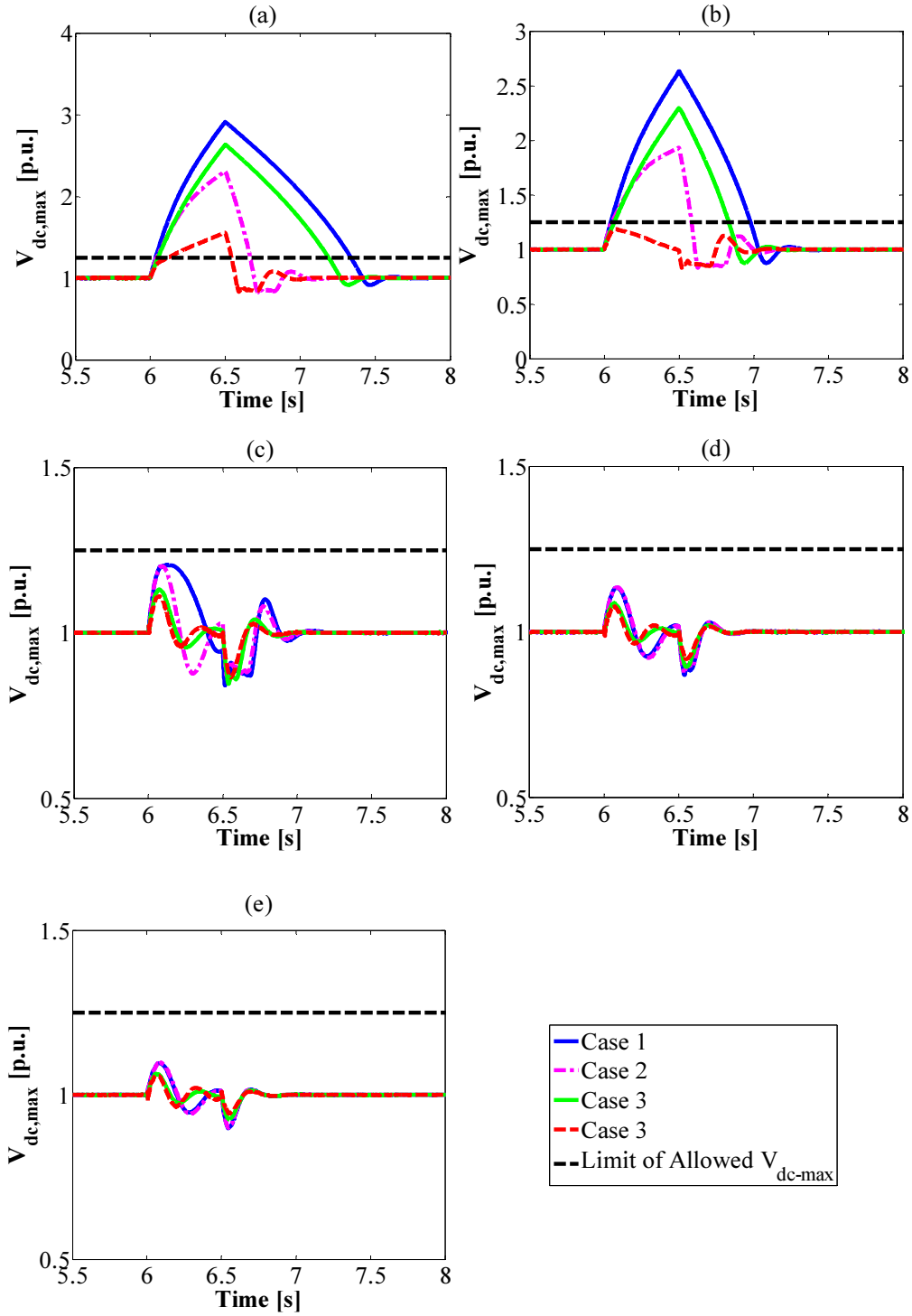

Figure 8-8 DC link voltage profiles of FCWGs for different case studies with wind speeds of: (a) 4m/s; (b) 12m/s; (c) 10m/s; (d) 8m/s; (e) 6m/s.

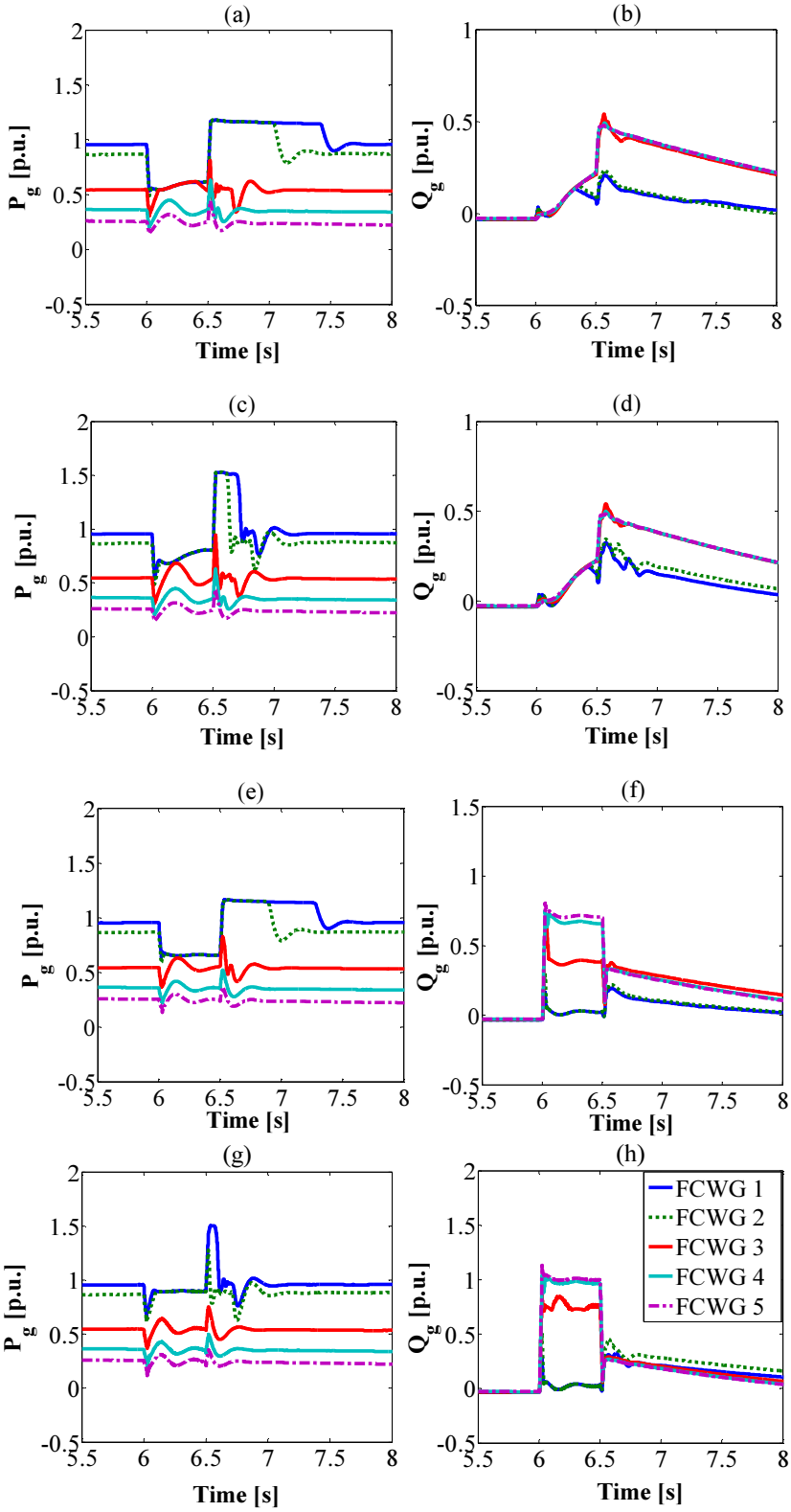

Figure 8-9 *PQ* response of FCWG for four different cases; (a)-(b) Case 1, (c)-(d) Case 2, (e)-(f) Case 3, (g)-(h) Case 4.

Moreover in detail for Case 1, the introduction of Type A1 fault [112] into the network causes the active power to drop to about 0.6 p.u. for FCWGs with wind speeds of 14m/s and 12m/s while other machines try to maintain their output active power similar to normal condition. As for reactive power, wind turbine with low wind rate tries to compensate the voltage drop by increasing a slightly more reactive power as compared to the higher level wind speeds. When the fault is cleared, this reactive power level soared to about 0.5 p.u. for FCWGs with wind speeds of 6, 8 and 10m/s and to about 0.2 p.u. for wind speeds of 12 and 14m/s. A similar trend for active power is also shown for Case 4 when the capacity of converter is increased up to 41%. However, the wind turbines are able to deliver more active and reactive power during and after fault clearance as compared to the Case 1. Clearly, an improvement in active power profile is obviously seen particularly for FCWGs with wind speeds of 14m/s and 12m/s.

8.3.2 Impacts of FCWGs on the nearby grid

The next demanding precaution of the recent grid codes is the contribution of the wind farm to help stabilize the network. Figure 8-10 shows the comparison of FRT curve for the four simulated control schemes. As the type A_1 voltage sags is sensed at PCC (B25), the voltage drop reaches 0.5 p.u. and slowly stabilizes when the fault is cleared. A significant improvement in voltage profile at PCC is achieved after the implementation of the proposed SPQC (Cases 3 and 4). Without SPQC, the voltage spans from 0.5 p.u. to about 0.55 p.u. for both Cases 1 and 2. With SPQC, the voltage increases to about 0.6 p.u. for wind turbines with rated capacity while an increase in converter capacity will also contribute to a higher voltage level, i.e. approximately 0.65 p.u. Table 8-5 also shows the profiles of the load connected at PCC. Among all simulated cases, the proposed SPQC with an extended capacity (Case 4) offers the best level of active and reactive power support to the network.

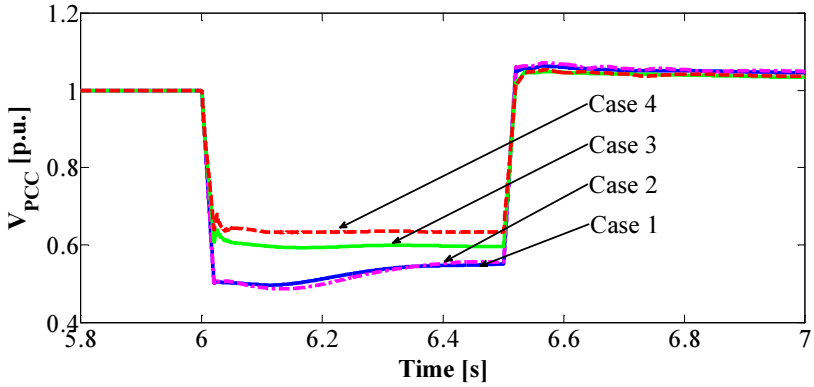

Figure 8-10 Voltage profiles at the PCC (B25) when a type A_1 fault is applied.

Table 8-5 Network Profiles at PCC Subject to the Type A1 Fault.

Simulation	V_{B25} [p.u]	V_{Load} [p.u]	P_{Load} [MW]	Q_{Load} [MVar]
Case 1	0.5004	0.4974	0.4937	0.1242
Case 2	0.5008	0.4978	0.4945	0.1243
Case 3	0.6068	0.6031	0.7293	0.1831
Case 4	0.6374	0.6335	0.8057	0.2029

Based on the above presented detailed simulations, it can be concluded that the proposed SPQC significantly utilizes the FCWGs to improve network performances during the fault. With the additional capacity extension of power converter, the FCWG is allowed to deliver more active power as compared to the conventional case while increasing its FRT capability.

8.4 CONCLUSION

This chapter proposes a new SPQC scheme for FCWGs to participate in the stability of the grid during fault events. The *PQ* capability of the FCWG is also extensively studied in accordance to the proposed control action. Simulation results confirm that the reactive power injection can be distributed across the FCWGs considering the ratio $\frac{\Delta I_{dg}}{\Delta V_{dc}}$ constant, where the FCWGs with lower wind speeds can provide more reactive power to the network. In addition, the proposed control scheme can also significantly reduce the level of DC link voltage while maximizing the output power injected to the nearby grid during and after the fault. Lastly, SPQC will also enhance the voltage profiles at PCC such that an optimal trade-off is achieved between the

network and machine capability. This has also been confirmed through detailed simulations by investigating the improvement in the FRT curve at PCC.

Chapter 9. Conclusions

This thesis proposes a new supervisory control scheme for full converter based WTGs in compliance with the latest international grid codes. The background, motivation and organization of this thesis are presented in Chapter 1. Literature review on grid connected full converter based WTGs is presented in Chapter 2. This chapter covers benefits of FCWGs over other wind turbine technologies as well as the latest trend of FCWGs utilization to meet international grid codes. The main research gaps that have motivated this research are also highlighted in this chapter.

Chapter 3 presents an up-to-date review of international grid codes in comparison with the Australian standards which is known as the most demanding one. The Australian grid codes refer to technical regulations set by the Australian Energy Market Operator (AEMO) and Western Power (WP) while the international standards includes regulations applied in several countries such as Canada (Hydro Quebec), Denmark (Energinet), Germany (Tennet), Ireland (EirGrid), Spain (REE), UK (NGET) and USA (WECC).

In Chapter 4, the transient responses of grid connected FCWGs are examined. Dynamic modelling and control of FCWGs is presented including general analysis on voltage control of FCWGs. In addition, theoretical analyses are also discussed to give supplementary justification on the simulation results. These results can assist in improving FRT capability of the FCWGs.

Chapter 5 addresses the extended PQ capability of FCWGs. The GSC control is assessed in order to temporarily increase the maximum converter current ability during the fault. The proposed schemes are in compliance with the Australian grid while also considering prioritization of reactive power over real power and vice versa

in order to give better perspectives in recovering voltage stability during fault event for network with FSIGs.

Chapter 6 investigates the benefit of interconnecting the weak network to the grid compliance FCWGs, previously explained in Chapter 5. The simulated weak network is developed in Matlab/Simulink and applying practical network data. The impacts of the proposed FCWGs are tested considering various fault types as well as fault locations within the weak network.

Chapter 7 of the thesis proposes an enhanced reactive power allocation methodology of FCWGs. The approach uses voltage drops at PCC and the wind speeds to define a power index for PQ control of FCWGs. Coordinated controllers allow distribution of reactive power support among FCWGs. The proposed power indexes are implemented both at the machine side and grid side controllers and are activated when voltage sag is detected at PCC. Detailed simulations are presented for a test system consisting of FCWGs connected to power grid subject to balanced and unbalanced faults. The proposed power indexes will not only distribute reactive power support among FCWGs but also reduce tear and wear of the DC link during fault onset.

Chapter 8 of the thesis recommends a new supervisory active and reactive power control (SPQC) that considers the individual FCWG wind speeds within the wind farm to improve the overall reactive power support to the network. The main idea is FCWG delivering less active power to inject more reactive power or temporarily increase their current ratings such that FCWG is able to help the nearby generators and loads to recover during severe fault conditions while working under safe operating area. The control command is centralized at the common point and the SPQC is independent of the wind turbine technology. Therefore, the proposed method may also be applied to other types of variable speed wind turbines. This will be beneficial for wind farm operator in providing reactive power support during fault among different level of wind speed.

Finally, this Chapter concludes the whole contents of the thesis by summarizing and highlighting main contributions and possible future research directions.

9.1 THESIS CONTRIBUTIONS

The main results of this thesis have been published in seven research papers as listed in Section 1.5. The primary contributions are as follow.

1) An up-to-date comparison of Australian grid codes with the other countries has been presented including discussion on recent issues in harmonization and grid code compliance.
2) A hypothesis on transient behavior of FCWTGs is defined considering both in symmetrical and asymmetrical faults. In addition, a comparative study on preliminary hypothesis and simulation results has been presented.
3) Enhanced reactive power control schemes to improve the FRT capabilities of FCWGs are explained, analyzed and compared to the conventional control schemes. A proposed enhanced reactive power control scheme is simulated to satisfy the most stringent reactive droop requirements, such as those listed in the Australian grid codes.
4) The main benefits of interconnecting the weak grid to the FCWTGs equipped with the proposed grid code compliant control schemes are also investigated. Detailed simulations results confirm the ability of the proposed control schemes to enhance the stability of the corresponding weak grid.
5) A coordinated reactive power allocation approach considering intermittent behavior of wind turbine is also proposed. Impacts on different fault types as well as reactive power droop are discussed in the simulation to confirm validity of the proposed method.
6) Finally, a new supervisory active and reactive power control (SPQC) for wind-park applications is proposed. The proposed SPQC ensures FCWGs are in compliance with the grid codes and ancillary services at PCC while working within their own safe operating margins. The novelty of the presented approach lies in the individual choice of set-points for the wind turbines in the park by taking into account their respective wind conditions.

9.2 FUTURE WORKS

The following topics are suggested for future research in continuation of this work.

1) Transient behaviors of other existing FCWG configurations are also important and need to be investigated. A popular example is FCWG equipped with multilevel converter or back-to-back converters.

2) It is also important to study the FCWGs having grid side controller other than PI-based current regulators, such as predictive methods.

3) Integration of mechanical protection (e.g. DC-choppers) and improved GSC control scheme are beneficial to reduce further excessive voltage at the DC link during extreme fault conditions.

4) A further investigation on transient response of FCWGs considering phase angle jump and extreme frequency excursions is also crucial. A further improvement on the system controllers is required to maintain system compliance with the recent grid codes.

5) There are future trends in the grid codes such as inertia emulation and power system stabilization. In order to be capable of adjusting with the new trends, a supplementary control loop incorporated into FCWGs in compliance with aforementioned requirements shall be suggested.

6) A more realistic power data with various generation units, load centers and communication systems shall be applied into the simulation. In this manner, a more accurate transient response on the proposed supervisory control of FCWGs can be achieved.

References

Every reasonable effort has been made to acknowledge the owners of copyright material. I would be pleased to hear from any copyright owner who has been omitted or incorrectly acknowledged.

[1] Global Wind Energy Council, " Global Wind Report: Annual Market Update 2013," April 2014. Available at http://www.gwec.net/publications/global-wind-report-2/global-wind-report-2013/.

[2] N. R. Ullah and T. Thiringer, "Variable Speed Wind Turbines for Power System Stability Enhancement," *IEEE Trans. Energy Conversion,* vol. 22, pp. 52-60, Mar. 2007.

[3] N. R. Ullah, T. Thiringer, and D. Karlsson, "Voltage and transient stability support by wind farms complying with the E.ON Netz grid code," *IEEE Trans. Power Systems*, vol. 22, no. 4, pp. 1647-1656, Nov. 2007.

[4] S. M. Muyeen, R. Takahashi, T. Murata, J. Tamura, M. H. Ali, Y. Matsumura, A. Kuwayama, and T. Matsumoto, "Low voltage ride through capability enhancement of wind turbine generator system during network disturbance," Renewable Power Generation, IET, vol. 3, pp. 65-74, Mar. 2009.

[5] S. M. Muyeen, R. Takahashi, T. Murata, and J. Tamura, "A Variable Speed Wind Turbine Control Strategy to Meet Wind Farm Grid Code Requirements," *IEEE Trans. Power Systems,* vol. 25, pp. 331-340, Feb. 2010.

[6] C. Zhe, J. M. Guerrero, and F. Blaabjerg, "A Review of the state of the art of power electronics for wind turbines," *IEEE Trans. Power Electronics*, vol. 24, no. 8, pp. 1859-1875, Aug. 2009.

[7] M. Tsili and S. Papathanassiou, “A review of grid code technical requirements for wind farms,” *IET Renewable Power Generation*, vol. 3, no. 3, pp. 308-332, Mar. 2009.

[8] M. Mohseni and S. M. Islam, “Review of international grid codes for wind power integration: Diversity, technology and a case for global standard,” *Renewable and Sustainable Energy Reviews*, vol. 16, no. 6, pp. 3876-3890, Apr. 2012.

[9] W. Christiansen and D. T. Johsen, “Analysis of requirements in selected grid codes,” Ørsted DTU, DK, Jan. 2006.

[10] F. Iov, A. D. Hansen, P. Sorensen, and N. A. Cutululis, “Mapping of grid faults and grid codes,” RISO National Laboratory, Tech. Univ. of Denmark, DK, Jul. 2007.

[11] AEMO. (2011, Oct.). Wind Integration: International Experience, WP2: Review of Grid Codes, A. E. M. Commission, AU.

[12] F. Blaabjerg, C. Zhe, and S. B. Kjaer, “Power electronics as efficient interface in dispersed power generation systems,” *IEEE Trans. Power Electronics*, vol. 19, no. 5, 1184-1194, Sep. 2004.

[13] F. Blaabjerg and M. Ke, "Future on Power Electronics for Wind Turbine Systems," *IEEE Journal Emerging and Selected Topics in Power Electronics,* vol. 1, pp. 139-152, Sep. 2013.

[14] F. Blaabjerg, M. Liserre, and M. Ke, "Power Electronics Converters for Wind Turbine Systems,"*, IEEE Trans. Industry Applications,* vol. 48, no. 2, pp. 708-719, Mar./Apr.2012.

[15] H. Polinder, J. A. Ferreira, B. B. Jensen, A. B. Abrahamsen, K. Atallah, and R. A. McMahon, "Trends in Wind Turbine Generator Systems," *IEEE Journal Emerging and Selected Topics in Power Electronics,* vol. 1, pp. 174-185, Sep. 2013.

[16] J. F. Conroy and R. Watson, “Low-voltage ride-through of a full converter wind turbine with permanent magnet generator,” *IET Renewable Power Generation*, vol. 1, no. 3, pp. 182-189, Sep. 2007.

[17] E. T. Ackermann, *Wind Power in Power System.* West Sussex, England: John Wiley & Sons, Ltd., 2005.

[18] H. Li and Z. Chen, “Overview of different wind generator systems and their comparisons,” *IET Renewable Power Generation*, vol. 2, no. 2, pp. 123-138, Jun. 2008.

[19] REN21. 2014. Renewables 2014 Global Status Report, REN21 Secretariat, Paris, FR.

[20] M. The Hon. Greg Hunt and M. The Hon. Ian Macfarlane. *Certainty and Growth for Renewable Energy*. Department of the Environment, Australian Government, 2015.

[21] Geoscience Australia and BREE. 2014. Australian Energy Resource Assessment. 2nd Ed, Geoscience Australia, Canberra, AU.

[22] L. Holdsworth, I. Charalambous, J. B. Ekanayake, and N. Jenkins, "Power system fault ride through capabilities of induction generator based wind turbines," *Wind Engineering,* vol. 28, pp. 399-409, Jan. 2004.

[23] R. Grunbaum, P. Halvarsson, D. Larsson, and P. R. Jones, "Conditioning of power grids serving offshore wind farms based on asynchronous generators," in *Proc. Power Electronics, Machines and Drives,* 2004, pp. 34-39 Vol.1.

[24] H. Gaztanaga, I. Etxeberria-Otadui, D. Ocnasu, and S. Bacha, "Real-Time Analysis of the Transient Response Improvement of Fixed-Speed Wind Farms by Using a Reduced-Scale STATCOM Prototype," *IEEE Trans. Power Systems,* vol. 22, pp. 658-666, Mar. 2007.

[25] M. Molinas, J. A. Suul, and T. Undeland, “Low voltage ride through of wind farms with cage generators: STATCOM versus SVC,” *IEEE Trans. Power Electronics*, vol. 23, no. 3, pp. 1104–1117, May 2008.

[26] H M. J. Hossain, H. R. Pota, V. A. Ugrinovskii, and R. A.Ramos, “Simultaneous STATCOM and pitch angle control for improved LVRT capability of fixed-speed wind turbines,” *IEEE Trans. Sustainable Energy*, vol. 1, no. 3, pp. 142–151, Oct. 2010.

[27] Z. Chen, Y. Hu and F. Blaabjerg, “Stability improvement of induction generator-based wind turbine systems,” *IET Renewable Power Generation*, vol. 1, no. 1, pp. 81–93, Mar. 2007.

[28] W. Freitas, A. Morelato, and W. Xu, “Improvement of induction generator stability using braking resistors,” *IEEE Trans. Power Systems*, vol. 19, no. 2, pp. 1247–1249, May 2004.

[29] S. Nomura, Y. Ohata, T. Hagita, H. Tsutsui, S. Tsuji-Iio, and R. Shimada, “Wind farms linked by SMES systems,” *IEEE Trans. Applied Superconductivity*, vol. 15, no. 2, pp. 1951–1954, Jun. 2005.

[30] S. M. Muyeen, M. Hasan Ali, R. Takahashi, T. Murata, J.Tamura, Y. Tomaki, A. Sakahara, and E. Sasano, “Comparative study on transient stability analysis of wind turbine generator system using different drive train models,” *IET Renewable Power Generation*, vol. 1, no. 2, pp. 131–141, Jun. 2007.

[31] IEA, 2009 *IEA wind annual report*, May 2010. Available: http://www.ieawind.org.

[32] J. Chi and W. Peng, "Enhancement of low voltage ride-through capability for wind turbine driven DFIG with active crowbar and battery energy storage system," in *Proc. IEEE Power and Energy Society General Meeting,* 2010, pp. 1-8.

[33] D. Chwa and K. B. Lee, "Variable Structure Control of the Active and Reactive Powers for a DFIG in Wind Turbines," *IEEE Trans Industry Applications,* vol. 46, pp. 2545-2555, Nov./Dec 2010.

[34] M. Mohseni and S. Islam, "An improved modeling and control approach for DFIG-based wind generation systems," in *Proc. Australasian Universities Power Engineering Conf.,*2009, pp. 1-6.

[35] C. Feltes, S. Engelhardt, J. Kretschmann, J. Fortmann, and I. Erlich, "Dynamic performance evaluation of DFIG-based wind turbines regarding new German grid code requirements," *Proc. IEEE Power and Energy Society General Meeting,* 2010, pp. 1-7.

[36] A. D. Hansen and G. Michalke, "Multi-pole permanent magnet synchronous generator wind turbines' grid support capability in uninterrupted operation during grid faults," *IET Renewable Power Generation,* vol. 3, pp. 333-348, Sept. 2009.

[37] G. Ramtharan, A. Arulampalam, J.B. Ekanayake, F.M. Hughes and N. Jenkins, "Fault ride through of fully rated converter wind turbines with AC and DC transmission," *IET Renewable Power Generation,* vol. 3, pp. 426-438, Dec. 2009.

[38] J. Li, Zhuying, X. He, and H. Xu, "Study on low voltage ride through characteristic of full power converter direct-drive wind power system," in *Proc. IEEE 6th Inter. Power Electronics and Motion Control Conf.*, 2009, pp. 2213-2216.

[39] D. Jingya, X. Dewei, W. Bin, and N. R. Zargari, "Unified DC-link current control for low-voltage ride-through in current-source-converter-based wind energy conversion systems," *IEEE Trans. Power Electronics*, vol. 26, no. 1, pp. 288-297, Jan. 2011.

[40] C. H. Ng, R. Li and J. Bumby, "Unbalanced-Grid-Fault Ride-Through Control for a Wind Turbine Inverter," *IEEE Trans. Industry Applications,* vol. 44, pp. 845-856, May/June 2008.

[41] M. Liserre, R. Cardenas, M. Molinas, and J. Rodriguez, "Overview of Multi-MW Wind Turbines and Wind Parks," *IEEE Trans. Industrial Electronics, ,* vol. 58, pp. 1081-1095, Apr. 2011.

[42] A. D. Hansen, F. Iov, F. Blaabjerg, and L. H. Hansen, "Review of Contemporary Wind Turbine Concepts and their Market Penetration," *Wind Engineering,* vol. 28, pp. 247-263, May. 2004.

[43] J. Sang-Yong, J. Hochang, H. Sung-Chin, J. Hyun-Kyo, and L. Cheol-Gyun, "Optimal Design of Direct-Driven PM Wind Generator for Maximum Annual Energy Production," *Magnetics, IEEE Transactions on,* vol. 44, pp. 1062-1065, Jun. 2008.

[44] S. M. Muyeen, R. Takahashi, and J. Tamura, "Operation and Control of HVDC-Connected Offshore Wind Farm," *IEEE Trans. Sustainable Energy,* vol. 1, pp. 30-37, Apr. 2010.

[45] Q. Ronghai, L. Yingzhen, and W. Jin, "Review of Superconducting Generator Topologies for Direct-Drive Wind Turbines," *IEEE Trans. Applied Superconductivity,* vol. 23, pp. 5201108-5201108, Jun. 2013.

[46] *SeaTitan™ 10 MW Wind Turbine*, AMSC, 2012. [Online]. Available: www.amsc.com.

[47] R. Carriveau. (2012, Nov. 21), *Advances in Wind Power*. [Online]. Available: http://www.intechopen.com

[48] J. Lloberas, A. Sumper, M. Sanmarti, and X. Granados, "A review of high temperature superconductors for offshore wind power synchronous generators," *Renewable and Sustainable Energy Reviews,* vol. 38, pp. 404-414, Oct. 2014.

[49] *ENERCON wind energy converters: Technology & Service*. ENERCON GmbH., 2014. [Online]. Available: www.enercon.de/p/downloads/EN_Eng_TandS_0710.pdf

[50] A. D. Hansen and G. Michalke, "Modelling and control of variable-speed multi-pole permanent magnet synchronous generator wind turbine," *Wind Energy,* vol. 11, pp. 537-554, May 2008.

[51] V. Akhmatov, "Analysis of dynamic behaviour of electric power systems with large amount of wind power," Ph.D. dissertation, Technical Univ. Denmark, Lyngby, 2003.

[52] J. Conroy and R. Watson, "Aggregate modelling of wind farms containing full-converter wind turbine generators with permanent magnet synchronous

machines: transient stability studies," *IET Renewable Power Generation,* vol. 3, pp. 39-52, Mar. 2009.

[53] D. S. Oliveira, M. M. Reis, C. Silva, L. Colado Barreto, F. Antunes, and B. L. Soares, "A Three-Phase High-Frequency Semicontrolled Rectifier for PM WECS," *Power Electronics, IEEE Transactions on,* vol. 25, pp. 677-685, Mar. 2010.

[54] A. Faulstich, J. K. Stinke, and F. Wittwer, "Medium voltage converter for permanent magnet wind power generators up to 5 MW," in *Proc. European Conf. Power Electronics and Applications,* 2005, pp. 9.

[55] S. Kouro, M. Malinowski, K. Gopakumar, J. Pou, L. G. Franquelo, W. Bin*, et al.*, "Recent Advances and Industrial Applications of Multilevel Converters," *IEEE Trans. Industrial Electronics,* vol. 57, pp. 2553-2580, Aug. 2010.

[56] V. Yaramasu, W. Bin, M. Rivera, and J. Rodriguez, "A New Power Conversion System for Megawatt PMSG Wind Turbines Using Four-Level Converters and a Simple Control Scheme Based on Two-Step Model Predictive Strategy-Part II: Simulation and Experimental Analysis," *IEEE Journal Emerging and Selected Topics in Power Electronics,* vol. 2, pp. 14-25, Mar. 2014.

[57] M. Cheng and Y. Zhu, "The state of the art of wind energy conversion systems and technologies: A review," *Energy Conversion and Management,* vol. 88, pp. 332-347, Dec. 2014.

[58] C. Jiawei, C. Jie, and G. Chunying, "On Optimizing the Aerodynamic Load Acting on the Turbine Shaft of PMSG-Based Direct-Drive Wind Energy Conversion System," *IEEE Trans. Industrial Electronics,* vol. 61, pp. 4022-4031, Aug. 2014.

[59] Z. Zhang, Y. Zhao, W. Qiao, and L. Qu, "A Space-Vector-Modulated Sensorless Direct-Torque Control for Direct-Drive PMSG Wind Turbines," *IEEE Trans. on Industry Applications,* vol. 50, pp. 2331-2341, Jul.-Aug. 2014.

[60] Z. Yue, W. Chun, Z. Zhe, and Q. Wei, "A Review on Position/Speed Sensorless Control for Permanent-Magnet Synchronous Machine-Based Wind Energy Conversion Systems," *IEEE Journal Emerging and Selected Topics in Power Electronics,* vol. 1, pp. 203-216, Dec. 2013.

[61] C.-M. Hong, C.-H. Chen, and C.-S. Tu, "Maximum power point tracking-based control algorithm for PMSG wind generation system without mechanical sensors," *Energy Conversion and Management,* vol. 69, pp. 58-67, May 2013.

[62] Q. Wei, Y. Xu, and G. Xiang, "Wind Speed and Rotor Position Sensorless Control for Direct-Drive PMG Wind Turbines," *IEEE Trans. Industry Applications,* vol. 48, pp. 3-11, Jan.-Feb. 2012.

[63] Z. Dawei and X. Lie, "Direct Power Control of DFIG With Constant Switching Frequency and Improved Transient Performance," *IEEE Trans. Energy Conversion, actions on,* vol. 22, pp. 110-118, Mar. 2007.

[64] F. Valenciaga and P. F. Puleston, "High-Order Sliding Control for a Wind Energy Conversion System Based on a Permanent Magnet Synchronous Generator," *IEEE Trans. Energy Conversion,* vol. 23, pp. 860-867, Sept. 2008.

[65] R. Melicio, V. M. F. Mendes, and J. P. S. Catalao, "Harmonic assessment of variable-speed wind turbines considering a converter control malfunction," *IET. Renewable Power Generation,* vol. 4, pp. 139-152, Mar. 2010.

[66] H. Weihao, C. Zhe, W. Yue, and W. Zhaoan, "Flicker Mitigation by Active Power Control of Variable-Speed Wind Turbines With Full-Scale Back-to-Back Power Converters," *IEEE Trans. Energy Conversion,* vol. 24, pp. 640-649, Sep. 2009.

[67] A. Mullane and G. Lightbody, "Wind-turbine fault ride-through enhancement," in *Power Engineering Society General Meeting, 2006. IEEE*, 2006, p. 1 pp.

[68] D. Jingya, D. D. Xu, and W. Bin, "A Novel Control Scheme for Current-Source-Converter-Based PMSG Wind Energy Conversion Systems," *IEEE Trans. Power Electronics,* vol. 24, pp. 963-972, Apr. 2009.

[69] M. Popat, W. Bin, and N. R. Zargari, "Fault Ride-Through Capability of Cascaded Current-Source Converter-Based Offshore Wind Farm," *IEEE Trans. Sustainable Energy,* vol. 4, pp. 314-323, Apr. 2013.

[70] S. M. Muyeen, R. Takahashi, T. Murata, and J. Tamura, "Integration of an Energy Capacitor System With a Variable-Speed Wind Generator," *IEEE Trans. Energy Conversion,* vol. 24, pp. 740-749, Sep. 2009.

[71] H. M. Hasanien and S. M. Muyeen, "Design Optimization of Controller Parameters Used in Variable Speed Wind Energy Conversion System by Genetic Algorithms," *IEEE Trans. Sustainable Energy,* vol. 3, pp. 200-208, Apr. 2012.

[72] W. Rebizant, J. Szafran, A. Wiszniewski, *Digital Signal Processing in Power System Protection and Control.* London : Springer, 2011.

[73] S. Alepuz, A. Calle, S. Busquets-Monge, S. Kouro, and W. Bin, "Use of Stored Energy in PMSG Rotor Inertia for Low-Voltage Ride-Through in Back-to-Back NPC Converter-Based Wind Power Systems," *IEEE Trans. Industrial Electronics,* vol. 60, pp. 1787-1796, May 2013.

[74] L. Jeong-Phil, P. Byung-Jun, H. Young-Hee, J. Se-yong, and S. Tae-Hyun, "Energy Loss by Drag Force of Superconductor Flywheel Energy Storage System With Permanent Magnet Rotor," *IEEE Trans. Magnetics,* vol. 44, pp. 4397-4400, Nov. 2008.

[75] J. Hee-Yeol, A. R. Kim, K. Jae-Ho, P. Minwon, Y. In-Keun, K. Seok-Ho*, et al.*, "A Study on the Operating Characteristics of SMES for the Dispersed Power Generation System," *IEEE Trans. Applied Superconductivity,* vol. 19, pp. 2028-2031, Jun. 2009.

[76] I. Ngamroo and T. Karaipoom, "Cooperative Control of SFCL and SMES for Enhancing Fault Ride Through Capability and Smoothing Power Fluctuation

of DFIG Wind Farm," *IEEE Trans. Applied Superconductivity,* vol. 24, pp. 1-4, Oct. 2014.

[77] *W. Tong, Wind power generation and wind turbine design.* Southampton : WIT Press, 2010

[78] Y. Xibo and L. Yongdong, "Control of variable pitch and variable speed direct-drive wind turbines in weak grid systems with active power balance," *IET. Renewable Power Generation,* vol. 8, pp. 119-131, Mar. 2014.

[79] Y. Jun, L. Hui, L. Yong, and C. Zhe, "An improved control strategy of limiting the DC-link voltage fluctuation for a doubly fed induction wind generator," *IEEE Trans. Power Electronics*, vol. 23, no. 3, pp. 1205-1213, May. 2008.

[80] *PM 3100 Data Sheet*, AMSC, 2012. [Online]. Available: http://www.amsc.com/pdf/PM3100W_DataSheet.pdf.

[81] *SEMISTAK Wind/Solar,* Semikron, Mar. 2010.

[82] *ENTSO-E Network Code for Requirements for Grid Connection Applicable to all Generator,* ENTSO-E, Brussels, Belgia. Mar 2013

[83] R. Teodorescu, M. Liserre, and P. Rodriguez, *Grid converters for photovoltaic and wind power systems*. Chichester, West Sussex : Wiley, 2011

[84] Technical Requirements for Wind Power and Photovoltaic Installations and Any Generating Facilities whose Technology does not Consists on a Synchronous Generator Directly Connected to the Grid: Offprint Form the O.P. 12.2 Outline, AEE, Spain, Oct. 2008.

[85] *EirGrid Grid Code Version 5.0*, EirGrid, Ireland. Oct. 2013.

[86] *National Electricity Rules Version 63*, A. E. M. Commission, AU, Jul. 2014.

[87] *Technical Rules*, Western Power, AU, Dec. 2011.

[88] Transmission Provider Technical Requirements for the Connection of Power Plants to the Hydro-Québec Transmission System, Hydro-Québec, Canada. Feb. 2009.

[89] Technical regulation 3.2.5 for wind power plants with a power output greater than 11 kW, Energinet, Denmark, Sep. 2010.

[90] *Grid Code: High and extra high voltage*, Tennet TSO GmbH, Bayreuth, German, Dec. 2012.

[91] The Grid Code, Issue 5, Revision 9, NGET, UK, Jul. 2014.

[92] The Technical Basis for the New WECC Voltage Ride Through (VRT) Standard, Western Electricity Coordinating Council, USA, Jun. 2007.

[93] *Implementation Guideline for Network Code: Requirements for Grid Connection Applicable to all Generators*, ENTSO-E, 2013.

[94] EWEA. (Feb. 2008). European Grid Code Requirements for Wind Power Generation, EWEA Working Group on Grid Code Requirements, Brussels, Belgium.

[95] Y. Coughlan, P. Smith, A. Mullane, and M. O'Malley, "Wind Turbine Modelling for Power System Stability Analysis – A System Operator Perspective," *IEEE Trans. Power Systems,* vol. 22, no. 3, pp. 929-936, Aug. 2007.

[96] A. Ellis, Y. Kazachkov, E. Muljadi, P. Pourbeik, and J. J. Sanchez-Gasca, "Description and technical specifications for generic WTG models – A status report," in *Proc. 2011 IEEE/PES Power Systems Conference and Exposition Conf.,* pp. 1-8.

[97] M. Asmine, J. Brochu, J. Fortmann, R. Gagnon, Y. Kazachkov, C. E. Langlois, C. Larose, E. Muljadi, J. MacDowell, P. Pourbeik, S. A. Seman, and K. Wiens, "Model validation for wind turbine generator models," in *Proc. 2011 IEEE Power and Energy Society General Meeting Conf.,* pp. 1-1.

[98] Z. Fan, T. Wehrend, T. Gehlhaar, and J. Meggers, "50/60 Hz Grid Code Test and Verification Experience," in Proc. 11th International Workshop on Large-Scale Integration of Wind Power into Power Systems as well as on Transmission Networks for Offshore Wind Power Plants Conf., 2012, pp.

[99] T. Gehlhaar. 2012. Grid Code Compliance beyond simple LVRT, Germanischer Lloyd, Germany.

[100] K. Argyriadis. 2013. GL Renewables Certification: Certification and Standards for Wind Turbines, Germanischer Lloyd, Germany.

[101] Alliance Power and Data. (2011). Our Key Services. [Online]. Available: http://apdpower.com.au/services.html.

[102] K. Chang, F. Xue, Y. Fang, and Y. Yu, "Comparative Simulation of Dynamic Characteristics of Wind Turbine Induction Generator Based on RTDS and MATLAB," in *Proc. 2010 Asia-Pacific Power and Energy Engineering Conf.,* pp. 1-5.

[103] AMSC. (Dec. 2013). Connecting Australia's Largest Wind Farm to the Power Grid. Australia.

[104] N. W. Miller, W.W. Price and J.J. Sanchez-Gasca, "Dynamic Modeling of GE 1.5 and 3.6 Wind Turbine-Generators," GE-Power Systems Energy Consulting, Oct. 2003. Available at http://www.easthavenwindfarm.com/filing/high/modeling.pdf.

[105] N. W. Miller, J. J. Sanchez-Gasca, W. W. Price, and R. W. Delmerico, "Dynamic modeling of GE 1.5 and 3.6 MW wind turbine-generators for stability simulations," in *Proc. IEEE Power Engineering Society General Meeting,* 2003, pp. 1977-1983, Vol. 3.

[106] M. O. L. Hansen, *Aerodynamics of wind turbines : rotors, loads and structure.* USA: Earthscan, 2008.

[107] J. F. Conroy and R. Watson, "Low-voltage ride-through of a full converter wind turbine with permanent magnet generator," *IET Renewable Power Generation,* vol. 1, pp. 182-189, Sept. 2007.

[108] S. Li, T.A. Haskew, E. Muljadi and C. Serrentino, "Characteristic Study of Vector-controlled Direct-driven Permanent Magnet Synchronous Generator in Wind Power Generation," *Electric Power Components and Systems,* vol. 37, pp. 1162 - 1179, Sep. 2009.

[109] B. Wu, Y. Lang, N. Zargari and S. Kouro, *Power conversion and control of wind energy systems*, N.J. : Wiley-IEEE Press, 2011.

[110] S. M. Muyeen, R. Takahashi, T. Murata, and J. Tamura, "A new control method of energy capacitor system in DC-based wind farm," in *Energy Conversion Congress and Exposition, 2009. ECCE 2009. IEEE*, Sep. 2009, pp. 1619-1625.

[111] K. Ohyama, S. Arinaga, and Y. Yamashita, "Modeling and simulation of variable speed wind generator system using boost converter of permanent magnet synchronous generator," in *Power Electronics and Applications, 2007 European Conference on*, Sep. 2007, pp. 1-9.

[112] M. Mohseni, S. Islam, and M. Masoum, "Impacts of symmetrical and asymmetrical voltage sags on DFIG-based wind turbines considering phase-angle jump, voltage recovery, and sag parameters," *IEEE Trans. Power Electronics*, vol. 26, no. 5, pp. 1587-1598, May. 2011.

[113] M. H. J. Bollen, *Understanding power quality problems: voltage sags and interruptions.* IEEE Press, NY, 2000.

[114] M. H. J. Bollen, "Voltage recovery after unbalanced and balanced voltage dips in three-phase systems," *IEEE Trans. Power Delivery,* vol. 18, pp. 1376-1381, Oct. 2003.

[115] M. Mohseni, S. Islam, and M. Masoum, "Enhanced Hysteresis-Based Current Regulators in Vector Control of DFIG Wind Turbines," *IEEE Trans. Power Elec.,* vol. 26, pp. 223-234, Jan 2011.

[116] M. Mohseni and S. M. Islam, "Transient control of DFIG-based wind power plants in compliance with the Australian grid code," *IEEE Trans. Power Electronics*, vol. 27, no. 6, pp. 2813-2824, Jun. 2012.

[117] H. T. Mokui, M. A. S. Masoum, M. Mohseni, and M. Moghbel, "Power system transient stability enhancement using direct drive wind generators," in Proc. *IEEE Power and Energy Society General Meeting,* 2012, pp. 1-6.

[118] N. R. Ullah, K. Bhattacharya, and T. Thiringer, “Wind farms as reactive power ancillary service providers─Technical and economic issues,” *IEEE Trans. Energy Conversion*, vol. 24, no. 3, pp. 661-672, Sep. 2009.

[119] O. Anaya-Lara, N. Jenkins, J. Ekanayake, P. Cartwright, and M. Hughes, *Wind energy generation : modelling and control.* Hoboken, NJ : John Wiley & Sons, 2009.

[120] B. Fox, D. Flynn L. Bryans, N. Jenkins, M. O' Malley, R. Watson and D. Milborrow*, Wind Power Integration: Connection and system operational aspects*. Institution of Engineering and Technology, 2007.

[121] P. Kundur, *Power System Stability and Control*, 1994.

[122] Y. Xibo, W. Fei, D. Boroyevich, L. Yongdong, and R. Burgos, "DC-link Voltage Control of a Full Power Converter for Wind Generator Operating in Weak-Grid Systems," IEEE Trans. Power Electronics, vol. 24, pp. 2178-2192, Sep. 2009.

[123] S. Grunau and F. W. Fuchs, "Effect of Wind-Energy Power Injection into Weak Grids," 2012. [online]. Available: www.tf.uni-kiel.de/etit/LEA/en/research/Publications/.../grunau_ewea_2012.pdf.

[124] N. P. W. Strachan and D. Jovcic, "Stability of a Variable-Speed Permanent Magnet Wind Generator with Weak AC Grids, "*IEEE Trans. Power Delivery,* vol. 25, pp. 2779-2788, Oct. 2010.

[125] The MathWorks Inc., *MATLAB and Simscape™ Power Systems™ Toolbox Release 2016a*. [CD-ROM]. Natick, Massachusetts, United States, 2016.

[126] M. S. El Moursi, B. Bak-Jensen, and M. H. Abdel-Rahman, "Coordinated Voltage Control Scheme for SEIG-Based Wind Park Utilizing Substation STATCOM and ULTC Transformer," *IEEE Trans. Sustainable Energy,* vol. 2, no. 3, pp. 246-255, Jul. 2011.

[127] M. El Moursi, G. Joos, and C. Abbey, “A secondary voltage control strategy for transmission level interconnection of wind generation,” *IEEE Trans. Power Electronics*, vol. 23, no. 3, pp. 1178-1190, May. 2008.

[128] H. Amaris, M. Alonso, and C. A. Ortega, *Reactive Power Management of Power Networks with Wind Generation.* London: Springer, 2013.

[129] *National Electricity Rules Version 41*, Australian Energy Market Operator, Jan. 2011.

[130] T. Stockmeier and T. Grasshoff, "Integrated power electronic solutions for renewable energy utilization," in *Proc. IEEE Energytech,* 2012, pp. 1-5.

Appendix A Simulation Parameters for FCWGs

Generator Parameters	
Rated Power	*2 MW*
Stator voltage/Frequency	*575 V / 60 Hz*
Rs	*0.006 p.u.*
Xd / Xq / Xl	*1.305 p.u / 0.474 p.u/0.18 p.u*
H	*2.32 Sec*
Vdc	*1100 Volt*
Grid side coupling inductor, L / R	*0.15 p.u / 0.03 p.u*
Boost converter inductance, L / R	*0.0012 H / 0.005* Ω
Wind Turbine parameters	
Nominal mechanical output power	*2 MW*
Base wind speed	*11 m/s*
Maximum power at base wind speed	*1.1 p.u.*
Initial pitch angle	0^o
Inertia Constant	*4.32 s*

Appendix B Simulation Parameters for FSIGs

Generator Parameters	
Rated power	*1.5 MW*
Rated Voltage/Rated frequency	*575 V, 50 Hz*
Stator/Rotor resistances	*0.005, 0.1248 p.u.*
Leakage / Mutual inductances	*0.4, 6.77 p.u.*
Local capacitor bank	*0.4 MVar*
Wind Turbine parameters	
Nominal mechanical output power	*1.5 MW*
Base wind speed	*9 m/s*
Maximum power at base wind speed	*1.0 p.u.*
Turbine inertia constant	*5.04 s*